Faculteit Geneeskunde en Gezondheidswetenschappen
Translationele Neurowetenschappen – Oogheelkunde

Het modelleren van emmetropisatie en myopisatie

Proefschrift ingediend voor het behalen van de graad van **Doctor in de Medische Wetenschappen** aan de Universiteit Antwerpen, ter verdediging door

Arezoo Farzanfar

Promotors:
Prof. Jos ROZEMA
Prof. dr. Carina KOPPEN

Antwerp, 2024

In this thesis, an artificial intelligence tool (ChatGPT) was used for grammar and spelling corrections.

PhD thesis submitted for the degree of **Doctor of Medical Sciences** at the University of Antwerp 2024

PROMOTORS:

Prof. Jos ROZEMA
University of Antwerp, Antwerp, Belgium

Prof. dr. Carina KOPPEN
University of Antwerp, Antwerp, Belgium

MEMBERS OF THE EXAMINATION COMMITTEE:

Prof. dr. Jan SIJBERS
University of Antwerp, Antwerp, Belgium

Prof. dr. Veva DE GROOT
University of Antwerp, Antwerp, Belgium

Prof. dr. Robert ISKANDER
Wroclaw University of Science and Technology, Wroclaw, Poland

Prof. dr. Linda LUNDSTRÖM
Royal Institute of Technology, Stockholm, Sweden

List of abbreviations *7*

Chapter 1. Thesis outline *9*

Chapter 2. Introduction *13*

ANATOMY OF THE EYE 13

Cornea *15*

Lens *16*

EYE DEVELOPMENT 16

Growth of ocular structures *17*

Eye development from infancy to early childhood *20*

Eye development from young adulthood to older age *20*

Role of sclera in refractive eye development *20*

Retinal image blur *21*

REFRACTIVE ERRORS 21

Hyperopia *22*

Myopia *22*

ENVIRONMENTAL FACTORS AFFECTING EYE GROWTH 25

Spatial contrast *25*

Light *25*

Wavelength of light *26*

Direction of light convergence *27*

Higher order aberrations (HOAs) *27*

Temporal integration of defocus signals *27*

REFRACTIVE DEVELOPMENT MODELING 28

Animal models *28*

Descriptive models *30*

Retinal feedback *32*

OCULAR COMPONENTS CONTRIBUTIONS TO REFRACTIVE ERROR 34

CONTRAST SENSITIVITY FUNCTION (CSF) 35

Age-related CSF *36*

Impact of refractive error (best corrected) on CSF *37*

Impact of defocus on CSF *38*

Chromatic CSF *38*

REFERENCES 40

Chapter 3. Bi-exponential description for different forms of refractive development *46*

INTRODUCTION 46

METHODS 46

RESULTS 51

DISCUSSION 53

REFERENCES 55

Chapter 4. Modelling normal and myopic eye growth *56*

INTRODUCTION 56

METHODS 58

RESULTS 63
DISCUSSION 67
REFERENCES 73

Chapter 5. The influence of color and defocus on contrast sensitivity function.... 76
INTRODUCTION 76
METHODS 77
RESULTS 80
DISCUSSION 84
REFERENCES 86

Chapter 6. The influence of variations in ocular biometric and optical parameters on differences in refractive error 88
INTRODUCTION 88
METHODS 89
RESULTS 94
DISCUSSION 97
REFERENCES 101

Chapter 7. Discussion 103

APPENDICES 113

Appendix A. Regressions by Jones et al. (2005) 114

Appendix B. Blur circle calculation 115

Appendix C. Spectral transmission of Dichroic filters 118

Appendix D. 120
SUPPLEMENTARY A: Additional Equations 120

APPENDIX E: Ocular biometry 126

APPENDIX F: Physiological constraints of visual pathway lead to more efficient coding of information in retina 128

APPENDIX G: Publications 129

APPENDIX H: Author contributions 130

English abstract 130

Nederlands abstract 132

Acknowledgements 133

List of abbreviations

Abbreviation	Meaning
Δ	Indicates Change In [Sth]
95CI	95% Confidence Interval
ACD	Anterior Chamber Depth
ACDtot	Anterior Chamber Depth (incl. corneal thickness)
ACs	Amacrine Cells
AL	Axial Length
AL/CR	Axial Length to Corneal Radius ratio
ANOVA	Analysis of Variance
CC	Corneal curvature
CCT	Central Corneal Thickness
CD	Corneal Diameter
CI	Confidence Interval
CL	Contact Lens
CLEERE	Collaborative Longitudinal Evaluation of Ethnicity and Refractive Error
COMET	Correction of Myopia Evaluation Trial
CP	Corneal Power
cpd	cycles per degree
CR	Corneal Radius
CS	Contrast Sensitivity
CSF	Contrast Sensitivity Function
CT	Choroidal Thickness
D	Diopter
FD	Form Deprivation
FVA	Functional Vision Analyzer
GA	Gestational age
HD	Hyperopic Defocus
HOA(s)	Higher Order Aberrations
IL	Innermost Layer
IOL	Intraocular Lens
LALES	Los Angeles Latino Eye Study
LCA	Longitudinal Chromatic Aberration
LogMAR	Logarithm Of the Minimal Angle Of Resolution
LP	Lens Power
LT	Lens Thickness
MAR	Minimum Angle of Resolution
M-cells	Midget Ganglion Cells
MD	Myopic Defocus
ML	Middle Layer
µL	Microliters
µm	Micrometer
ml	Milliliters
mm	Millimeters
OA	Optical Aberration
OCT	Optical Coherence Tomography
ODEs	Ordinary Differential Equations
OL	Outer Layer
OLSM	Orinda Longitudinal Study of Myopia
PCD	Posterior Chamber Depth
P-cells	Parasol Ganglion Cells
Q	Asphericity
RGCs	Retinal Ganglion Cells

ROP	Retinopathy of Prematurity
RPE	Retinal Pigment Epithelium
S	Spherical refractive error
SA	Spherical Aberration
SCORM	Singapore Cohort Study of the Risk Factors for Myopia
SD	Standard Deviation
SE	Spherical Equivalent
SNR	Signal-to-Noise Ratio
T	Corneal Thickness
VA	Visual Acuity
VC	Vitreous Chamber
VCD	Vitreous Chamber Depth
VF	Visual Field

Chapter 1. Thesis outline

Refractive error is a common vision problem that can affect individuals of all ages. It arises from an imbalance between the axial length (AL) of the eye and its optical power, which is the combined power of the cornea and lens.[1] Myopia, commonly referred to as nearsightedness, is a refractive error where parallel rays of light entering the eye are focused in front of the retina. Flitcroft et al.[2] describe this condition as primarily resulting from either excessive axial elongation of the eyeball (axial myopia) or changes in the refractive elements of the eye, such as increased corneal curvature or lens power (refractive myopia). These two forms of myopia, while distinct in origin, contribute to the growing public health challenge of myopia globally.

Axial myopia is of particular interest in this thesis due to its association with more severe complications, such as pathologic myopia. Pathologic myopia involves structural changes in the posterior segment of the eye, leading to vision loss. Proper coordination between the growth of different ocular components (like AL and optical power of the eye) ensures that light is accurately focused on the retina, leading to clear vision.

Over the past decades, extensive research has highlighted the influence of genetic, environmental, and lifestyle factors on the development of myopia. For example, school-age myopia is believed to result from a complex interplay of multiple minor genetic factors and major environmental influences, such as outdoor activity and educational pressures (environmental factors).[3-5] Following this, **Chapter 2** (Introduction) discusses some animal models to explain how environmental factors such as ambient lighting conditions and the spatial contrast of visual stimuli affect eye growth.

To gain a comprehensive understanding of myopia, it is essential to explore models of refractive eye development and precisely comprehend the changes that occur in ocular components over time. Many descriptive studies have focused on the initial stages of eye development and the associated biometric changes. Notably, Mutti and colleagues (2018)[6] examined individual ocular biometric parameters from infancy to early school age. Building on these studies, Rozema (2023)[7] recently demonstrated that most ocular parameters exhibit a bi-exponential growth pattern. These descriptive models are explained in Chapter 2. In **Chapter 3**, inspired by these bi-exponential functions for axial power and total eye power, we demonstrate that various courses of refractive development known from the literature, ranging from normal to high hyperopia or early myopia can be simulated. This chapter[8] demonstrates how bi-exponential growth function coefficients can effectively replicate refractive development patterns for both normal and abnormal eyes. Although bi-exponential growth functions describe

changes in AL and eye power over time, it could be improved by considering the interactions between axial length, total eye power, and external factors. Our model in Chapter 3 assumes that these parameters are independent, while actual refractive development involves complex interactions between the eye's optical and sensory components for clear vision.

Based on the literature, it was determined that a feedback controller[9] is necessary to assess how changes in one ocular parameter influence the growth rates of other parameters, ultimately optimizing the quality of the image projected onto the retina. Thus, in **Chapter 4** we introduced a system of first-order ordinary differential equations (ODEs) using the bi-exponential descriptions of the axial and optical power of the eye and a closed-loop feedback control to model normal refractive development based on the interactions between both powers, as well as the impact of external influences. The feedback function used in this model is based on the retinal blur diameter of a distant object. Moreover, we simulated myopic refractive development by adding an extra term Δ to the feedback function to account for external factors like behavioral or environmental factors affecting myopia. The proposed model can replicate findings from numerous animal experiments and clinical studies such as form deprivation (FD). This model enhances our understanding of the origins of refractive errors and holds potential for future innovations in myopia management.

Eye growth modeling should include a precise regulator that considers the effects of external factors like ocular wavefront distortions, light levels, color, spatial frequency, and contrast. These predominant environmental factors are processed by the retina. Therefore, in the next stage, we aim to develop a version of eye growth modeling that incorporates alternative feedback functions to address the effects of environmental and behavioral factors, better understanding the relationship between ocular growth and external influences. To this end, we conducted experiments to evaluate the influence of wavelength and defocus on contrast sensitivity function (CSF) in both emmetropes and myopes (**Chapter 5**) and the results showed that both defocus and color significantly influence CSF. Also, chapter 5 describes the study design method employed in this experiment. As a future goal, we need to find a general function for contrast sensitivity that includes factors such as light, color, defocus, and spatial frequency. Then, we must find a way to incorporate this function into the feedback control of eye growth.

Moreover, it has been well established that understanding the origins of refractive error is crucial because the way the structure of the eye components develops determines how well the eye can focus light onto the retina. Variations in these ocular dimensions can cause normal vision, myopia, or hyperopia. Therefore, we introduced a paraxial approach for estimating how variations in ocular biometry impact refractive error in **Chapter 6**.[10] We found that alterations in

ocular refraction are predominantly driven by changes in AL, lens power (LP), and cornea power (CP). However, the extent to which lens and corneal power contribute varies among different populations.[10]

In future work, we aim to integrate alternative feedback mechanisms to better account for environmental and behavioral factors, bringing the model closer to a physiological feedback system.

REFERENCES

1. Harb EN, Wildsoet CF. Origins of refractive errors: environmental and genetic factors. Annu. Rev. Vis. Sci. 2019;5(1):47-72.
2 Flitcroft DI, He M, Jonas JB, Jong M, Naidoo K, Ohno-Matsui K, et al. IMI–defining and classifying myopia: a proposed set of standards for clinical and epidemiologic studies. Invest. Ophthalmol. Vis. Sci. 2019;60(3):M20-M30.
3. Hyman L, Gwiazda J, Hussein M, Norton TT, Wang Y, Marsh-Tootle W, et al. Relationship of age, sex, and ethnicity with myopia progression and axial elongation in the correction of myopia evaluation trial. Arch. Ophthalmol. 2005;123(7):977-87.
4. Johnson G, Matthews A, Perkins E. Survey of ophthalmic conditions in a Labrador community. I. Refractive errors. Br. J. Ophthalmol. 1979;63(6):440-8.
5. Morgan I, Rose K. How genetic is school myopia? Prog. Retin. Eye Res. 2005;24(1):1-38.
6. Mutti DO, Sinnott LT, Mitchell GL, Jordan LA, Friedman NE, Frane SL, et al. Ocular component development during infancy and early childhood. Optom. Vis. Sci. 2018;95(11):976-85.
7. Rozema JJ. Refractive development I: biometric changes during emmetropisation. Ophthalmic Physiol. Opt. 2023;43(3):347-67.
8. Fzanfar A, Rozema JJ. Bi-exponential description for different forms of refractive development. J. Vis. 2024;24(7):3-.
9 Medina A. The cause of myopia development and progression: theory, evidence, and treatment, Surv. Ophthalmol. 2022;67(2);488-509.
10. Farzanfar A, Lockett-Ruiz V, Navarro R, Koppen C, Rozema JJ. The influence of variations in ocular biometric and optical parameters on differences in refractive error. Ophthalmic Physiol. Opt. 2024;44(5):1000-9.

Chapter 2. Introduction

Refractive development of the eye depends on a delicate balance between the optical powers of the cornea and the crystalline lens, as well as the position of the retina. Any mismatch in this balance leads to refractive errors. Despite significant eye growth during childhood, the refractive power of the eye typically adjusts to maintain this balance, preventing the onset of ametropia. However, the mechanisms underlying this adaptive process remain largely unclear. So, to understand how ocular components grow and interact, it is essential to examine the anatomical details of the eye as these structures significantly impact refractive development. Therefore, this chapter begins with a brief overview of the anatomy of the eye and the growth patterns of ocular components across different ages. Then, the factors that affect eye growth and can lead to the development of myopia are provided in this chapter. Finally, various refractive eye development models are introduced to have a comprehensive understanding of myopia.

ANATOMY OF THE EYE

The human eye plays a crucial role in processing sensory information, serving as the primary organ for gathering environmental information and enabling interaction with it. It is a highly complex system in terms of both optics and physiology. Figure 1.1 illustrates its main components. Its structure is nearly spherical and divided into two chambers by the crystalline lens.

The eyeball is structured into three concentric layers. The outer layer (OL) consists of the transparent cornea at the front and the opaque sclera at the back, both composed of collagen fibers, protecting the inner eye structures. The middle layer (ML), known as the uvea, includes the iris, ciliary body, and choroid. The innermost layer (IL) is the retina, which processes visual signals transmitted to the brain via the optic nerve. The sclera, the eye's white outer shell, is transparent at the cornea, letting light enter from outside.[1]

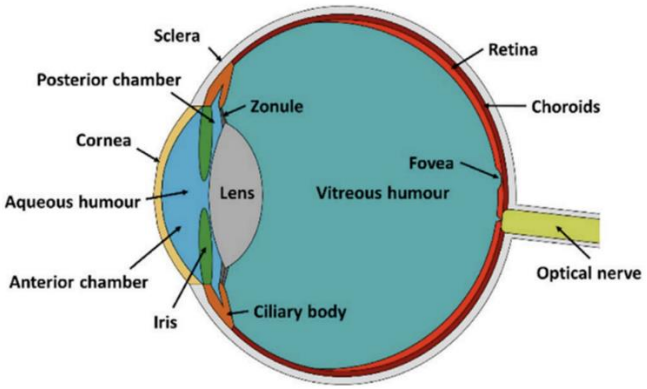

Figure 1.1. Schematic cross-section of a human eye.[2]

Light enters through the cornea, initiating the visual process. The cornea is crucial for refracting light and is essential for clear vision.

The anterior chamber (AC) is the space between the cornea and the iris, containing aqueous fluid with an average volume of 200 microliters (µL) and a depth of around 3 millimeters (mm). This chamber helps maintain intraocular pressure and provides nutrients for the eye structure. The posterior chamber (PC) is the space between the iris and the anterior surface of the lens, holding about 60 µL of aqueous fluid. The vitreous cavity is the largest part of the eye, making up about two-thirds of its total volume (5-6 milliliters (mL)),[3] and it contains a gel-like substance called vitreous gel.

The pupil adjusts its size to regulate the amount of light reaching the retina. It controls light exposure, which is vital for optimal vision under varying lighting conditions.
The crystalline lens, located just behind the iris and pupil, modulates its curvature via the ciliary muscle, enabling visual accommodation for varying distances (focusing images at varying distances).

The retina, covering the inner two-thirds of the eyeball, is nourished by the vitreous humor and the choroid. Bruch's membrane acts as a barrier between the choroid and the retinal pigment epithelium (RPE) which surrounds the ends of rod and cone photoreceptors. The neural retina, in front of the RPE, is made up of photoreceptors (rods and cones), horizontal cells, bipolar cells, amacrine cells, and ganglion cells organized into five distinct layers. Light passes through blood vessels and four transparent cell layers before reaching the photoreceptors.[4] The retina has approximately 115 million rods and 6.5 million cones, distributed unevenly. Cones are most concentrated in the fovea, which is specialized for high-resolution vision. Rods detect low light, while cones perceive color and brightness, categorized into S (426 nm), M (530 nm), and L (557 nm) types based on their sensitivity to wavelengths. The retina also includes the optic disc, known

as the retina's "blind spot," where the optic nerve exits and lacks photoreceptors. Adjacent to the optic disc is the macula, which contains protective yellow pigments. At the center of the macula lies the fovea, measuring 1.5 mm and specialized for high-resolution vision.[4]

Around one million retinal ganglion cells (RGCs) are also unevenly distributed, absent in the center of the fovea. Two primary types of RGCs exist: midget ganglion cells (M-cells) and parasol ganglion cells (P-cells). P-cells connect to specific brain layers, processing detailed information such as contrast, form, and red-green color, while M-cells focus on motion changes.

One of the most crucial measurements in understanding optical performance and image formation in the eye is axial length (AL).[5] Axial length is defined as the distance between the anterior surface of the cornea and the posterior retina, plays a role in ocular structure and function. Its variations are closely associated with changes in choroidal thickness, influencing ocular physiology and disease mechanisms. Normal vision, known as emmetropia, is typically associated with AL ranging between 21 and 26 mm. Achieving emmetropia requires approximately 55-70 diopters (D) of refractive power to correctly focus images onto the retina.

Given that the primary components influencing image formation are the cornea and the crystalline lens, they are explained more below. These components, responsible for refracting light, need to be very transparent and have precise optical characteristics for good visual quality.

Cornea

The cornea, covered by a tear film, serves as the eye's first refractive element through which light enters. It contributes approximately two-thirds of the total refractive power of the eye, around 60 diopters (D), and acts as a protective barrier. The cornea consists of several layers including the epithelium, Bowman's membrane, the stroma, Descemet's membrane, and the endothelium.[1]

The epithelium, a protective layer, ranges from 50 to 54 micrometers (μm) in thickness and has an average refractive index of 1.401. Bowman's and Descemet's membranes are thin layers measuring 8–12 μm. The stroma, which constitutes nearly 90% of the corneal thickness (Mean stromal thickness is thinner in the center (415 ± 34) compared to the periphery ($536 \pm 29\ \mu m$))[6] maintains transparency and strength through its collagenous lamellae and has an average refractive index of 1.376, with variations reported from 1.38 at the anterior to 1.373 at the posterior stroma.[7] Finally, the endothelium, a single-cell layer, is approximately 5 μm thick, and its refractive index is currently unknown.

The cornea exhibits different curvatures at the center and periphery, a feature known as asphericity, which is crucial for visual optics and retinal image quality.[8] Asphericity is commonly

described using conical sections, characterized by two parameters: the apical radius and the shape factor.[9,10] Various descriptors, such as eccentricity (e), asphericity (Q), and the form factor (p),[11] interrelate as $Q = -e^2 = p - 1$.

The shape of the corneal surface includes anterior and posterior parts, influenced by asphericity (Q). The anterior corneal surface typically has a negative Q, with a steeper center and flatter periphery, which helps reduce spherical aberrations and improves visual clarity. In contrast, the posterior corneal surface generally has a positive Q value, indicating flattened shape with a flatter center and steeper periphery, contributing to the overall balance of the eye.[1]

The radius of curvature varies between the anterior and posterior surfaces, with the anterior surface having a larger radius (7.81 ± 0.27 mm) compared to the posterior surface (6.40 ± 0.28 mm). The anterior corneal surface contributes about +48 D of refractive power, while the posterior surface reduces the anterior power by 6 D and compensates for astigmatism and spherical aberration (SA). Any irregularities in corneal fibers due to scarring or swelling can reduce transparency, leading to increased light scattering and diminished image quality.[1, 12, 13] The corneal shape varies between individuals, but consistently maintains a regular convex and aspheric form in healthy corneas.

Lens

The crystalline lens is a flexible optical component enclosed within a capsule. It has special features such as its ability to change shape, its varying refractive index, and its position within the ciliary ring, making it crucial for focusing light and adjusting vision. The crystalline lens is the most adaptable part of the eye, changing shape significantly with age.[14] It contains densely packed lens fibers composed of epithelial cells, leading to a non-uniform distribution of its gradient index. The gradient index is higher at the center and gradually decreases towards the edges.[1]

The crystalline lens accounts for approximately one-third of the eye's refractive power (about 22-26 D). This power can be adjusted through a process called accommodation, where the ciliary muscle contracts to increase the curvature of the lens.[15-17] The crystalline lens increases in thickness by about 24 μm each year.

EYE DEVELOPMENT

The development of the human eye is a gradual process from infancy to adulthood, culminating in achieving and maintaining a sharp retinal image. Understanding how newborn eyes adapt to clear vision requires precise information. Studying premature infants provides valuable insights as it offers early-stage data on prenatal development. Premature infants often present

myopia at birth, which is more pronounced with greater prematurity.[18] In utero, infants gradually reduce this myopia until the eye has a mild hyperopia at birth. These changes primarily result from natural eye growth without visual stimuli, highlighting early eye growth dynamics.[14]

During prenatal development, the eye grows proportionally (scaled growth), ensuring that components like the cornea, lens, and retina maintain correct shapes and proportions.[14,19-22] After birth, the eye adjusts its growth in response to visual stimuli (active growth).[14,23,24] Continuous and coordinated growth of ocular components is crucial for maintaining sharp retinal images. Disruptions in this harmonious growth, particularly in childhood, can lead to conditions such as myopia.

Emmetropization ensures harmonious growth of eye components, allowing images to be focused sharply on the retina.[25] Mismatching between the eye's focusing power and its axial length can lead to refractive errors.[26] During the first two years of life, emmetropization relies primarily on cornea power. After age two, cornea power stabilizes and has minimal impact on further emmetropization. Clear vision is primarily maintained through changes in AL rather than corneal power (CP).[27] Emmetropization is generally completed by age 2-3, with further fine-tuning of refractive components continuing into childhood to achieve emmetropia or near-emmetropic status.[26, 28, 29, 30]

The development of the ocular and visual system is highly susceptible to visual-environmental factors. Continuous coordinated growth remains essential throughout early childhood and beyond to ensure that the eye adapts to changing visual demands. Any disruptions in this process during school-age years can result in refractive errors such as school myopia.

The human eye normally grows until around age 6 without vision issues unless conditions like cataract intervene.

This section first explores changes in ocular biometry from prenatal infants until adulthood, followed by the progression of human eye development from infancy to childhood and from young adulthood to old age.[31] Then, the next section delves into myopia and the impact of visual-environmental factors on its development.

Growth of ocular structures

Understanding refractive error development in the human eyes requires knowledge of ocular biometry changes from prenatal stages through adulthood (Figure 1.2).[22, 28, 32, 33] Below are some significant biometric changes over time.

AL exhibits a bi-exponential growth pattern. During the prenatal period (20 to 40 weeks gestation), it grows rapidly at 0.16 mm per week. This rate slows significantly to about 0.03 mm per week during the first year of life. Growth continues at a slower pace, approaching adult size at 16-18 years.[22, 33, 34]

The anterior chamber (AC) undergoes significant changes during development. In embryonic stages, the lens and cornea touch until the corneal endothelium forms, causing the lens to move back and AC to form and deepen. This trend continues until about 10–12 years of age when the process reverses as the lens thickens and the AC becomes shallower. These shifts slightly affect the overall focusing power of the eye.[14]

Changes in corneal parameters also influence refraction over time. AL increases rapidly by about 5 mm from birth to three years, accompanied by a flattening corneal curvature (CC) and a reduction in lens power (LP) to compensate for these changes. The fetal cornea is steep and round but flattens by about 2 years old.[14] Changes in the shape of the cornea as individuals age primarily consist of alterations in its front and back radii of curvatures (r_{ca} and r_{cp}). Specifically, the mean value of r_{ca} increases from 5.65 mm three months before birth to 6.94 at birth, eventually reaching 7.77 mm by the age of 3 years.[35] Also, CP decreases slightly from 43 D at age 3 to 42.7 D at age 14.[36-39] The central thickness of the cornea remains largely unchanged throughout life, except for a short time after birth when it reduces swelling.[14]

The growth patterns of the crystalline lens are complicated, as certain dimensions such as the anterior and posterior radii of curvature (r_{la} and r_{lp}) show biphasic exponential changes, but the crystalline lens thickness (LT) follows a growth pattern consisting of three phases: initially an rapid increase, reaching approximately 3.80 mm at birth, followed by a decrease to 3.50 mm at ages 10–12 years (while LP reduces from 23 D to 20 D), and finally a steady increase throughout adolescence and adulthood. The lens diameter grows quickly before birth and more slowly afterward. Initially, the lens becomes flatter, then it gradually gets rounder.[14] This process leads to a decrease in the lens's power after birth, which is understandable when the lens flattens.[14] Infant lenses also have higher refractive indices than adults.[40]

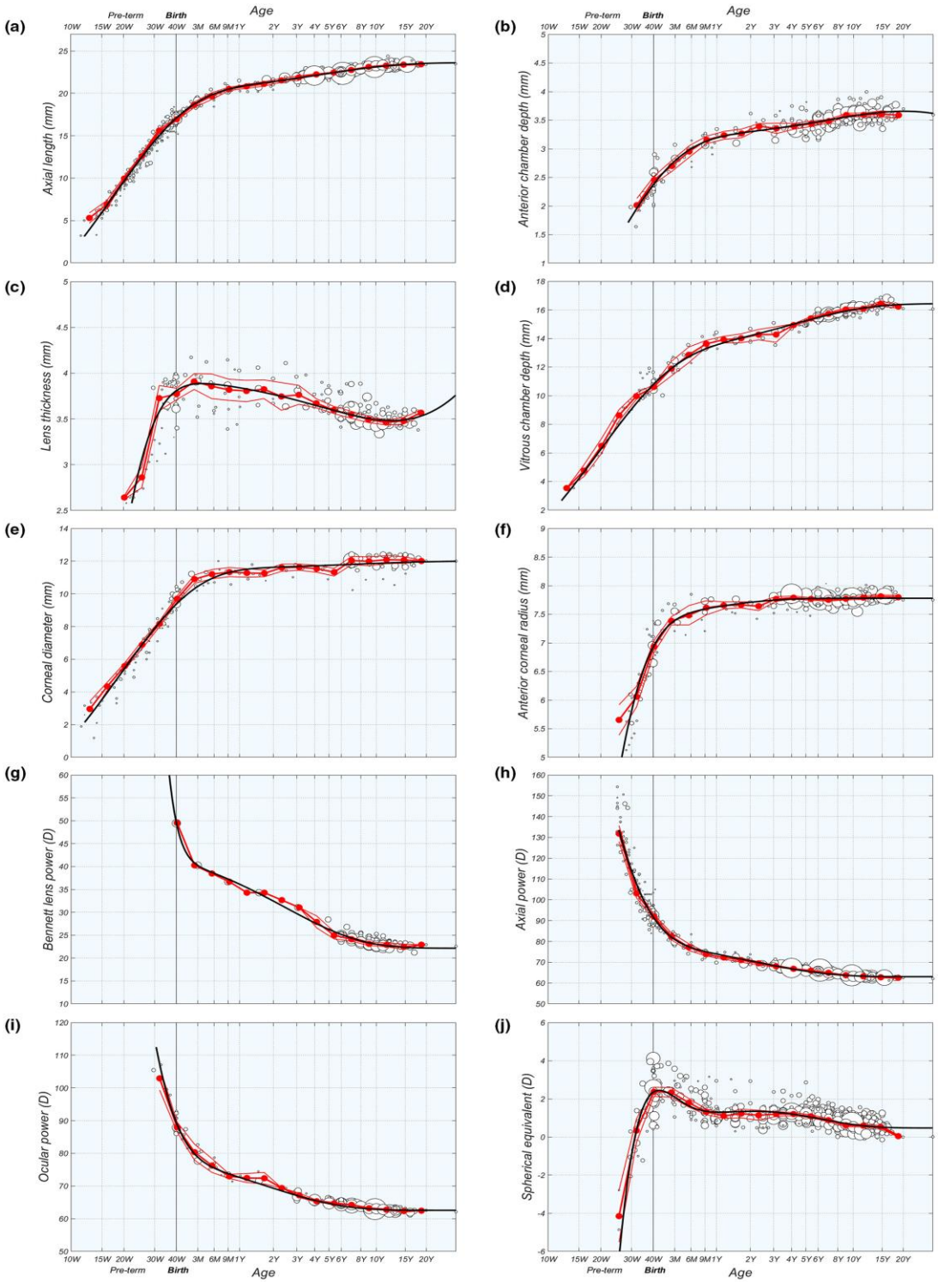

Figure 1.2. Changes in ocular measurements before and after birth were compiled by integrating several previous datasets for a) axial length; b) anterior chamber depth; c) lens thickness; d) vitreous chamber depth; e) corneal diameter; f) anterior corneal radius of curvature; g) Bennett lens power; h) axial power; i) whole eye power; j) spherical equivalent refractive error. [38, 40]

Eye development from infancy to early childhood

The refractive components of the eye grow rapidly during the first year of life, but they do so at varying rates and in interaction with each other.[32] Parameters like corneal curvature (CC), lens thickness (LT), and AL coordinate their growth during the emmetropization process to minimize average ocular refraction and achieve clear vision. AL increases significantly in the first year, but at the same time, the average powers of the cornea and the lens decrease.[24, 41] The rates of the change in these parameters vary, causing the average cycloplegic refraction to decrease by approximately 1 diopter, though individual differences can range up to 3 diopters.[22, 42] According to Pennie et al. (2001), infants aged 3 to 7 months typically exhibit hyperopia, which decreases rapidly within the first year, shifting towards emmetropia by 15 months of age.[14, 22, 18, 43-45] After that, the homeostasis period where the refractive error is stable and gradually facilitates toward emmetropia (1.25-18 years).[46]

Eye development from young adulthood to older age

After age 18, the ocular structures remain mostly stable, with only minimal refractive changes from young adulthood to older age.[47, 48] Older eyes tend to become slightly more hyperopic due to small adjustments in the cornea, lens, and AL.[49, 50] These changes are coordinated by the emmetropization process.

As people age, the lens grows, and its refractive index changes, causing the eye to become slightly more myopic. Research suggests that adult eyes may shorten their AL to balance these changes, keeping refractive error relatively stable overall.[51]

Role of sclera in refractive eye development

As mentioned in previous sections, ocular growth has a multifaceted nature, emphasizing the importance of understanding the contributions of various components such as corneal and lens growth, scleral growth, retinal neural signal processing, and ocular neurochemistry.[52] The sclera plays a crucial role in regulating eye growth by remodeling in response to visual signals. This remodeling involves changes in thickness and biomechanical properties to adjust the eye's AL. Dopamine, a neurotransmitter released by amacrine cells (ACs), influences eye growth by modulating the level of axial elongation. Amacrine cells affect various retinal layers through volume transmission, where neuromodulators diffuse and impact proteoglycan synthesis. This synthesis modulates scleral growth, with animal studies showing that increased proteoglycan synthesis correlates with a thicker sclera and reduced axial elongation.[53, 54]

Retinal image blur

Previous research highlighted the significant impact of retinal image blur on eye growth and emmetropization and suggested that clear images stabilize eye growth, whereas blurred images prompt the eye to elongate to minimize blur. This hypothesis was initially supported by experiments with monkeys and tree shrews.[26, 55, 56]

Later investigations revealed a more complex reality. In chicks, eye growth induced by form deprivation (FD) is more closely related to specific image patterns rather than overall blurriness.[57] Moreover, monkeys and tree shrews demonstrated the ability to adjust to both positive and negative lens-induced blur, correcting vision regardless of defocus type.[58-62] These insights indicate that factors beyond image clarity, such as image patterns and the eye's adaptability to different kinds of defocus, play crucial roles in emmetropization.[21, 34] In the animal model section, both form FD and lens-induced blue are explained in more detail.

Moreover, studies on retinal defocus magnitude showed that weak diffusers lead to a small increase in growth rate, while strong diffusers cause a larger increase.[27] Research combining diffusers and astigmatic lenses suggests that eye growth is influenced more by the type of defocus than the level of blur.[63, 64] Normally, diffusers cause myopia, but when paired with positive lenses, chick eyes develop hyperopia. Similarly, strong astigmatic lenses cause hyperopia with positive lenses and myopia with negative lenses, indicating that eyes adjust based on defocus type to maintain clear vision.[65, 66]

These findings underscore the complexity of eye growth regulation, highlighting the roles of retinal image patterns, defocus types, and the adaptive mechanisms in maintaining visual clarity.

REFRACTIVE ERRORS

Understanding the natural growth of ocular components is crucial for explaining the behavior of refractive errors with age. Comparing individuals with emmetropia to those with refractive errors provides insights into ocular growth mechanisms, the progression of myopia, the stability of emmetropia, and hyperopia.

Studies by Jones et al. examined AL, VCD, and CP among emmetropes, myopes, emmetropizing hyperopes, and persistent hyperopes for ages between 6 and 14 years. They found that the crystalline LP decreases with age across all groups. LT decreases to around 9.5 years, then increases, with no significant differences between groups. AL elongated more slowly in young emmetropes compared to hyperopes and myopes. After age 10 years, myopes show a steeper increase in VCD compared to persistent emmetropes. CP remains constant in myopes, and

decreases in persistent emmetropes, and slightly increases in emmetropizing hyperopes.[67]

In this section, two of the most important courses of refraction development, hyperopia and myopia are explained (Figure 1.3). Then, the factors affecting myopia development are explained.

Hyperopia

Hyperopia, or farsightedness, happens when close objects appear blurry because the focus point of light is behind the retina. Convex (positive) lenses correct this by directing light onto the retina. Hyperopia is typically around +1–3 diopters (D) at birth and often improves to near emmetropia by adolescence.[68, 69]

Hyperopia can be caused by several factors such as short AL, flat cornea, or weak LP.[70] In children, the most common type is axial hyperopia, where a 1 mm reduction in AL results in approximately 3.00 D of hyperopia.[70] Another type is curvature hyperopia, which occurs when the cornea or lens is flatter than normal, with a 1 mm increase in the radius of curvature leading to about 6.00 D of hyperopia.[71]

Myopia

Myopia, or near-sightedness, arises when the optical power of the eye is not properly aligned with its AL, resulting in blurred distance vision. It ranges from low myopia (-0.50 D to -6.00 D) to high myopia (≥ -6.00 D).[72] Pathologic myopia involves an excessive elongation of the eyeball, leading to degenerative retinal changes, such as myopic retinopathy or maculopathy.[73]

The prevalence of myopia has significantly increased over the past few decades, particularly in high-income regions such as Asia, North America, and Europe. In these areas, the rates of myopia ranged from 27% to 48% in 2010, projected to increase to 34% to 53% by 2020. By 2050, myopia is expected to affect half of the world's population, making a notable increase from 28% in 2010, reflecting a 1.7 times increase over four decades.[74]

Axial length to cornea radius ratio

As mentioned in the previous section, myopia occurs due to a mismatch between CP, LP, and AL of the eye. Sorsby (1962) observed that discrepancies in AL and CP can lead to high myopia or hyperopia.[36] The AL to CR ratio (AL/CR) is crucial for identifying myopia risk; a ratio exceeding 3 indicates a longer AL and a steeper cornea, common in myopia.[37] Longitudinal studies such as Orinda and Collaborative Longitudinal Evaluation of Ethnicity and Refractive Error (CLEERE) have identified these factors as predictive of myopia development. Changes in AL significantly contribute to myopia progression with age.[75]

Risk factors associated with myopia

Given the rising prevalence and serious implications of myopia, understanding its causes and developing effective interventions, especially for children, is essential.
Research indicates that myopia results from a complex interaction of genetic and environmental factors. Studies in East Asia and Western countries have identified critical risk factors for its onset and progression.

Early studies by Burns (1949) and Jablonski (1922) provided foundational insights into the genetic causes of myopia. Burns observed significant heritability trends in myopia over three generations of twins, while Jablonski found reduced variability in refractive errors among identical twins compared to fraternal twins, emphasizing genetic predisposition. Later studies by Knobloch et al. (1985) confirmed the high heritability of myopia, even in identical twins raised separately.[76-79]

Parental myopia significantly increases the likelihood of children developing myopia, with some studies suggesting a risk increase of up to 6.4 times if both parents are myopic.[80] Ethnicity also plays a role, with East Asian children more likely to develop myopia than European children.[81] Age of onset is crucial, as early-onset myopia tends to progress more rapidly and lead to higher levels of myopia in adulthood. Meanwhile, higher education levels and extensive near-work activities, such as reading and computer use, are linked to increased myopia prevalence.[82-85]

Recent investigations have also highlighted a link between spending more time outdoors[86,87] and lower rates of myopia, particularly among children.[85, 88, 89] Studies by Dirani et al. (2009), Jones et al. (2007), and Rose et al. (2008) consistently indicate that greater time spent outdoors is associated with a lower likelihood of developing myopia. This correlation is believed to stem from heightened exposure to natural light and reduced engagement in indoor near work.[85, 87, 90 -92]

Studies[93] have found that urban and indoor environments, which have fewer spatial frequencies than natural outdoor environments, might contribute to myopia. Thus, understanding the roles of spatial frequency and light exposure is important for myopia development.[93]

Myopia can be classified by the age of onset: juvenile myopia generally develops between the ages of 6 and adolescence, while myopia of prematurity (MOP) occurs shortly after premature birth due to lens and cornea alterations.[94-96] MOP is characterized by a sharply curved cornea and a thicker crystalline lens, differing from juvenile myopia, which typically presents with an elongated eye shape.[97]

The majority of these infants' eyes gradually recover and develop normal vision as they

grow older. However, some infants develop a lasting form of myopia that is often severe and remains stable, like congenital myopia. Within this group, there are cases where the myopia transitions into a more typical childhood myopia, which has the potential to worsen over time.[96]

Myopia treatment

Myopia typically necessitates the use of glasses, contact lenses (CLs), or refractive surgery for correction. However, these methods do not address the fundamental issue of excessive eye growth. High myopia increases the risk of serious complications like retinal detachment, myopic retinal degeneration, and glaucoma.[98]

As mentioned before, both genetic factors (such as parental myopia and ethnicity) and environmental factors (such as the high prevalence in Asian countries) contribute to the development of myopia.[99, 100] Animal studies suggest that changing optical conditions during eye development could offer potential new treatments.

Current methods to slow myopia progression have mixed results. Strategies like bifocal lenses and under-correction have shown limited success.[101] Atropine eye drops, as one of the myopia treatments are effective but can cause side effects like blurred vision and potential retinal damage.[102,103] Retinal feedback provides a comprehensive framework for understanding the mechanisms by which atropine mitigates myopia progression.[103] Atropine is known to affect the eye's ability to accommodate, with higher doses leading to significant reductions in accommodative response, making near objects appear blurry. However, in low-dose atropine treatment, the impact on accommodation is minimal, and it remains a popular option for myopia control due to its balance of efficacy and tolerance. Individuals treated with atropine may need to remove their glasses or use a positive lens for near tasks. Studies by Chia and colleagues demonstrated that groups using different doses of atropine showed varying rates of myopia progression, with lower doses associated with slower progression and less accommodative impact, supporting the role of retinal feedback. This highlights the importance of myopia research to discover more effective and safer treatment methods.

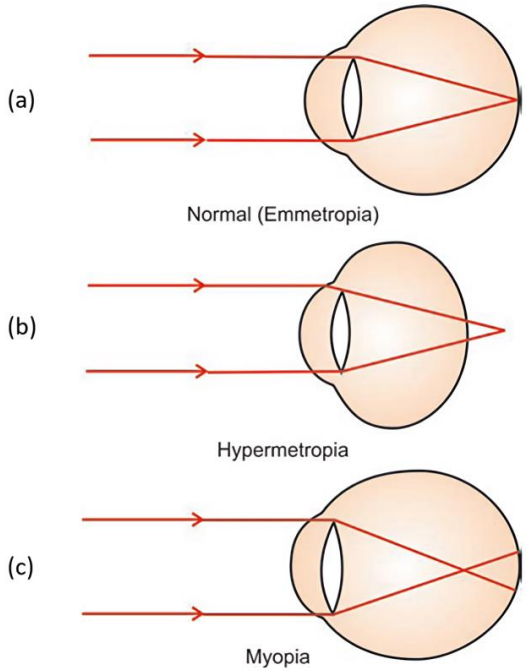

Figure 1.3. Schematic representations of a) emmetropia b) myopia c) hyperopia.[104]

ENVIRONMENTAL FACTORS AFFECTING EYE GROWTH

As mentioned in previous sections, eye growth is influenced by a variety of factors, including environmental and genetic factors. Key factors include ambient lighting conditions, including intensity, wavelength, and its convergence direction which impact retinal signaling and neurotransmitter release. Additionally, the spatial contrast of visual stimuli in the environment plays a critical role in shaping ocular growth patterns. Below, it is explained how these factors affect eye growth.

Spatial contrast

The contrast and spatial details in our visual environment play a crucial role in the proper growth of the eyes. Animal studies have demonstrated that reducing contrast or specific visual details through the use of filters can induce myopia experimentally.[105] Additionally, some research suggests that reduced outdoor activity and exposure to environments with fewer clear visual details may contribute to the development of myopia in children.[87] Despite these findings, the exact mechanisms by which these visual factors influence eye growth remain largely unknown.

Light

Experimental data show that the emmetropization process is influenced by lighting

conditions, including the duration, rhythmicity, spectral composition, and intensity of ambient light.[62] Animal research has demonstrated that high levels of light intensity result in shorter AL and hyperopia in both chicks and rhesus monkeys.[106, 107] This protective effect against myopia is associated with increased dopamine release in the retina, which fluctuates with light exposure.[108] For example, previous literature found that chicks raised under bright daytime light (10,000 lux) remain hyperopic, unlike those kept indoors under lower light (500 lux), which become myopic. High light intensities up to 40,000 lux reduce form-deprivation myopia (FDM) in chicks and provide protective effects in rhesus monkeys, tree shrews, and mice, preventing myopia.[62]

On the other hand, it was reported that the effectiveness of bright light in preventing myopia depends on factors such as duration and timing of exposure. Longer daily exposures (5-7.5 hours) are more effective across species, whereas shorter periods may not provide sufficient protection. Timing also plays a role; afternoon or evening exposures are more effective in reducing myopic eye growth compared to morning exposures.[62]

Moreover, studies[109, 110] have shown that chick eyes grow in a rhythmic pattern, growing more during the day. When their vision is blurred, their eyes grow faster at night, changing the normal growth rhythm. Detailed research using advanced measurement techniques revealed that the AL and choroidal thickness (CT) follow 24-hour cycles, with the CT peaking at midnight, opposite to the AL. New techniques like optical coherence tomography (OCT) and laser interferometry have shown these rhythms in humans as well, with AL and CT following opposite cycles.[62]

In conclusion, the impact of light intensity on ocular development underscores its potential as a factor in managing myopia. Insights from animal studies suggest that outdoor exposure and higher light levels may help counteract the global rise in myopia prevalence, potentially through mechanisms involving retinal signaling and adaptation to light conditions.[62]

Wavelength of light

Experimental data suggest that longitudinal chromatic aberration (LCA) may serve as a directional cue for both accommodation and emmetropization. LCA occurs because the eye's refractive index varies with the wavelength of light, causing long wavelengths (e.g., red light) to undergo less refraction compared to shorter wavelengths (e.g., blue light). This results in LCA ranging from 1.24 D to 1.95 D across wavelengths from 400 nm (blue) to 700 nm (red) in chicks, creating subtle color fringes around retinal images that change based on the eye's refractive state. Specifically, in hyperopic defocus (HD), red components of the image appear more blurred than blue components, while in myopic defocus (MD), blue components are more blurred than red

components. [55, 111]

LCA is consistent across individuals and species and remains unaffected by changes in pupil size or accommodation,[112] making it a reliable signal for guiding emmetropization. Studies with chicks identified various strategies by which the eye uses LCA cues. The previous study[55] found that when the image was sharp in the red channel, the eye became shorter, while sharpness in the blue channel led to elongation, indicating that the retina uses the difference in focus between red and blue to regulate eye growth, though this mechanism fails in already myopic eyes.[55, 111]

Additionally, temporal changes in LCA signals influence emmetropization. Experiments with flickering light sources have shown that rapid changes in color contrast can affect the direction of eye growth. High temporal frequencies, which indicate an in-focus image, slow eye growth, while low temporal frequencies promote growth, especially under specific color conditions.[111]

Direction of light convergence

The direction of light convergence serves as a cue for detecting blur direction and influences eye growth in animals, although the exact mechanism remains unclear.[113] Fincham hypothesized that light falling on different parts of the eye affects photoreceptors differently, with temporal light causing myopic defocus and nasal light causing hyperopic defocus.[114] Animal experiments have shown myopic defocus thickens the choroid temporarily, while hyperopic defocus thins the choroid.[61, 115]

Higher order aberrations (HOAs)

Recent research demonstrated that higher order aberrations (HOAs) notably impact retinal image quality and may lead to improper eye growth responses. These aberrations can impair the eye's ability to accurately detect and respond to defocus, potentially contributing to refractive errors such as myopia. Two critical aspects of how monochromatic and polychromatic aberrations affect retinal image quality in the nasal visual field were highlighted. The first relies on chromatic optical anisotropy in the peripheral retina to provide a consistent cue for defocus, irrespective of pupil size. The other depends on the blur shape, where myopes exhibit vertically elongated blur for wavelengths longer than 455nm, while emmetropes and hyperopes show horizontally elongated blur.[116]

Temporal integration of defocus signals

Previous studies indicated that temporal integration of defocus signals significantly influences eye growth by affecting how the eye compensates for visual changes. It was reported that the frequency and duration of defocus exposure, rather than just the total amount of time, have

a greater impact on eye growth. For instance, frequent interruptions of defocus with short periods of normal vision can reduce myopia development and slow down eye elongation. This suggests that the eye's response to visual signals is non-linear and that timing plays a crucial role in guiding eye growth.[117]

REFRACTIVE DEVELOPMENT MODELING

Modeling refractive development is essential for understanding the intricate interactions between the eye's optical and sensory components that are crucial for maintaining clear vision as the eye grows. While experimental animal models have provided valuable insights, their applicability to human refractive development is limited due to species differences and environmental factors. Therefore, advanced numerical models offer a powerful alternative. These models can simulate how changes in one ocular parameter influence others through feedback mechanisms aimed at optimizing retinal image quality. Such models are essential for deepening our understanding of refractive development and guiding future research and clinical interventions. So, in this section, we first discuss animal and descriptive models, followed by our alternative numerical model.

Animal models

Animal models have been conducted to understand early refractive development and the mechanisms behind emmetropization and myopia.[111] By controlling the visual environment, researchers can investigate how various visual cues affect eye growth in animal studies. These studies have identified mechanisms such as local retinal control and biochemical signaling pathways that translate visual stimuli into changes in eye structure, affecting refractive errors.[111] Research shows that myopia in animal models is linked to disruptions in eye regulation mechanisms, resulting in increased variability and regulatory failure.[118, 119] Initial studies involved depriving animals of clear visual stimuli, which induced myopia and resulted in greater variability in refractive outcomes. Another experimental approach used lenses to induce myopia or hyperopia in animals. These findings are important for developing optical and pharmacological treatments to manage and prevent myopia, a growing public health concern.[111] Both deprivation and lens-based studies are discussed in detail below.[58, 61, 120, 121]

Form deprivation myopia

Form deprivation (FD) refers to a condition characterized by the absence of clear-form vision, such as in darkness or with blurred lenses, which results in abnormal eye growth and myopia.[111] For example, previous studies have demonstrated that suturing the eyelids of monkeys leads to eye elongation, suggesting a link between FD and abnormal emmetropization.[122] This

phenomenon occurs because the blurred images seen through closed eyelids do not provide sufficient clear visual information. Additionally, FD myopia can be induced by placing diffusers in front of the eyes or by manipulating the visual environment to restrict spatial and contrast details. These methods highlight the importance of clear visual input in normal eye development. Also, it emphasizes that form-deprivation myopia is an open-loop condition where the eye cannot use visual feedback to regulate its growth.[123, 124] In fact, deprivation myopia shows an open loop condition since the eye continues to grow despite not enhancing retinal image quality, disrupting emmetropization. So, the researchers can measure how the eye responds to blurred images by growing. Blurry retinal images stimulate this eye growth, like how the eye adjusts to correct slight hyperopia. It is noteworthy that the extent of FD myopia depends on the environment and genetics, with earlier and longer periods of FD causing more severe myopia.[111]

Lens- induced defocus

Previous research has investigated how blurring lenses affect eye growth. Positive lenses cause images to focus in front of the retina (myopic defocus), prompting the eye to slow its growth to bring the retina closer to the focal point. Conversely, negative lenses cause images to focus behind the retina (hyperopic defocus), leading the eye to accelerate its growth to achieve proper focus.

For instance, experiments conducted on monkeys exposed different parts of their retina to various types of defocus, leading to distinct refractive changes in those regions.[125] Animal studies demonstrate these adaptive changes reflect the eye's active response to different types of defocus by adjusting its growth accordingly.[61, 126-128]

Anatomical changes from induced refractive errors

Inducing refractive errors in experiments leads to changes in different parts of the eye, especially the VC. These changes affect the retina, choroid, and sclera. Experimental studies demonstrate that obstructing clear vision or inducing blur through lenses alters gene activity in the retina, resulting in accelerated growth at the retina periphery.[111]

The choroid, a vascular layer between the retina and sclera, influences eye size and shape by adjusting its thickness in response to visual stimuli. As mentioned before, myopic defocus thickens the choroid, while hyperopic defocus thins it, with changes occurring rapidly until structural adjustments are ensured.[127, 129, 130] Though CT was thought to predict eye growth rates, studies show various results. These changes involve fluid movement and smooth muscle activity, highlighting the choroid's regulatory role in eye growth and its potential in treating eye conditions.[111]

The sclera, the eye's outer layer, varies across species. In many animals, it comprises an inner cartilaginous layer and an outer dense tissue, sometimes with bony parts. Humans and most mammals have mostly fibrous sclera with leftover cartilage. Changes in the sclera's structure affect eye growth and myopia. Both mammals and birds experience scleral thinning in myopia, but birds also grow cartilage in their sclera. In mammals, myopia involves changing the scleral structure and making it more flexible, while young birds actively grow new scleral tissue during myopization. Changes in the posterior sclera during myopia are influenced by differential growth patterns of various eye components and the associated pressures, crucial for controlling eye growth across different animals.[111]

Local retinal mechanisms

Researchers have determined that the mechanisms controlling eye growth in response to visual signals are inherently local to the eye. They used diffusers and lenses, and various experimental manipulations to show that these mechanisms operate independently of the central nervous system. Important experiments showed that removing the visual cortex, severing the optic nerve, blocking retinal ganglion cells, or disrupting sensory nerves did not prevent refraction. This suggests that visual signals are intrinsic regulators of eye development.

Further studies, including MRI examinations of macaque eyes, confirmed local changes in eye development and refractive error in response to changes in the visual field. These findings confirm that local retinal mechanisms detect defocus and regulate eye growth in specific regions. Thus, eye development and refractive growth are governed primarily by these retinal local mechanisms, independent of central nervous system inputs. These mechanisms likely contribute to observed patterns of myopia and refractive errors in various species under specific visual conditions.[111]

However, these experimental findings may have limitations when applied to humans. For instance, while under-correction of myopia results in emmetropia in chickens,[131] it has minimal to no impact on humans.[132, 133] This discrepancy led to the development of the retinal feedback,[103, 25, 134] which explains how alterations in one part of the eye influence others to optimize retinal image quality. Retinal feedback will be explained in more detail in the following sections.

Descriptive models

Numerous studies investigated ocular biometric changes with age and their correlation with each other to provide a comprehensive dataset for understanding refractive development. In 1979, Hirano and colleagues measured changes in AL without considering refraction. In 2001, Pennie and colleagues collected long-term data on the growth and refraction of full-term infants'

eyes during their first year of life, using cycloplegia for accurate measurements. This research revealed that different components of the eye grow at varying rates during the first year. AL expands based on a quadratic equation with age, and ACD grows linearly. However, the LT remains unchanged.[22]

In 2018, Mutti and colleagues followed a group of infants over the first 6 years of their life.[135, 24] This study uses long-term data on eye components from infancy to childhood to identify average growth patterns.[135] They found that certain parts of the eye, such as AL, grew consistently with other studies, showing about a 3.4 mm increase from three months to 6.5 years. Other aspects, like LT, changed gradually over time.[135]

Although various longitudinal and cross-sectional studies have been conducted on refractive development, many are constrained by the age range or specific parameters considered. Recently, a meta-regression analysis examined refractive and biometric changes from the prenatal stages to adulthood, emphasizing interactions between the optical and sensory components of the eye.[40] Among 34,409 references, only 294 contained usable data.[6] In 2023, Rozema reported that the growth patterns of nearly all ocular parameters can be described by a bi-exponential growth pattern (equation 1-1), characterized by a rapid initial phase before and immediately after birth, transitioning into a slower phase once retinal feedback starts.[40]

$$a_0 + a_1\, exp(a_2 \times Age) + a_3\, exp(a_4 \times Age) + a_5 \times Age \qquad (1\text{-}1)$$

The coefficient values of the biometric parameters fitted to the function for each parameter are available in the Rozema study.[40] Due to the rapid initial growth phase, the logarithm of gestational age (GA) was employed instead of birth age at birth for sampling. Age is in years and pre-term ages are denoted as negative values.[40]

By considering the eye as a simplified optical system, a single lens represents the total refractive power of the eye (axial power, P_{eye}) and the AL of the eye expressed in diopters (D), P_{ax}. Both P_{ax} (the power that eye needs to have a sharp image on the retina), and P_{eye} (the combined powers of the cornea and lens) can be calculated using bi-exponential functions (equation 1-2). Both powers exceed 130 D three months before birth, drop to 87-89 D at birth, and reach 62 D in adulthood.

$$\begin{cases} P_{ax}(t) = c_1 e^{c_2 t} + c_3 e^{c_4 t} + C_1 \\ P_{eye}(t) = c_5 e^{c_6 t} + c_7 e^{c_8 t} + C_2 \end{cases} \qquad (1\text{-}2)$$

The difference between these two powers corresponds with the refractive error S. For optimal vision, the values of P_{ax} and P_{eye} must remain close to each other.

$$S = P_{ax} - P_{eye} \quad (1\text{-}3)$$

These functions describe two stages of eye development: an initial rapid growth phase before and shortly after birth, followed by a slower growth phase where feedback starts to influence the growth. In Chapter 3, we will demonstrate that by adjusting the coefficients of these functions, we can simulate various courses of refractive development known from literature.[46]

Additionally, we could estimate the underlying changes in P_{ax} and P_{eye} which is an advantage over a simple description of the refractive error alone. Since this model does not account for interactions between these powers, a real refractive development requires considering the effect of different ocular components on each other. So, to better understand how different parts of the eye work together, researchers have used animal studies.

Retinal feedback

Emmetropization, first identified in early 20th-century Dutch and German studies,[25, 136, 137] describes the shift of refractive errors from a Gaussian distribution at birth to a more concentrated (leptokurtic) distribution around the mean as people age. Initially, researchers did not consider that eye growth regulation might be controlled by retinal feedback systems, but retinal feedback is currently the leading explanation for emmetropization and myopization.[103, 25, 134]

Retina feedback underscores the retina's role in regulating eye growth to maintain clear vision. During postnatal development, the eye adjusts its growth in response to visual signals to ensure proper retinal focus. Hyperopic defocus stimulates eye growth, while myopic defocus inhibits it.[61, 126, 138-141] Retinal feedback involves an optical signal related to refractive error and the adjustment of axial length to correct this error.[103]

Sorsby and colleagues (1960) proposed that eye regulation operates through an open-loop system. In contrast, Van Alphen (1961)[134] suggested it relies on a closed-loop system, incorporating feedback mechanisms based on refractive error. Supporting the closed-loop system, studies by Brown and Young (1981) and Greene and Guyton (1986) demonstrated exponential alterations in monkey eye refraction. Medina (1987)[142] proposed a second-order feedback system model for accurately predicting eye refractions, which performs better than non-feedback models. Medina, Korb, and Fariza (1988) later found that a simpler first-order feedback system might be sufficient since an exponential curve matches refraction data well.[143] In 1988, Schaeffel & Howland postulated that accommodation contributes to visual development, proposing a mathematical model applied to the eyes of chick.[144]

Hung and Ciuffreda later proposed a detailed model using genetic growth programming

and feedback from retinal blur circles, which is closely linked to refractive error. Their model simulates normal eye growth and experimental results with lenses, and diffusers.[31, 145] Their results represented that a negative lens decreases the blur circle size by reducing neuromodulator release like dopamine and increasing axial growth, but a positive lens increases the blur circle size by enhancing neuromodulator release which leads to axial growth decrease.[17]

However, these models have their drawbacks. For example, Hung's model overlooked the influence of the crystalline lens during emmetropization. To address this, we present a first-order differential equation model (ODE) using bi-exponential descriptions for axial power and eye power to model ocular growth from prenatal stages until adulthood. This model focuses on ocular and axial powers with closed-loop feedback based on retinal blur size (Chapter 4). It is the first model to consider the influence of the crystalline lens on refractive development and features a modular design for its feedback function and growth term in a way that can replicate various animal studies and clinical findings.

The emmetropization feedback has been extensively discussed in the literature as a central framework for explaining the mechanisms underlying myopia development. It says that myopia results from the disruption of the feedback mechanisms that normally regulate eye growth. Although the precise mechanisms of how retinal feedback causes the eye to grow are not fully understood, various observations support the retinal feedback.[146] These include the impact of near work, atropine treatment, corrective lenses, visual defocus, the contrast between outdoor and indoor activities, higher and peripheral aberrations,[147-149] chromatic aberrations,[55, 112, 150] optical properties of photoreceptors,[151] environmental light,[152] and spatial frequencies.[103,93] In Chapter 5, we assessed the impact of wavelength and defocus on contrast sensitivity function (CSF) for two groups of emmetropes and myopes. In the first version of our ODE model , we considered the simplest version of the feedback function, but in future stages, we want to modulate this with the general CSF, including factors such as luminance, spatial frequency, wavelength, and defocus. In the future, to develop a realistic model for eye growth, we need to thoroughly explore the influence of external factors by making the retinal feedback mechanism more complex.

Additionally, retinal feedback explains both FD and lens-induced myopia by highlighting the crucial role of the feedback loop in visual development. Disruptions in this loop, rather than retinal image blur, lead to myopia by preventing proper retinal focus.[103] Historically, experiments involving lid sutures inspired the hypothesis that blurred retinal images cause myopia. However, inducing myopia with high-power lenses has been inconsistent. It was found that lower-power lenses could induce myopia or hyperopia without noticeable blur, challenging the idea that only blurred images lead to myopia. Despite many researchers citing retinal blur as key in myopia

development, the evidence does not support this. Refractive error, rather than blur, is a more direct indicator for emmetropization and feedback.[103]

OCULAR COMPONENTS CONTRIBUTIONS TO REFRACTIVE ERROR

A detailed biometric evaluation of the eye can clarify the underlying reasons for age-related changes in refractive error and provide insights into mitigating the impact of refractive error-related visual impairment on quality of life and daily activities. Numerous studies have been conducted in this regard, some of which are highlighted below.

The relationship between ocular components, age, and ethnicity was assessed in a diverse cohort of children in the United States using data from the Orinda Longitudinal Study of Myopia Orinda Longitudinal Study of Myopia (OLSM) and CLEERE studies. These studies showed that older children tend to be more myopic across all ethnic groups, with children from the Tohono O'odham Nation (TON) having longer AL than white children.[153] Differences in CP and ACD were also noted across genders and ethnicities, with girls typically having greater CP and boys having deeper AC.[153]

In another study,[154] the ocular biometrics of individuals from a village in Myanmar were compared with those of Chinese Singaporeans. It was found that Burmese individuals have shorter AL compared to Chinese Singaporeans and Latinos. The ACD of Burmese individuals was like that of Chinese Singaporeans but shallower than that of the Los Angeles Latino Eye Study (LALES) population. In younger Burmese, VCD is a predictor of myopia.[154]

A comparison between the rate of myopia and ocular biometric data of the Mongolian population and East Asian groups showed that, unlike other East Asian populations, Mongolians do not show significant AL differences across age groups, indicating stability in ocular dimensions. Despite high literacy rates, the less intensive Mongolian education system might contribute to lower myopia rates compared to industrialized East Asia.[155]

The Los Angeles Latino Eye Study (LALES) addresses age-related refractive errors and finds significant differences in ocular measurements between men and women. Men generally have more emmetropic vision, longer axial lengths, and less lens opalescence. Older individuals have shallower AC, thicker, more opalescent lenses, and significant lens opalescence contributing to myopic shifts.[156]

Ocular component measurements in a Middle Eastern population (Jordanian adults) provided a comprehensive database on refractive error prevalence. The prevalence of myopia in Jordan is similar to the Western population but lower than in far Eastern societies. Linear regression analysis showed that AL has the strongest correlation with refractive error. Differences

in AL between individuals with refractive errors were mainly attributed to variations in the depth of the VC. Myopic eyes tended to have deeper VCs, whereas hyperopic eyes had shallower ones. LT generally decreased as the degree of myopia increased. Age-related changes included an increase in LT and a decrease in ACD.[157]

Findings on ACD vary between studies. The Shahroud Eye Cohort study focuses on these relationships among adults aged 40 to 64, reporting that axial length and CP are major contributors to refractive errors in severe cases (both high myopia and high hyperopia), with anterior segment components playing a more significant role in hyperopia.[158]

The Correction of Myopia Evaluation Trial (COMET) study which monitored children for 14 years and outlined that AL elongation plays a crucial role in the development and stabilization of juvenile-onset myopia.[159]

The Reykjavik Eye study investigated people over 55 years old to determine how refractive components like CP and LP, alongside AL, influence refractive error. The study reported that ocular refraction shows a statistically significant correlation not only with AL but also with LP, and to a lesser extent, CP. There was a considerable variation in crystalline LP, proposing its potential role in modulating ocular refraction during development.[160]

Based on the studies above, eye measurements like AL and VCD consistently have a link with refractive error. However, studies on other measurements such as CP, CCT, ACD, and LT may also have a relationship with refractive error. Some studies propose a connection between CP and refractive errors, while others do not find significant associations. So, there is some contradiction between the studies regarding the contribution of other ocular components like CP and LP.

In Chapter 6,[161] we present a method to understand how ocular components contribute to refractive error during infancy and childhood using the error propagation method explained in detail in the paper. Despite existing data on eye development, an analytical understanding of the mechanisms controlling spherical refraction is still lacking. This analysis helps to identify which ocular component variations are more associated with changes in refractive error in various population datasets.[161]

CONTRAST SENSITIVITY FUNCTION (CSF)

Vision, a fundamental human sense, encompasses key elements such as visual acuity (VA), contrast Sensitivity (CS), and color perception. VA measures how well the eye can see fine details using high-contrast symbols like letters or numbers. VA is determined by the visual angle formed by eye detail, which depends on the object's size and the viewing distance. It is often assessed using

the inverse of the Minimum Angle of Resolution (MAR), where a larger value of VA indicates better vision, while a smaller value of MAR indicates better vision. Normal vision is a logMAR of 0, which is also 1.0 in decimals or 6/6 in the Snellen chart. VA assessment is essential for diagnosing eye conditions, but it doesn't fully capture overall visual function and quality.[162-164]

CSF tests provide a comprehensive evaluation of spatial vision to determine how well an individual detects variations in light intensity. This assessment typically involves presenting stimuli with varying contrast levels to determine the smallest detectable contrast, known as the contrast threshold. There is an inverse relationship between CS and this threshold.

Evaluating CS provides insights into practical vision, particularly how individuals perceive objects of different sizes and contrasts in daily activities. This practical vision is essential for tasks like driving, reading, and recognizing faces, as it reflects both the optical properties of the eye and neural processing within the retina.[165] Studies have shown that CS can detect visual impairments even when VA remains normal, making it valuable in diagnosing conditions such as central serous chorioretinopathy and glaucoma.[166-168] Furthermore, conditions like cataracts, diabetes, and various disorders of the eye and nervous system can impact CS, highlighting its importance in assessing outcomes of surgeries such as cataract and refractive procedures. So, identifying and managing deficits in CS is essential for improving patients' overall quality of life.

The Michelson formula is a fundamental tool in vision science used to calculate CS, particularly with periodic patterns like sine-wave gratings. It is defined as the reciprocal of the threshold contrast.

$$CS = \frac{1}{\text{threshold contrast}} \qquad (1\text{-}4)$$

This definition highlights the relationship between the minimum detectable contrast and the visual system's sensitivity.

There are several factors affecting CSF and understanding these factors is essential for optimizing visual function and quality of life. Some of these factors are explained below.

Age-related CSF

The increasing number of elderly individuals in society presents a considerable challenge, as aging often leads to a decline in visual performance. This decline is evident in daily activities such as household tasks, workplace duties, and driving, where older adults typically struggle more than their younger counterparts. Extensive research aims to understand the causes of this gradual

deterioration in vision with age.[169]

Visual acuity generally starts to diminish after the age of 40, primarily due to changes in the eye's lens and decreased transparency. Although CS tests are common in clinical practice, further population-based studies are needed to investigate its correlation with age, gender, and geographic variations.[169] While it is generally accepted that CS decreases with age, research findings are inconsistent. Some studies report no changes, others note declines across all spatial frequencies, and some observe losses only at specific frequencies. These discrepancies are often due to variations in study methodologies and testing systems.[170]

Research focusing on an aging population of white males aged 35-80 has shown a decline in CS across various spatial frequencies (3, 6, 12, 18 cycles per degree), with higher frequencies being more affected.[170] The reduction in CS with age may result from increased internal noise (such as visual distortions) or a reduced ability to detect targets within this noise, necessitating a higher signal-to-noise ratio (SNR) for detection. Internal noise can stem from optical factors like smaller pupil size or lens densification, as well as neural factors such as increased spontaneous neural activity.[171]

Impact of refractive error (best corrected) on CSF

Refractive errors such as myopia, hyperopia, and astigmatism can significantly affect CSF, and this relationship is further influenced by age-related changes in the eye. Individuals with hyperopia often demonstrate diminished VA, indicating a refractive error or other ocular conditions. People with mild hyperopia (up to 2 D) typically maintain normal CS, whereas those with severe hyperopia (5 D or more) often experience a marked decrease in their ability to perceive contrasts.[172]

A previous study investigated how age and refractive errors affect vision in 92 healthy Chinese adults. The findings revealed that advancing age is linked to increased hyperopia, poorer near vision, and reduced CS. Age remains a significant factor impacting CS even after adjusting for refractive error, gender, and types of vision tests. These findings emphasize the critical role of age in determining VA in this cohort.[173]

Additionally, severe myopia and astigmatism reduce the ability to distinguish contrasts because corrective lenses cause retinal images to appear smaller. This highlights the significance of comprehending these factors when assessing visual performance, especially in clinical contexts. Previous literature assessed the impact of severe myopia on CS in central vision, revealing that myopes generally perceived a lower contrast, especially in discerning negative contrasts. This

deficit tends to worsen with increased myopia severity, despite efforts to correct vision.[174]

Furthermore, research has shown that people with high levels of myopia who wear glasses often struggle with contrast clarity, possibly due to optical aberrations or early retinal problems. Switching to contact lenses can improve CS, especially for those with severe myopia, but these cannot completely correct retina impairments.[175]

Impact of defocus on CSF

The literature indicates that visual accommodation, the eye's ability to focus, is influenced by retinal defocus.[57, 61, 126, 176] Studies show that specific ocular aberrations affect static accommodation, and variations in SA may play a role in myopia development. Theoretical research suggests that negative SA in an accommodated eye, along with a slight lag in accommodation (negative defocus), might enhance letter detection despite reducing image contrast, potentially promoting eye growth, and contributing to myopia. Thus, examining the effect of defocus on CSF could be crucial for understanding vision development and developing interventions for vision disorders.[177]

Several studies investigated the impact of defocus on the CSF, revealing that defocus leads to a reduction in CSF, especially at higher spatial frequencies.[178, 179] Moreover, research shows that the depth of focus tends to increase with age, especially for a 4-mm pupil. However, CS at high defocus levels (12 diopters) declines with age, though less sharper than at optimal focus. Increased OAs in aging eyes may mitigate defocus effects, suggesting older individuals may be less affected by defocus compared to younger ones.[180]

Chromatic CSF

Previous studies demonstrated that normal eye development in chicks is critically dependent on visual stimulation. Continuous FD leads to severe myopia, while intermittent exposure to environments with restricted spatial frequencies can effectively mitigate this condition. These findings emphasize the significance of specific visual cues, such as mid-range spatial frequencies and adequate contrast, in promoting normal eye growth in chicks. The potential involvement of chromatic aberration cues has been suggested as a contributing factor in this process.[181] Hence, understanding the effect of chromaticity on CS can be essential.

Human color vision includes luminance and chromatic dimensions, allowing for contrasts in terms of luminance or chromaticity. Achromatic contrast relates to differences in luminance, perceived as variations in lightness, like black-and-white photographs. In contrast, chromatic contrast relates to differences in chromaticity along the chromatic dimensions rather than

luminance, forming the complement to achromatic contrast. Thus, while achromatic contrast is about luminance differences, chromatic contrast involves differences in color properties.[182]

Achromatic and chromatic CSFs have been extensively studied.[183-185] Various analytical models of CSF have been proposed, primarily focusing on frequency effects. However, luminance has the most significant impact on pattern detection. Barten and Daly developed comprehensive CSF models incorporating luminance effects through complex formulas fitted to data from previous studies. Barten's model integrates fundamental concepts like optical transfer functions (OTFs) and psychometric functions, successfully predicting many historical CSF measurements.[186]

In 1975, Cavonius et al. assessed CS using individual color filters, specifically Wratten filters, across spatial frequencies ranging from 0 to 32 cycles per degree (cpd). Their findings indicated that both red and green filters exhibited similar CSFs, whereas sensitivity was notably reduced for the blue filter. This reduction is believed to be associated with chromatic aberration in the human eye, which affects how different colors are perceived and distinguished at varying spatial frequencies.[187]

REFERENCES

1. *Oyster CW. The human eye: structure and function. (No Title). 1999.*
2. *Regal S, Troughton J, Djenizian T, Ramuz M. Biomimetic models of the human eye, and their applications. Nanotechnology. 2021;32(30):302001.*
3. *Forrester JV, Dick AD, McMenamin PG, Roberts F, Pearlman E. The eye: basic sciences in practice: Elsevier Health Sci; 2015.*
4. *Kanski Jack J, Brad B. Clin. Ophthalmol -A Systematic Approach. pg. 2007;536.*
5. *Wyszecki G, Stiles WS. Color science: concepts and methods, quantitative data and formulae: John wiley & sons; 2000.*
6. *Bergmanson JP, Burns AR, Walker MK. Central versus peripheral thickness in the human cornea explained. Cont Lens Anterior Eye. 2024 Jun 1;47(3):102165.*
7. *Barbero S. Refractive power of a multilayer rotationally symmetric model of the human cornea and tear film. J. Opt. Soc. Am. A. 2006;23(7):1578-85.*
8. *Marcos S. Image quality of the human eye. Int Ophthalmol Clin. 2003 Apr 1;43(2):43-62.*
9. *Davis WR, Raasch TW, Mitchell GL, Mutti DO, Zadnik K. Corneal asphericity and apical curvature in children: a cross-sectional and longitudinal evaluation. Invest Ophthalmol Vis Sci. 2005 Jun 1;46(6):1899-906.*
10. *Calossi A. Corneal asphericity and spherical aberration. J Refract Surg. 2007 May 1;23(5):505-14.*
11. *Gatinel D, Haouat M, Hoang-Xuan T. Etude des paramètres permettant la description mathématique de l'asphéricité cornéenne. J Fr Ophtalmol. 2002;25:81-90.*
12. *Kiely PM, Smith G, Carney LG. The mean shape of the human cornea. Opt. Acta. 1982;29(8):1027-40.*
13. *Carney LG, Mainstone JC, Henderson BA. Corneal topography and myopia. A cross-sectional study. Invest. Ophthalmol. Vis. Sci. 1997;38(2):311-20.*
14. *Rozema J, Dankert S, Iribarren R. Emmetropization and nonmyopic eye growth. Surv. Ophthalmol. 2023;68(4):759-83.*
15. *Dubbelman M, Van der Heijde G, Weeber HA. Change in shape of the aging human crystalline lens with accommodation. Vis. Res. 2005;45(1):117-32.*
16. *Charman W. Physiological optics in 2008: standing on Helmholtz's shoulders. Wiley Online Libr. 2009. pp. 209-10.*
17. *Glasser A, Campbell MC. Presbyopia and the optical changes in the human crystalline lens with age. Vis. Res. 1998;38(2):209-29.*
18. *Saunders KJ, McCulloch DL, Shepherd A, Wilkinson AG. Emmetropisation following preterm birth. Br. J. Ophthalmol. 2002;86(9):1035-40.*
19. *Brown NP, Koretz JF, Bron AJ. The development and maintenance of emmetropia. Eye. 1999;13(1):83-92.*
20. *Troilo D. Neonatal eye growth and emmetropisation—a literature review. Eye. 1992;6(2):154-60.*
21. *Hunter JJ, Campbell MC, Kisilak ML, Irving EL. Blur on the retina due to higher-order aberrations: Comparison of eye growth models to experimental data. J Vis. 2009;9(6):12-.*
22. *Pennie FC, Wood IC, Olsen C, White S, Charman WN. A longitudinal study of the biometric and refractive changes in full-term infants during the first year of life. Vis Res. 2001;41(21):2799-810.*
23. *Saunders KJ, Woodhouse JM, Westall CA. Emmetropisation in human infancy: rate of change is related to initial refractive error. Vis Res. 1995;35(9):1325-8.*
24. *Mutti DO, Mitchell GL, Jones LA, Friedman NE, Frane SL, Lin WK, et al. Axial growth and changes in lenticular and corneal power during emmetropization in infants. Invest. Ophthalmol. Vis. Sci. 2005;46(9):3074-80.*
25. *Straub M. Über die Atiologie der Brechungsanomalien des Auges und den Ursprung der Emmetropie. Albrecht von Graefes Arch. Clin. Exp. Ophthalmol. 1909;70:130-99.*
26. *Wallman J, Winawer J. Homeostasis of eye growth and the question of myopia. Neuron. 2004;43(4):447-68.*
27. *Hung GK, Ciuffreda KJ. A unifying theory of refractive error development. Bull. Math. Biol. 2000;62(6):1087-108.*
28. *Gwiazda J, Thorn F, Bauer J, Held R. Emmetropization and the progression of manifest refraction in children followed from infancy to puberty. Clin. Vis. Sci. 1993;8(4):337-44.*
29. *Mum DO, Zadnik K. The utility of three predictors of childhood myopia: a Bayesian analysis. Vis. Res. 1995;35(9):1345-52.*
30. *Iribarren R, Morgan IG, Chan YH, Lin X, Saw S-M. Changes in lens power in Singapore Chinese children during refractive development. Invest. Ophthalmol. Vis. Sci. 2012;53(9):5124-30.*
31. *Rosenfield M. Refractive status of the eye. In: Borish's Clin. Refraction, 2006. pp. 3-34.*
32. *Fledelius HC, Christensen AC. Reappraisal of the human ocular growth curve in fetal life, infancy, and early childhood. Br. J. Ophthalmol. 1996;80(10):918-21.*
33. *Cook A, White S, Batterbury M, Clark D. Ocular growth and refractive error development in premature infants without retinopathy of prematurity. Invest. Ophthalmol. Vis. Sci. 2003;44(3):953-60.*
34. *LARSEN JS. The sagittal growth of the eye: IV. Ultrasonic measurement of the axial length of the eye from birth to puberty. Acta Ophthalmol. 1971;49(6):873-86.*
35. *York MA, Mandell RB. A new calibration system for photokeratoscopy. Part II—Corneal contour measurements. Optom. Vis. Sci. 1969;46(11):818-25.*

36. Augusteyn RC, Nankivil D, Mohamed A, Maceo B, Pierre F, Parel J-M. Human ocular biometry. Exp. Eye Res. 2012;102:70-5.
37. Sorsby A, Leary G, Richards MJ. Correlation ametropia and component ametropia. Vis. Res. 1962;2(9-10):309-13.
38. Grosvenor T, Goss DA. Role of the cornea in emmetropia and myopia. Optom. Vis. Sci. 1998;75(2):132-45.
39. Wiesel TN, Hubel DH. Extent of recovery from the effects of visual deprivation in kittens. J. Neurophysiol. 1965;28(6):1060-72.
40. Rozema JJ. Refractive development I: biometric changes during emmetropisation. Ophthalmic Physiol. Opt. 2023;43(3):347-67.
41. Inagaki Y. The rapid change of corneal curvature in the neonatal period and infancy. Arch. Ophthalmol. 1986;104(7):1026-7.
42. Mayer DL, Hansen RM, Moore BD, Kim S, Fulton AB. Cycloplegic refractions in healthy children aged 1 through 48 months. Arch. Ophthalmol. 2001;119(11):1625-8.
43. Ehrlich DL, Braddick OJ, Atkinson J, Anker S, Weeks F, Hartley T, et al. Infant emmetropization: longitudinal changes in refraction components from nine to twenty months of age. Optom. Vis. Sci. 1997;74(10):822-43.
44. Hirsch M, Weymouth F. Prevalence of refractive anomalies. Refractive Anomalies: Refractive Anomalies: Res. Clin. Appl. 1991:15-38.
45. Saunders KJ. Early refractive development in humans. Surv. Ophthalmol. 1995;40(3):207-16.
46. Farzanfar A, Rozema JJ. Bi-exponential description for different forms of refractive development. J. Vis. 2024;24(7):3-.
47. Fledelius HC. Ophthalmic changes from age of 10 to 18 years: A Longitudinal study of sequels to low birth weight.: III. Ultrasound oculometry and keratometry of anterior eye segment. Acta ophthalmol. 1982;60(3):393-402.
48. Grosvenor T, Scott R. Comparison of refractive components in youth-onset and early adult-onset myopia. Optom. Vis. Sci. 1991;68(3):204-9.
49. Brown N. The change in lens curvature with age. Exp. Eye Res. 1974;19(2):175-83.
50. Hirsch MJ. Changes in refractive state after the age of forty-five. Optom. Vis. Sci. 1958;35(5):229-37.
51. Leighton D, Tomlinson A. Changes in axial length and other dimensions of the eyeball with increasing age. Acta ophthalmol. 1972;50(6):815-26.
52. Ong E, Ciuffreda K. Accommodation, Nearwork, and Myopia: Optometric Extension Program Foundation. Inc, Santa Ana, CA. 1997:76-96.
53. Christensen AM, Wallman J. Evidence that increased scleral growth underlies visual deprivation myopia in chicks. Invest. Ophthalmol. Vis. Sci. 1991;32(7):2143-50.
54. Siegwart Jr JT, Norton TT. Regulation of the mechanical properties of tree shrew sclera by the visual environment. Vis Res. 1999;39(2):387-407.
55. Swiatczak B, Schaeffel F. Myopia: why the retina stops inhibiting eye growth. Sci Rep. 2022;12(1):21704.
56. Smith III EL. Optical treatment strategies to slow myopia progression: effects of the visual extent of the optical treatment zone. Exp. Eye Res. 2013;114:77-88.
57. Diether S, Schaeffel F. Local changes in eye growth induced by imposed local refractive error despite active accommodation. Vis Res. 1997;37(6):659-68.
58. Irving E, Callender M, Sivak J. Inducing myopia, hyperopia, and astigmatism in chicks. Optom. Vis. Sci. 1991;68(5):364-8.
59. Schaeffel F, Howland H. Visual optics in normal and ametropic chickens. Clin. Vis. Sci. 1988;3(2):83-&.
60. Amedo AO, Norton TT. Visual guidance of recovery from lens-induced myopia in tree shrews (Tupaia glis belangeri). Ophthalmic Physiol. Opt. 2012;32(2):89-99.
61. Hung L-F, Crawford ML, Smith EL. Spectacle lenses alter eye growth and the refractive status of young monkeys. Nat. Med. 1995;1(8):761-5.
62. Zhu X, McBrien NA, Smith EL, Troilo D, Wallman J. Eyes in various species can shorten to compensate for myopic defocus. Invest. Ophthalmol. Vis. Sci. 2013;54(4):2634-44.
63. Smith EL, Hung L-F, Huang J, Blasdel TL, Humbird TL, Bockhorst KH. Effects of optical defocus on refractive development in monkeys: evidence for local, regionally selective mechanisms. Invest Ophthalmol Vis Sci. 2010;51(8):3864-73.
64. Kee C-S, Hung L-F, Qiao-Grider Y, Roorda A, Smith EL. Effects of optically imposed astigmatism on emmetropization in infant monkeys. Invest Ophthalmol Vis Sci. 2004;45(6):1647-59.
65. Schmid KL, Wildsoet CF. Natural and imposed astigmatism and their relation to emmetropization in the chick. Exp. Eye Res. 1997;64(5):837-47.
66. McLean RC, Wallman J. Severe astigmatic blur does not interfere with spectacle lens compensation. Invest. Ophthalmol. Vis. Sci. 2003;44(2):449-57.
67. Jones LA, Mitchell GL, Mutti DO, Hayes JR, Moeschberger ML, Zadnik K. Comparison of ocular component growth curves among refractive error groups in children. Invest. Ophthalmol. Vis. Sci. 2005;46(7):2317-27.
68. Castagno VD, Fassa AG, Vilela MAP, Meucci RD, Resende DPM. Prevalência de hipermetropia e fatores associados em escolares do ensino fundamental. Ciênc. Saúde Colet. 2015;20:1449-58.
69. Ip JM, Robaei D, Kifley A, Wang JJ, Rose KA, Mitchell P. Prevalence of hyperopia and associations with eye findings in 6-and 12-year-olds. Ophthalmol. 2008;115(4):678-85. e1.
70. Aaron M, Solley W, Broocker G. CHAPTER 1-General Eye Examination. Palay DA, Krachmer JHBT-PCO (Second E, editors Philadelphia: Mosby. 2005.

71. Dhanjal S. Treasure Island (FL): StatPearls Publishing Copyright© 20232023.
72. Flitcroft DI, He M, Jonas JB, Jong M, Naidoo K, Ohno-Matsui K, et al. IMI–defining and classifying myopia: a proposed set of standards for clinical and epidemiologic studies. Invest. Ophthalmol. Vis. Sci. 2019;60(3):M20-M30.
73. Verkicharla PK, Ohno-Matsui K, Saw SM. Current and predicted demographics of high myopia and an update of its associated pathological changes. Ophthalmic Physiol. Opt. 2015;35(5):465-75.
74. Holden BA, Fricke TR, Wilson DA, Jong M, Naidoo KS, Sankaridurg P, et al. Global prevalence of myopia and high myopia and temporal trends from 2000 through 2050. Ophthalmol. 2016;123(5):1036-42.
75. Mutti DO, Hayes JR, Mitchell GL, Jones LA, Moeschberger ML, Cotter SA, et al. Refractive error, axial length, and relative peripheral refractive error before and after the onset of myopia. Invest. Ophthalmol. Vis. Sci. 2007;48(6):2510-9.
76. Burns R. Hereditary myopia in identical twins. Br. J. Ophthalmol. 1949;33(8):491.
77. Jablonski W. A contribution to the heredity of refraction in human eyes. Arch Augenheilk. 1922;91:308-28.
78. Knobloch WH, Leavenworth NM, Bouchard TJ, Eckert ED. Eye findings in twins reared apart. Ophthalmic Pediatr. Genet. 1985;5(1-2):59-66.
79. Tedja MS, Haarman AE, Meester-Smoor MA, Kaprio J, Mackey DA, Guggenheim JA, et al. IMI–myopia genetics report. Invest. Ophthalmol. Vis. Sci. 2019;60(3):M89-M105.
80. Mutti DO, Mitchell GL, Moeschberger ML, Jones LA, Zadnik K. Parental myopia, near work, school achievement, and children's refractive error. Invest. Ophthalmol. Vis. Sci. 2002;43(12):3633-40.
81. Pan CW, Ramamurthy D, Saw SM. Worldwide prevalence and risk factors for myopia. Ophthalmic Physiol. Opt. 2012;32(1):3-16.
82. Morgan A, Young R, Narankhand B, Chen S, Cottriall C, Hosking S. Prevalence rate of myopia in schoolchildren in rural Mongolia. Optom. Vis. Sci. 2006;83(1):53-6.
83. Young FA, Leary GA, Baldwin WR, West DC, Box RA, Harris E, et al. The transmission of refractive errors within Eskimo families. Optom. Vis. Sci. 1969;46(9):676-85.
84. Jung S-K, Lee JH, Kakizaki H, Jee D. Prevalence of myopia and its association with body stature and educational level in 19-year-old male conscripts in Seoul, South Korea. Invest. Ophthalmol. Vis. Sci.2012;53(9):5579-83.
85. Morgan IG, Wu P-C, Ostrin LA, Tideman JWL, Yam JC, Lan W, et al. IMI risk factors for myopia. Invest. Ophthalmol. Vis. Sci. 2021;62(5):3-.
86. Guggenheim JA, Northstone K, McMahon G, Ness AR, Deere K, Mattocks C, et al. Time outdoors and physical activity as predictors of incident myopia in childhood: a prospective cohort study. Invest. Ophthalmol. Vis. Sci. 2012;53(6):2856-65.
87. Rose KA, Morgan IG, Ip J, Kifley A, Huynh S, Smith W, et al. Outdoor activity reduces the prevalence of myopia in children. Ophthalmol. 2008;115(8):1279-85.
88. He M, Xiang F, Zeng Y, Mai J, Chen Q, Zhang J, et al. Effect of time spent outdoors at school on the development of myopia among children in China: a randomized clinical trial. Jama. 2015;314(11):1142-8.
89. French AN, Morgan IG, Mitchell P, Rose KA. Risk factors for incident myopia in Australian schoolchildren: the Sydney adolescent vascular and eye study. Ophthalmol. 2013;120(10):2100-8.
90. Dirani M, Tong L, Gazzard G, Zhang X, Chia A, Young TL, et al. Outdoor activity and myopia in Singapore teenage children. Br. J. Ophthalmol. 2009;93(8):997-1000.
91. Jones LA, Sinnott LT, Mutti DO, Mitchell GL, Moeschberger ML, Zadnik K. Parental history of myopia, sports and outdoor activities, and future myopia. Invest. Ophthalmol. Vis. Sci. 2007;48(8):3524-32.
92. Lingham G, Mackey DA, Lucas R, Yazar S. How does spending time outdoors protect against myopia? A review. Br. J. Ophthalmol. 2020;104(5):593-9.
93. Flitcroft DI, Harb EN, Wildsoet CF. The spatial frequency content of urban and indoor environments as a potential risk factor for myopia development. Invest. Ophthalmol. Vis. Sci. 2020;61(11):42-.
94. Grosvenor T. A review and a suggested classification system for myopia on the basis of age-related prevalence and age of onset. Optom. Vis. Sci.1987;64(7):545-54.
95. GOSS DA, WINKLER RL. Progression of myopia in youth: age of cessation. Optom. Vis. Sci.1983;60(8):650-8.
96. Fledelius H. Myopia of prematurity, clinical patterns. Ophthalmic Lit 1996;3(49):211.
97. Fledelius HC. Myopia of prematurity, clinical patterns: A follow-up of Danish children now aged 3–9 years. Acta Ophthalmol. Scand. 1995;73(5):402-6.
98. Lam DS, Fan DS, Chan W-M, Tam BS, Kwok AK, Leung AT, et al. Prevalence and characteristics of peripheral retinal degeneration in Chinese adults with high myopia: a cross-sectional prevalence survey. Optom. Vis. Sci. 2005;82(4):235-8.
99. Morgan R, Speakman J, Grimshaw S. Inuit myopia: an environmentally induced" epidemic"? CMAJ. 1975;112(5):575.
100. SORSBY A. Transmission of refractive errors within Eskimo families. Optom. Vis. Sci. 1970;47(3):244-6.
101. Gwiazda J, Hyman L, Hussein M, Everett D, Norton TT, Kurtz D, et al. A randomized clinical trial of progressive addition lenses versus single vision lenses on the progression of myopia in children. Invest. Ophthalmol. Vis. Sci. 2003;44(4):1492-500.
102. Fan DS, Lam DS, Chan CK, Fan AH, Cheung EY, Rao SK. Topical atropine in retarding myopic progression and axial length growth in children with moderate to severe myopia: a pilot study. Jpn. J. Ophthalmol. 2007;51:27-33.
103. Medina A. The cause of myopia development and progression: theory, evidence, and treatment. Surv. Ophthalmol. 2022;67(2):488-509.
104. Renu J. Basic Ophthalmology. 4/e ed2009.
105. Diether S, Gekeler F, Schaeffel F. Changes in contrast sensitivity induced by defocus and their possible relations

to emmetropization in the chicken. Invest. Ophthalmol. Vis. Sci. 2001;42(12):3072-9.
106. Ashby R. Animal studies and the mechanism of myopia—protection by light? Optom. Vis. Sci. 2016;93(9):1052-4.
107. Smith EL, Hung L-F, Huang J. Protective effects of high ambient lighting on the development of form-deprivation myopia in rhesus monkeys. Invest. Ophthalmol. Vis. Sci. 2012;53(1):421-8.
108. Cohen Y, Peleg E, Belkin M, Polat U, Solomon AS. Ambient illuminance, retinal dopamine release and refractive development in chicks. Exp. Eye Res. 2012;103:33-40.
109. Chakraborty R, Ostrin LA, Nickla DL, Iuvone PM, Pardue MT, Stone RA. Circadian rhythms, refractive development, and myopia. Ophthal Physiol Opt. 2018;38(3):217-45.
110. Liu J, Pendrak K, Capehart C, Sugimoto R, Schmid GF, Stone RA. Emmetropisation under continuous but non-constant light in chicks. Exp Eye Res.
111. Troilo D, Smith EL, Nickla DL, Ashby R, Tkatchenko AV, Ostrin LA, et al. IMI–Report on experimental models of emmetropization and myopia. Invest. Ophthalmol. Vis. Sci. 2019;60(3):M31-M88.
112. Gawne TJ, Grytz R, Norton TT. How chromatic cues can guide human eye growth to achieve good focus. J Vis. 2021;21(5):11-.
113. Stiles WS, Crawford B. The luminous efficiency of rays entering the eye pupil at different points. Proceedings of the Royal Society of London Series B, Containing Papers of a Biological Character. 1933;112(778):428-50.
114. Fincham EF. The accommodation reflex and its stimulus. Br J Ophthalmol.1951;35(7):381.
115. Park TW, Winawer J, Wallman J. Further evidence that chick eyes use the sign of blur in spectacle lens compensation. Vis Res. 2003;43(14):1519-31.
116. Zheleznyak L, Liu C, Winter S. Chromatic cues for the sign of defocus in the peripheral retina. Biomed Opt Exp. 2024;15(9):5098-114.
117. Zhu X, Kang P, Troilo D, Benavente-Perez A. Temporal properties of positive and negative defocus on emmetropization. Sci Rep. 2022;12(1):3582.
118. Raviola E, Wiesel TN. An animal model of myopia. N Engl J Med. 1985;312(25):1609-15.
119. Wallman J, Turkel J, Trachtman J. Extreme myopia produced by modest change in early visual experience. Science. 1978;201(4362):1249-51.
120. McBRIEN NA, Gentle A, Cottriall C. Optical correction of induced axial myopia in the tree shrew: implications for emmetropization. Optom Vis Sci. 1999;76(6):419-27.
121. Irving E, Sivak J, Callender M. Refractive plasticity of the developing chick eye. Ophthalmic Physiol Opt. 1992;12(4):448-56.
122. Wiesel TN, Raviola E. Myopia and eye enlargement after neonatal lid fusion in monkeys. Nature. 1977;266(5597):66-8.
123. Bartmann M, Schaeffel F. A simple mechanism for emmetropization without cues from accommodation or colour. Vis Res. 1994;34(7):873-6.
124. Smith III EL, Hung L-F. Form-deprivation myopia in monkeys is a graded phenomenon. Vis Res. 2000;40(4):371-81.
125. Smith III EL, Hung L-F. The role of optical defocus in regulating refractive development in infant monkeys. Vis Res. 1999;39(8):1415-35.
126. Schaeffel F, Glasser A, Howland HC. Accommodation, refractive error and eye growth in chickens. Vis Res. 1988;28(5):639-57.
127. Read SA, Collins MJ, Sander BP. Human optical axial length and defocus. Invest. Ophthalmol. Vis. Sci. 2010;51(12):6262-9.
128. Graham B, Judge S. The effects of spectacle wear in infancy on eye growth and refractive error in the marmoset (Callithrix jacchus). Vis Res. 1999;39(2):189-206.
129. Wang D, Chun RKM, Liu M, Lee RPK, Sun Y, Zhang T, et al. Optical defocus rapidly changes choroidal thickness in schoolchildren. PloS one. 2016;11(8):e0161535.
130. Chiang STH, Phillips JR, Backhouse S. Effect of retinal image defocus on the thickness of the human choroid. Ophthalmic Physiol Opt. 2015;35(4):405-13.
131. Schaeffel F, Troilo D, Wallman J, Howland HC. Developing eyes that lack accommodation grow to compensate for imposed defocus. Vis neurosci. 1990;4(2):177-83.
132. Wildsoet CF, Chia A, Cho P, Guggenheim JA, Polling JR, Read S, et al. IMI–interventions for controlling myopia onset and progression report. Invest. Ophthalmol. Vis. Sci. 2019;60(3):M106-M31.
133. Chung K, Mohidin N, O'Leary DJ. Undercorrection of myopia enhances rather than inhibits myopia progression. Vis Res. 2002;42(22):2555-9.
134. Van Alphen G. On Emmetropia and Ametropia (supplementum ad Ophthalmogica, Vol. 142). S. Karger, Basel & New York, 1961.
135. Mutti DO, Sinnott LT, Mitchell GL, Jordan LA, Friedman NE, Frane SL, et al. Ocular component development during infancy and early childhood. Optom. Vis. Sci. 2018;95(11):976-85.
136. Steiger A. Die Entstehung der spharischen Refraktionen des menschlichen Auges: S. Karger; 1913.
137. Wibaut F. Über die Emmetropisation und den Ursprung der sphärischen Refraktionsanomalien. Graefes Arch. Clin. Exp. Ophthalmol. 1926;116:596-612.
138. Benavente-Pérez A, Nour A, Troilo D. Axial eye growth and refractive error development can be modified by exposing the peripheral retina to relative myopic or hyperopic defocus. Invest. Ophthalmol. Vis. Sci. 2014;55(10):6765-73.
139. Cottriall CL, McBrien NA. The M1 muscarinic antagonist pirenzepine reduces myopia and eye enlargement in

the tree shrew. Invest. Ophthalmol. Vis. Sci. 1996;37(7):1368-79.
140. Norton T, Siegwart Jr J. Animal models of emmetropization: matching axial length to the focal plane. J Am Optom Assoc. S1995;66(7):405-14.
141. Smith E, Harwerth R, Crawford M. Spatial contrast sensitivity deficits in monkeys produced by optically induced anisometropia. Invest. Ophthalmol. Vis. Sci. 1985;26(3):330-42.
142. Medina A. A model for emmetropization: predicting the progression of ametropia. Ophthalmologica. 1987;194(2-3):133-9.
143. Medina A, Fariza E. Emmetropization as a first-order feedback system. Vis Res. 1993;33(1):21-6.
144. Schaeffel F, Howland HC. Mathematical model of emmetropization in the chicken. JOSA A. 1988;5(12):2080-6.
145. Hung GK, Ciuffreda KJ. Model of human refractive error development. Curr Eye Res. 1999;19(1):41-52.
146. Gajjar S, Ostrin LA. A systematic review of near work and myopia: measurement, relationships, mechanisms and clinical corollaries. Acta Ophthalmol. 2022;100(4):376-87.
147. Hughes RP, Vincent SJ, Read SA, Collins MJ. Higher order aberrations, refractive error development and myopia control: a review. Clin Exp Optom. 2020;103(1):68-85.
148. Romashchenko D, Rosén R, Lundström L. Peripheral refraction and higher order aberrations. Clin Exp Optom. 2020;103(1):86-94.
149. Zheleznyak L. Peripheral blur may provide the eye with a cue for the sign of defocus. J Vis. 2023;23(11):83-.
150. Rucker FJ, Wallman J. Chick eyes compensate for chromatic simulations of hyperopic and myopic defocus: evidence that the eye uses longitudinal chromatic aberration to guide eye-growth. Vis Res. 2009;49(14):1775-83.
151. Vohnsen B. Geometrical scaling of the developing eye and photoreceptors and a possible relation to emmetropization and myopia. Vis Res. 2021;189:46-53.
152. Cohen Y, Iribarren R, Ben-Eli H, Massarwa A, Shama-Bakri N, Chassid O. Light intensity in nursery schools: a possible factor in refractive development. Asia Pac J Ophthalmol. 2022;11(1):66-71.
153. Twelker JD, Mitchell GL, Messer DH, Bhakta R, Jones LA, Mutti DO, et al. Children's ocular components and age, gender, and ethnicity. Optom Vis Sci. 2009;86(8):918-35.
154. Warrier S, Wu HM, Newland HS, Muecke J, Selva D, Aung T, et al. Ocular biometry and determinants of refractive error in rural Myanmar: the Meiktila Eye Study. Br J Ophthalmol. 2008;92(12):1591-4.
155. Wickremasinghe S, Foster PJ, Uranchimeg D, Lee PS, Devereux JG, Alsbirk PH, et al. Ocular biometry and refraction in Mongolian adults. Invest. Ophthalmol. Vis. Sci. 2004;45(3):776-83.
156. Shufelt C, Fraser-Bell S, Ying-Lai M, Torres M, Varma R. Refractive error, ocular biometry, and lens opalescence in an adult population: the Los Angeles Latino Eye Study. Invest. Ophthalmol. Vis. Sci. 2005;46(12):4450-60.
157. Mallen EA, Gammoh Y, Al-Bdour M, Sayegh FN. Refractive error and ocular biometry in Jordanian adults. Ophthalmic Physiol Opt. 2005;25(4):302-9.
158. Hashemi H, Khabazkhoob M, Emamian MH, Shariati M, Miraftab M, Yekta A, et al. Association between refractive errors and ocular biometry in Iranian adults. J Ophthalmic Vis Res. 2015;10(3):214.
159. Hou W, Norton TT, Hyman L, Gwiazda J, Group C. Axial elongation in myopic children and its association with myopia progression in the correction of myopia evaluation trial. Eye & contact lens. 2018;44(4):248-59.
160. Olsen T, Arnarsson A, Sasaki H, Sasaki K, Jonasson F. On the ocular refractive components: the Reykjavik Eye Study. Acta Ophthalmol Scand. 2007;85(4):361-6.
161. Farzanfar A, Lockett-Ruiz V, Navarro R, Koppen C, Rozema JJ. The influence of variations in ocular biometric and optical parameters on differences in refractive error. Ophthalmic Physiol. Opt. 2024;44(5):1000-9.
162. Colenbrander A. The historical evolution of visual acuity measurement. Vis Impairment Res. 2008;10(2-3):57-66.
163. Ricci F, Cedrone C, Cerulli L. Standardized measurement of visual acuity. Ophthalmic Epidemiol. 1998;5(1):41-53.
164. Universale CO. Visual acuity measurement standard. Visual Functions Committee. 1984.
165. Sieiro RdO, Coelho LM, Boas PCV, Fonseca SC, Souza SR, Guimarães TdP. Contrast sensitivity assessment in different age group in medium and high spatial frequency. Rev Bras Oftalmol. 2016;75:296-9.
166. Chylack L, Padhye N, Khu PM, Wehner C, Wolfe J, McCarthy D, et al. Loss of contrast sensitivity in diabetic patients with LOCS II classified cataracts. Br J Ophthalmol. 1993;77(1):7-11.
167. Georgakopoulos CD, Eliopoulou MI, Exarchou AM, Tzimis V, Pharmakakis NM, Spiliotis BE. Decreased contrast sensitivity in children and adolescents with type 1 diabetes mellitus. J Pediatr Ophthalmol Strabismus. 2011;48(3):92-7.
168. Dosso AA, Bonvin ER, Morel Y, Golay A, Assal JP, Leuenberger PM. Risk factors associated with contrast sensitivity loss in diabetic patients. Graefes Arch Clin Exp Ophthalmol. 1996;234:300-5.
169. Joulan K, Brémond R, Hautière N. Towards an Analytical Age-Dependent Model of Contrast Sensitivity Functions for an Ageing Society. Sci World J. 2015;2015(1):625034.
170. Sia DI, Martin S, Wittert G, Casson RJ. Age-related change in contrast sensitivity among Australian male adults: Florey Adult Male Ageing Study. Acta Ophthalmol. 2013;91(4):312-7.
171. Allard R, Renaud J, Molinatti S, Faubert J. Contrast sensitivity, healthy aging and noise. Vis Res. 2013;92:47-52.
172. Ilyas A, Fatima D. Comparison of contrast sensitivity in low and high Hypermetropes. Ophthalmol Pak .2023;13(1):21-5.
173. Li Z, Hu Y, Yu H, Li J, Yang X. Effect of age and refractive error on quick contrast sensitivity function in Chinese

adults: a pilot study. Eye. 2021;35(3):966-72.
174. Stoimenova BD. The effect of myopia on contrast thresholds. Invest Ophthalmol Vis Sci. 2007;48(5):2371-4.
175. Liou S-W, Chiu C-J. Myopia and contrast sensitivity function. Curr Eye Res. 2001;22(2):81-4.
176. Ohlendorf A, Schaeffel F. Contrast adaptation induced by defocus–A possible error signal for emmetropization? Vis Res. 2009;49(2):249-56.
177. Del Águila-Carrasco AJ, Kruger PB, Lara F, López-Gil N. Aberrations and accommodation. Clin. Exp. Optom. 2020;103(1):95-103.
178. Charman W. Effect of refractive error in visual tests with sinusoidal gratings. Br J Physiol Opt. 1979;33(2):10-20.
179. Kay C, Morrison JD. A quantitative investigation into the effects of pupil diameter and defocus on contrast sensitivity for an extended range of spatial frequencies in natural and homatropinized eyes. Ophthalmic Physiol Opt. 1987;7(1):21-30.
180. Nio Y, Jansonius N, Fidler V, Geraghty E, Norrby S, Kooijman A. Age-related changes of defocus-specific contrast sensitivity in healthy subjects. Ophthalmic Physiol Opt. 2000;20(4):323-34.
181. Schmid KL, Wildsoe CF. Contrast and spatial-frequency requirements for emmetropization in chicks. Vis res. 1997;37(15):2011-21.
182. Díez-Ajenjo MA, Capilla P. Spatio-temporal contrast sensitivity in the cardinal directions of the colour space. A review. J Optom. 2010;3(1):2-19.
183. Rucker FJ. The role of luminance and chromatic cues in emmetropisation. Ophthalmic Physiol Opt. DOptics. 2013;33(3):196-214.
184. Mullen KT. The contrast sensitivity of human colour vision to red-green and blue-yellow chromatic gratings. J Physiol. 1985;359(1):381-400.
185. Kim KJ, Mantiuk R, Lee KH, editors. Measurements of achromatic and chromatic contrast sensitivity functions for an extended range of adaptation luminance. Hum Vis Electron Imaging XVIII; 2013: SPIE.
186. Barten PG. Contrast sensitivity of the human eye and its effects on image quality: SPIE press; 1999.
187. Cavonius C, Estévez O. Contrast sensitivity of individual colour mechanisms of human vision. J Physiol. 1975;248(3):649-62.

Chapter 3. Bi-exponential description for different forms of refractive development

Previously published as:

Arezoo Farzanfar, Jos J Rozema
Bi-exponential description for different forms of refractive development

Journal of Vision, 2024 Jul 2;24(7):3.

INTRODUCTION

The human eye undergoes an intricate refractive development between infancy and adolescence, culminating in the achievement and preservation of a sharp retinal image while the eye grows.[1-3] Refractive development occurs fastest during the first two years of life when the eye grows fastest[1, 4-5] by varying the growth rates of the different ocular components.[5, 6-8] At birth, the eye is typically hypermetropic,[3, 5, 9] which gradually decreases through emmetropization, a continuous dynamic process that aims to fine-tune the refractive state of the eye to reach a sharp image on the retina.[2, 5] Although many factors contribute to emmetropization, it can be described in its most basic form as a fine-tuning of the axial length and the total optical power of the eye through coordinated growth to minimize spherical refractive errors.[2] However, emmetropia cannot always be achieved, as refractive development may be influenced by genetic, environmental, and lifestyle factors.[10] Several descriptive studies have explored early eye development and its underlying biometric changes, most notably Mutti and colleagues,[8] who examined individual ocular biometric parameters between infancy and early school age.

Based in part on those works, a model was recently developed that describes the growth of refractive and biometric factors of the eye from before birth until adulthood as a bi-exponential function, a sum of two exponential functions.[1] These functions correspond with the two phases of ocular growth: genetically preprogrammed prenatal growth (or scaled growth) and postnatal coordinated growth. Inspired by this descriptive model, current work investigates the function of the different coefficients of the bi-exponential functions and whether these functions can be used to describe various healthy and pathological refractive development courses known from literature.

METHODS

Model

The eye can be described as a simplified optical system that must balance two components:

the axial length of the eye, expressed in diopters as P_{ax} (or axial power), and the total refractive power of the eye, P_{eye}, consisting of the combined powers of the cornea and lens. These two parameters represent the power that the eye requires for a sharp retinal image and the power that the ocular optics can provide, respectively. Any difference between them would then correspond with the spherical refractive error S:

$$S = P_{ax} - P_{eye} \qquad (2\text{-}1)$$

Consequently, the values of P_{ax} and P_{eye} must remain close to one another for the best chance of successful emmetropization.

Recently, it was established[1] that, like most ocular parameters, P_{ax} and P_{eye} may be described by the following bi-exponential functions as a function of time t (age in years):

$$P_{ax}(t) = a_0 + a_1 e^{a_2 t} + a_3 e^{a_4 t}$$
$$P_{eye}(t) = a_5 + a_6 e^{a_7 t} + a_8 e^{a_9 t} \qquad (2\text{-}2)$$

where a_0, …, a_9 are the model coefficients. Equation 2-2 corresponds to the fast initial scaled growth phase before and short after birth when retinal feedback is not yet active, followed by a second, slower growth phase during which the feedback controls (part of) the growth. As Equation 2-2 is purely descriptive, no interaction is assumed between P_{ax} and P_{eye}.

Note that, although most biometric parameters of the eye can be described by a bi-exponential function, refractive error S is a notable exception, as it displays more complicated, somewhat oscillating behavior.[1-2] Hence, it was modeled by combining Equations 2-1 and 2-2, thus representing the relationship among all three parameters using a total of 10 coefficients ai. These coefficients can be adjusted to match various courses of refractive development based on the literature [5, 8, 11] as well as those of pathologies such as school-age myopia and infant pseudophakia.

To simulate the sudden onset of school-age myopia, coefficients a_3 and a_7 were modulated by a Gompertz function,[12] an asymmetric sigmoid function used for this purpose before in the literature[13]:

$$P_{ax}(t) = a_0 + a_1 e^{a_2 t} + a_3 (1 + G(t)) e^{a_4 t}$$
$$P_{eye}(t) = a_5 + a_6 e^{a_7 t} + a_8 (1 + G(t)) e^{a_9 t} \qquad (2\text{-}3)$$
$$\text{where } G(t) = \exp[-\exp(0.5 - 5 \cdot t)].$$

Courses of refractive development

Longitudinal refractive data from prior studies[5, 8, 11] demonstrate that there are several distinct courses in refractive development, ranging from normal to high hyperopia or early myopia. Considering cycloplegic refractive errors, the following courses of refractive development can be identified:

1. *Modulated development*—At birth, the eye has a refractive error of about +2.5 diopters (D) and becomes more hypermetropic until a maximum value is reached at the age of 3 months. In the following months, the eye emmetropizes toward +1D, when the refractive error stabilizes under continued eye growth.[5, 8] The overall development displays the wavy behavior that gives it its name.[8, 14]

2. *Instant emmetropization*—The maximum hypermetropic refractive error is reached at birth, and the eye begins emmetropizing immediately, followed by homeostasis.

3. *Instant homeostasis*—The eye is born with a refractive error near +1D, negating the need for emmetropization, homeostasis.[2, 5, 8]

4. *Emmetropizing hyperopia*—This is similar to modulated development, but here emmetropization takes several years rather than 1 year.

5. *Persistent hyperopia*—The eye is hypermetropic at birth and remains so over time.

6. *Developing hyperopia*— The eye emmetropizes normally but gradually becomes hypermetropic with age.

7. *Infant myopia*— Although rare, some eyes are born with mild myopia. Although in some cases this myopia may emmetropize during the first year of life,[3] this generally leads to high levels of myopia later on. This is seen in, for example, severely premature infants.[15]

8. *School-age myopia*— The eye emmetropizes but gradually becomes myopic with age due to a combination of genetic, behavioral, and environmental factors affecting axial growth. [2, 16-18] This case requires Equation 2-3.

9. *Infant pseudophakia*— Infants with congenital cataract must be treated at the earliest possible age to avoid negatively affecting their refractive development. Often such eyes are implanted with an intraocular lens. As such a lens has a fixed power, it hinders normal refractive development, leading to high myopia.[19-21] This pathological course of development was added to test the limits of what the bi-exponential description can

handle.

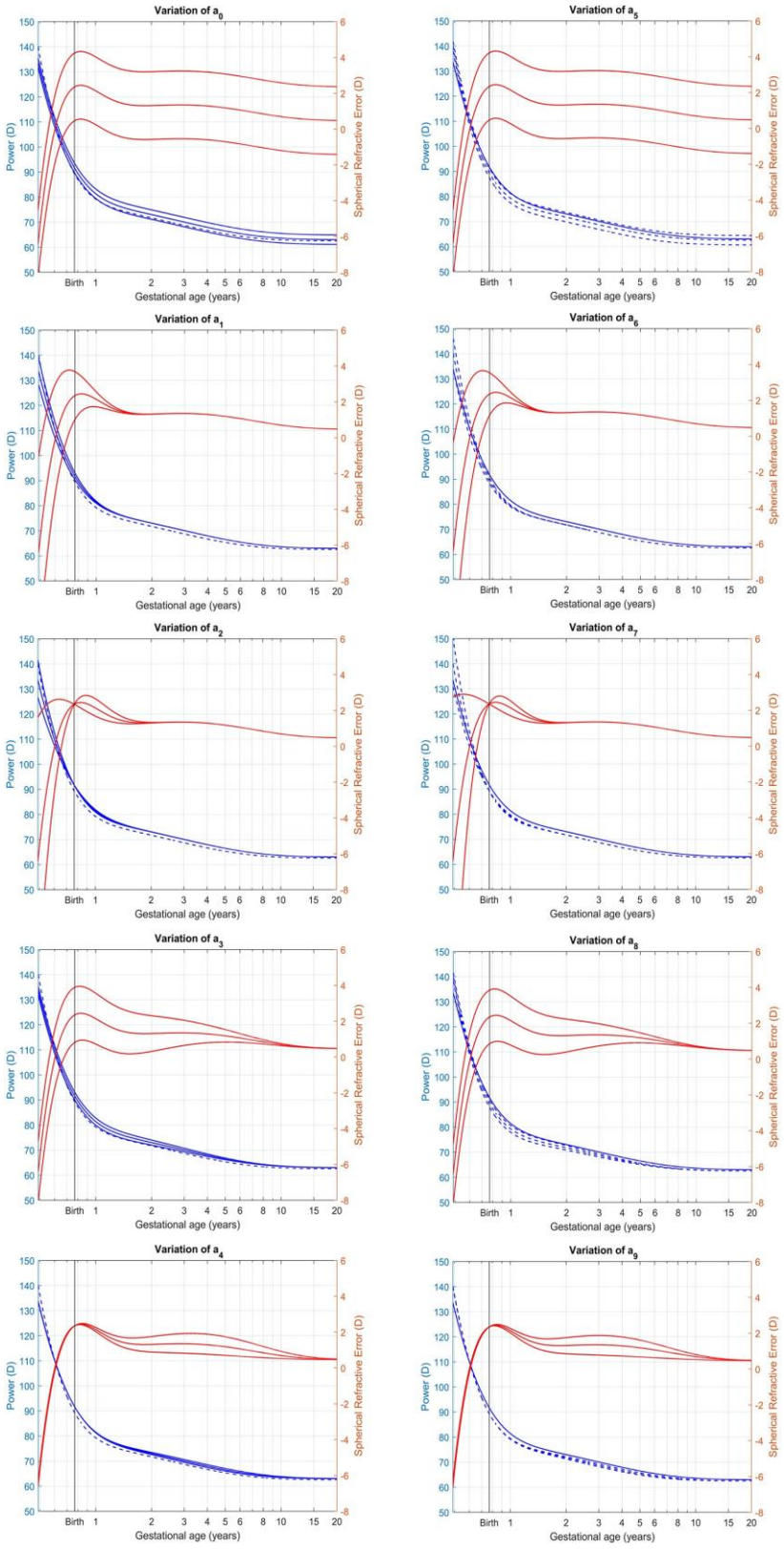

Figure 2.1. Influence of individual ai parameters on S (red), axial (blue), and optical power (dashed blue). Middle red and blue lines correspond with the model from Rozema (2023).[1]

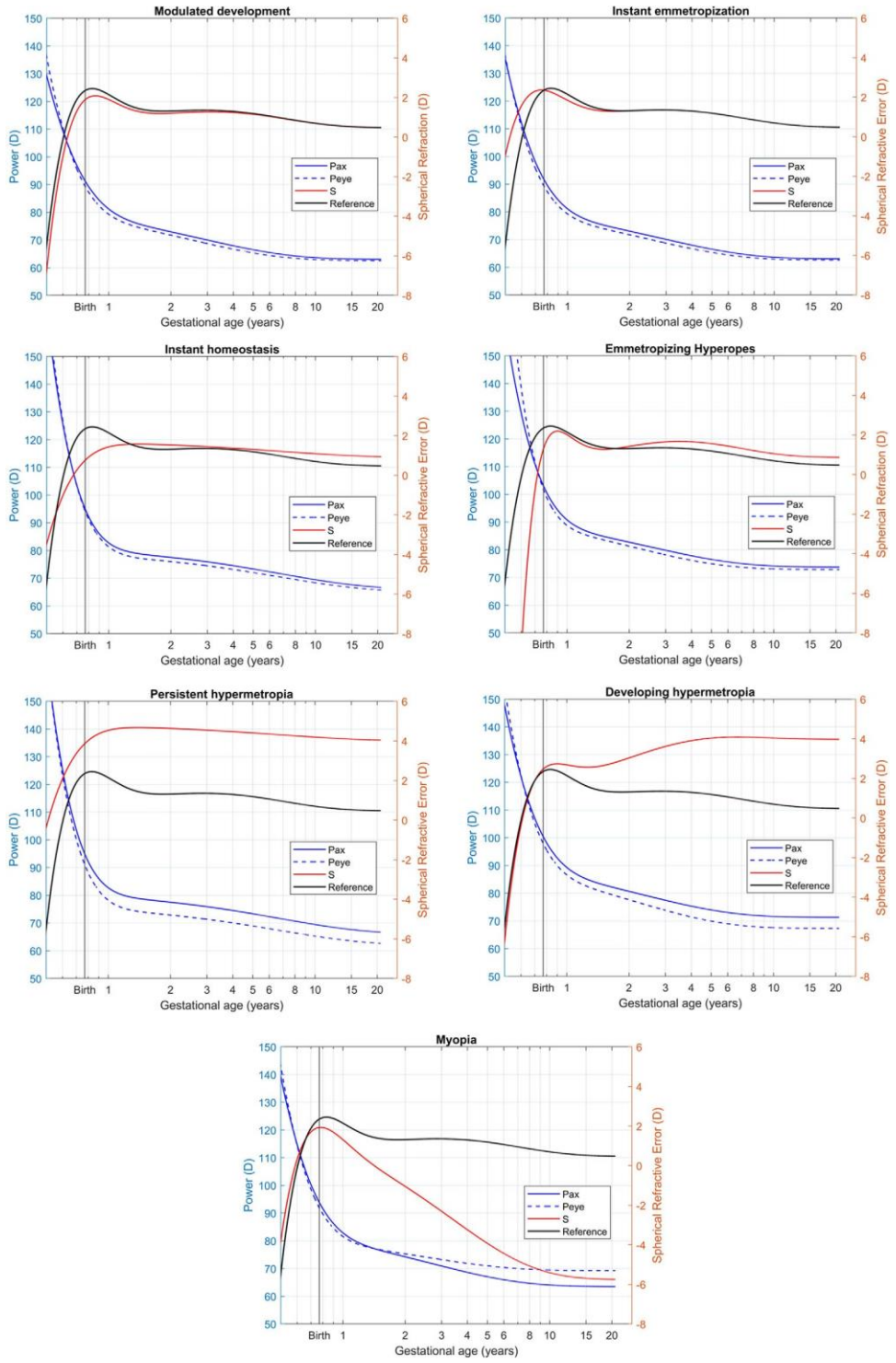

Figure 2.2 Simulated refractive development courses. The black line represents the references based on Rozema (2023).[1]

Comparison with literature

Jones et al. (2005)[11] published ocular component growth curves for emmetropes, emmetropizing hyperopes, persistent hyperopes, and myopes based on statistical fits for each ocular biometry variable as a function of age (Appendix A). These can be used to estimate the axial

and whole eye power [22] for comparison with the bi-exponential functions.

RESULTS

Influence of a_i parameter variations

To investigate the influence of the individual ai coefficients on spherical refractive error *S* and the axial and ocular powers, each was varied by a certain percentage (a_0 and a_5 by ±3% and all others by $\pm 10\%$) (Figure 2.1). Due to the symmetry in Equation 2-2, coefficients should be considered in pairs that affect the curves of P_{ax} and P_{eye}, respectively:

1. a_0 and a_5—The initial values of the axial and ocular powers; variations cause a vertical shift of the graphs.
2. a_1 and a_6—Amplitude of the axial and ocular powers during the scaled eye growth; lower values correspond with excessive eye growth, causing the focal point of the image to fall in front of the retina and resulting in myopia.
3. a_2 and a_7—Dampening of the scaled eye growth; these parameters determine the time scale over which this phase remains active and play a critical role in shaping the initial development.
4. a_3 and a_8—Amplitude of the axial and ocular powers during the coordinated eye growth, which is linked to the strength of the retinal feedback mechanism.
5. a_4 and a_9— Dampening of the coordinated eye growth; this determines the time scale over which the retinal feedback remains active but does not seem to affect the final refractive error.

Parameter	a_0	a_1	a_2	a_3	a_4	a_5	a_6	a_7	a_8	a_9
Modulated development	63.02	13.00	−4.98	15.20	−0.35	62.57	11.82	−5.85	14.96	−0.39
Instant emmetropization	63.04	13.29	−5.30	15.37	−0.35	62.57	11.82	−5.85	14.96	−0.39
Instant homeostasis	66.00	15.10	−6.50	13.84	−0.15	65.10	16.00	−6.50	13.08	−0.15
Emmetropizing hyperopes	73.77	14.78	−5.91	14.51	−0.40	72.90	13.90	−7.50	14.96	−0.50
Persistent hyperopia	66.00	15.10	−6.50	13.84	−0.15	62.00	16.00	−6.50	13.08	−0.15
Developing hyperopia	71.30	13.41	−5.50	15.68	−0.42	67.32	12.44	−6.21	18.15	−0.46
Myopia	63.50	13.41	−5.38	16.88	−0.37	69.26	12.54	−5.97	10.07	−0.42
School myopia	69.42	15.4	−5.07	17.57	−0.33	71	12.77	−5.99	16.05	−0.42
Pseudophakia	58.04	20	−2.55	6.84	−0.1	61	15	−3.7	6.68	−0.01
Reference [1]	63.04	13.29	−4.98	15.37	−0.35	62.57	11.82	−5.84	14.96	−0.39

Table 2.1. Parameters required to simulate the above refractive development courses.

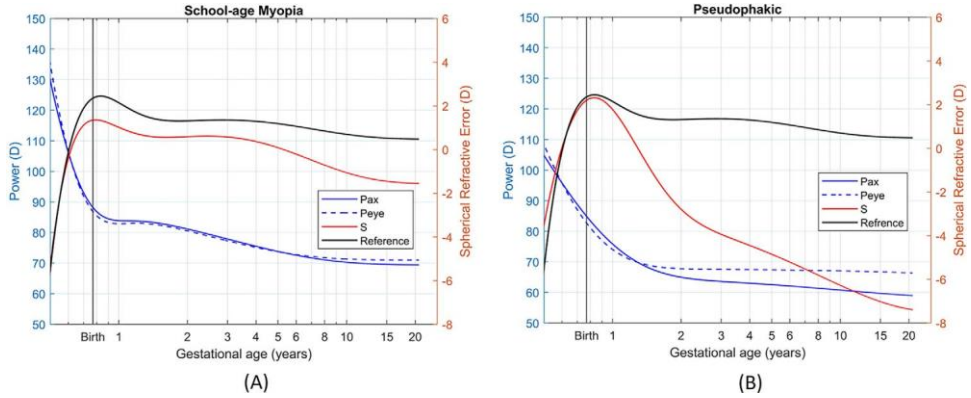

Figure 2.3. Simulation of refractive development for school-age myopia (A) and pseudophakic eye (B) with the underlying changes in P_{ax} and P_{eye}.

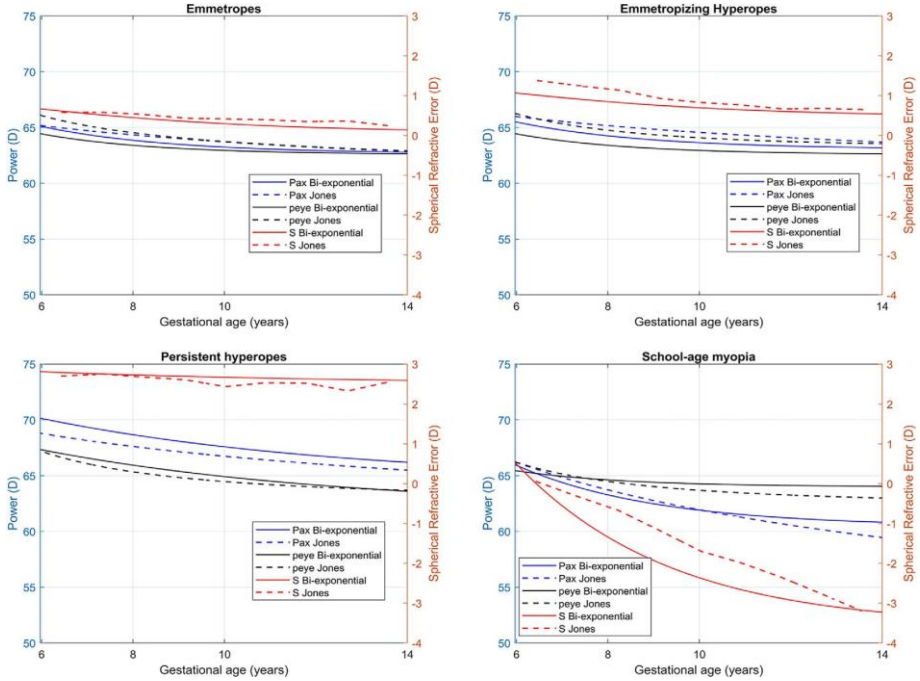

Figure 2.4. Comparison among four refractive development courses adapted from Jones et al. (2005)[11] alongside their underlying changes in P_{ax} and P_{eye} with the results of bi-exponential function.

Simulation of normal refractive development courses

By making different combinations of the ai coefficients, Equation 2-2 can simulate all forms of refractive development listed above. Examples of the changes in S, Pax, and Peye are shown in Figure 2.2, and the corresponding values for the ai coefficients are provided in Table 2.1. The coefficient values for the population average are provided as a referenc.1 Equation 2-2 can also be adjusted to show the refractive development of pseudophakia and, with a small adjustment using Equation 2-3, school-age myopia (Figure 2.3). All these courses closely resemble those reported

in the previous literature.

Comparison with literature

Comparing the four refractive development groups identified by Jones et al. (2005)[11] for ages between 6 and 14 years with the bi-exponential functions, it can be seen that both behave similarly for axial and optical powers, as well as spherical refractive error (Figure 2.4).

DISCUSSION

This paper has explored how the coefficients of the bi-exponential growth functions can be used to successfully reproduce various courses of refractive development for emmetropic and ametropic eyes found in the literature (Figure 2.2), as well as pathological refractive developments, such as infant pseudophakia and school-age myopia (Figure 2.3). Consistent with previous literature,[19] congenital cataract produced myopic shifts in pseudophakic eyes, indicating a greater risk of myopia due to the presence of the intraocular lens.

The bi-exponential description also reproduced the refractive development courses reported by Jones et al. (2005)[11] for four refractive categories of children ages 6 to 14 years (Figure 2.4). In addition to reproducing the literature, these simulations also estimated the changes in P_{ax} and P_{eye} underlying the changes in refractive error. This is a distinct advantage over a simple description of the refractive error alone, especially given the observation by Benjamin, Davey, Sheridan, Sorsby, and Tanner (1957)[23] that there is a considerable overlap between the ocular biometry values of emmetropes and ametropes between ±4D. It is therefore important to determine the underlying mismatch in ocular biometry, expressed as P_{ax} and P_{eye}, when trying to understand the origin of a refractive error.

Although bi-exponential growth functions provide a good description of the evolution of axial and whole eye power over time, these functions could conceivably be adapted further by considering the mutual influence between P_{ax} and P_{eye}, as well as the influence of external factors. Although the current model assumes independence between both parameters, real refractive development consists of intricate interactions between the optical and sensory components of the eye, crucial for achieving emmetropization. Such models were developed earlier by Medina (2022)[24] and Medina and Fariza (1993),[25] who described refractive error without intervention and a single exponential function, as well as by Hung and Ciuffreda (2000),[26] who combined refractive error, axial length, and various scleral factors.

In conclusion, this work demonstrates the viability of bi-exponential functions to simulate diverse refractive development courses and offers insights into their differences. This

research forms a foundation for future investigations into the complex interplay between ocular parameters during eye growth. Potential applications of the proposed descriptions may be the analysis of the refractive development profiles of individual eyes.

ACKNOWLEDGMENTS

Funding from the European Union's Horizon 2020 research and innovation program under the Marie Skłodowska Curie Grant Agreement No. 956720.

REFERENCES

1. Rozema JJ. Refractive development I: biometric changes during emmetropisation. Ophthalmic Physiol. Opt. 2023;43(3):347-67.
2. Rozema J, Dankert S, Iribarren R. Emmetropization and nonmyopic eye growth. Surv. Ophthalmol. 2023;68(4):759-83.
3. Wood IC, Hodi S, Morgan L. Longitudinal change of refractive error in infants during the first year of life. Eye. 1995 Sep;9(5):551-7.
4. Mutti DO, Mitchell GL, Jones LA, Friedman NE, Frane SL, Lin WK, Moeschberger ML, Zadnik K. Axial growth and changes in lenticular and corneal power during emmetropization in infants. Invest. Ophthalmol. Vis. Sci. 2005 Sep 1;46(9):3074-80.
5. Pennie FC, Wood IC, Olsen C, White S, Charman WN. A longitudinal study of the biometric and refractive changes in full-term infants during the first year of life. Vis Res. 2001 Sep 1;41(21):2799-810.
6. EHRLICH DL, BRADDICK OJ, ATKINSON J, ANKER S, WEEKS F, HARTLEY T, WADE J, RUDENSKI A. Infant emmetropization: longitudinal changes in refraction components from nine to twenty months of age. Optom. Vis. Sci. 1997 Oct 1;74(10):822-43.
7. Mutti DO. To emmetropize or not to emmetropize? The question for hyperopic development. Optom. Vis. Sci. 2007 Feb 1;84(2):97-102.
8. Mutti DO, Sinnott LT, Mitchell GL, Jordan LA, Friedman NE, Frane SL, Lin WK. Ocular component development during infancy and early childhood. Optom. Vis. Sci. 2018 Nov 1;95(11):976-85.
9. Edwards M. The refractive status of Hong Kong Chinese infants. Ophthalmic Physiol. Opt. 1991 Oct;11(4):297-303.
10. Morgan I, Rose K. How genetic is school myopia? Prog. Retin. Eye Res. 2005 Jan 1;24(1):1-38.
11. Jones LA, Mitchell GL, Mutti DO, Hayes JR, Moeschberger ML, Zadnik K. Comparison of ocular component growth curves among refractive error groups in children. Invest. Ophthalmol. Vis. Sci. 2005 Jul 1;46(7):2317-27.
12. Gompertz B. XXIV. On the nature of the function expressive of the law of human mortality, and on a new mode of determining the value of life contingencies. In a letter to Francis Baily, Esq. FRS &c. Philos. Trans. R. Soc. Lond. 1825 Dec 31(115):513-83.
13. Thorn F, Gwiazda J, Held R. Myopia progression is specified by a double exponential growth function. Optom. Vis. Sci. 2005 Apr 1;82(4):E286.
14. Medina A. El origen de las ametropías¿ Qué es emetropía. Arch Soc Esp Oftalmol. 1980 Feb;40:156-61.
15. Fledelius HC. Myopia of prematurity, clinical patterns. Ophthalmic Lit. 1996;3(49):211.
16. Lingham G, Mackey DA, Lucas R, Yazar S. How does spending time outdoors protect against myopia? A review. Br. J. Ophthalmol. 2020 May 1;104(5):593-9.
17. Morgan IG, French AN, Ashby RS, Guo X, Ding X, He M, Rose KA. The epidemics of myopia: aetiology and prevention. Prog. Retin. Eye Res.2018 Jan 1;62:134-49.
18. Troilo D, Smith EL, Nickla DL, Ashby R, Tkatchenko AV, Ostrin LA, Gawne TJ, Pardue MT, Summers JA, Kee CS, Schroedl F. IMI–Report on experimental models of emmetropization and myopia. Invest. Ophthalmol. Vis. Sci.2019 Feb 28;60(3):M31-88.
19. Chan JJ, Wong ES, Lam CP, Yam JC. Ten-year refractive and visual outcomes of intraocular lens implantation in infants with congenital cataract. Hong Kong Med J. 2023 Feb 1;29(1):22-30.
20. Hoevenaars NE, Polling JR, Wolfs RC. Prediction error and myopic shift after intraocular lens implantation in paediatric cataract patients. Br. J. Ophthalmol. 2011 Aug 1;95(8):1082-5.
21. McClatchey SK, Dahan E, Maselli E, Gimbel HV, Wilson ME, Lambert SR, Buckley EG, Freedman SF, Plager DA, Parks MM. A comparison of the rate of refractive growth in pediatric aphakic and pseudophakic eyes. Ophthalmology. 2000 Jan 1;107(1):118-22.
22. Rozema JJ. Estimating principal plane positions for ocular power calculations in children and adults. Ophthalmic Physiol. Opt. 2021 Mar;41(2):409-13.
23. Benjamin B, Davey JB, Sheridan M, Sorsby A, Tanner JM. Emmetropia and its aberrations; a study in the correlation of the optical components of the eye. Spec. Rep. Ser. Med. Res. Counc. (Gr. Brit.). 1957;11(293):1-69.
24. Medina A. The cause of myopia development and progression: theory, evidence, and treatment. Surv. Ophthalmol. 2022 Mar 1;67(2):488-509.
25. Medina A, Fariza E. Emmetropization as a first-order feedback system. Vis Res. 1993 Jan 1;33(1):21-6.
26. Hung GK, Ciuffreda KJ. A unifying theory of refractive error development. Bull. Math. Biol. 2000 Nov 1;62(6):1087-108.

Chapter 4. Modelling normal and myopic eye growth

Previously published as:
Jos J Rozema, Arezoo Farzanfar
Modelling normal and myopic eye growth
Ophthalmic and Physiological Optics, 2024

INTRODUCTION

Normal refractive development involves delicate interactions between the optical and sensory components of the eye to produce and preserve a sharp retinal image while the eye grows.[1-4] The most important interaction is that between the axial length and the optical power of the eye, both of which must be closely tuned to each another to ensure a good retinal image quality. This is a continuous process, where in the first two years of life the ocular components adjust their growth rates so that the eye gradually assumes a near-emmetropic refractive error of *+1D* (*emmetropization*),[5] followed by a period during which the eye continues to grow while preserving this near-emmetropic error (*homeostasis*).[1-4] Any failure during this process can lead to ametropia, of which the excessive axial growth during myopization is the best known example.[6, 7] The exact causes of this excessive growth remain under investigation, but various behavioral and environmental factors,[8] such as the amount of near vision activities,[9] time spent outdoors,[10, 11] and ambient light[12, 13] are known to be major influences.

The first paper in this series established that most ocular components grow in two phases that can each be described by a bi-exponential curve,[2] corresponding to a fast initial phase before and shortly after birth, followed by a slower phase once the retinal feedback starts. The first phase is roughly synchronous for most ocular components, creating scaled growth, while during the slower phase, each component follows its own unique growth curve that eventually helps reduce refractive error.[2] Consequently, while axial length increases from *16.50 mm* at birth to about *23.75 mm* in young adults, the cornea and crystalline lens rapidly lose power to compensate. For the cornea, this power loss ends after only *2 – 3* years,[2, 14] while the lens continues to lose power throughout life.[2, 14-16] However, achieving emmetropization and homeostasis relies on a delicate balance between axial length and optical power. So, the timing and amplitude of this refractive power loss need to be precisely regulated to achieve emmetropization and homeostasis, which in turn depend on interactions between the eye's optical and sensory components.[17]

To better understand these interactions, several cross-sectional,[18, 19] longitudinal,[14] and meta-analysis studies[2, 20] have investigated early eye growth, examining how individual ocular biometric parameters change with age and how these changes correlate with one another.[21] Although these studies yielded valuable data about early refractive development, they were all descriptive, observational, and non-interventional in nature due to obvious ethical concerns regarding human testing. Hence, to obtain deeper insights into the interactions between the optical parameters, researchers have used experimental animal models[22, 23] to identify the most important mechanisms for emmetropization and myopia development, as well as environmental factors such as the intensity and color of the ambient light, viewing distance, contrast, etc.[22, 23] However, while valuable, results from animal studies depend on the species being considered[1, 18] and questions have been raised about how well testing protocols reflect real human environments or behavior.[24] Consequently, some treatments that work well in animals can be far less effective in humans, such as the observation that undercorrection of myopia leads to emmetropia in chickens,[25] while in humans[26, 27] this effect is absent or weak at best.[21, 22] Consequently, there are limits to using animal models to understand human refractive development.

A potentially powerful alternative is active numerical models that assess how changes in one ocular parameter trigger changes in the growth rates of other parameters, regulated through closed-loop feedback to optimize retinal image quality. Based on observations that refractive changes over time correlate with the amount of refractive error at baseline,[21, 28, 29] it is reasonable to assume that the feedback controller is closely associated with refractive error. This is also supported by a multitude of animal experiments that consistently demonstrate how induced changes in refractive focus alter the optical characteristics of the eye.[22, 23]

Retinal feedback models were first conceptually described by van Alphen,[30] Medina[31] and Carroll,[32] and were first implemented numerically in *1987* by Medina.[33, 34] His model used retinal defocus as a feedback controller and provided a closer match to clinical data than a similar system without feedback.[34] One year later, Schaeffel and Howland[35] presented a model that successfully reproduced their myopia experiments in chickens.[36] Later, in *1998*, Flitcroft[37] proposed a refractive development model based on earlier descriptions of accommodative lag and vergence,[38-40] which was later expanded by Blackie and Howland[41] to include the influence of illumination on the pupil size. Finally, Hung and Ciuffreda[42, 43] developed a more elaborate model that combined genetically pre-programmed growth with feedback controlled by the retinal blur circle, which is closely related to the refractive error. Their system included refractive error, ocular axial length, as well as various retinal and scleral factors, and not only reproduced normal emmetropia eye growth, but also the growth observed in animal experiments involving imposed lenses, occluders and diffusers. All these models have their limitations, however, as Medina and

Flitcroft did not consider the biometric aspects of refractive development, while Hung's model does not consider the contributions of the crystalline lens. But as crystalline lens power loss occurs at a higher rate during myopization than in normal development,[44-46] the lens likely plays an important role in emmetropization and homeostasis as well.

Hence, this paper presents a system of first-order ordinary differential equations (*ODEs*) based on bi-exponential descriptions[2] of the ocular and axial powers with a closed-loop feedback control based on the retinal blur size to describe normal and abnormal ocular growth from before birth until adulthood. The model presented here establishes the underlying concepts and assesses the influence of the relative proportions of the pre-programmed growth and feedback. Subsequently, the model's features and limits are explored by varying the model parameters.

METHODS

The eye can be described as a simplified optical system that balances two components: the axial length of the eye expressed in diopters, P_{ax} (*dioptric distance* or *axial power*), and a single lens that represents the total refractive power of the eye P_{eye}, consisting of the combined powers of the cornea and lens. Simply put, these two parameters represent the power that the eye requires for a sharp retinal image and the power that the ocular optics can provide, respectively. Any difference between them would then correspond with the refractive error *SE*:

$$SE = P_{ax} - P_{eye} \tag{3-1}$$

Consequently, the values of P_{ax} and P_{eye} must remain close to one another for the best chance of successful emmetropization. Recently, it was shown [2] that P_{ax} and P_{ax} may each be described by a bi-exponential function as a function of time t:

$$\begin{cases} P_{\mathrm{ax}}(t) = c_1 e^{c_2 t} + c_3 e^{c_4 t} + C_1 \\ P_{\mathrm{eye}}(t) = c_5 e^{c_6 t} + c_7 e^{c_8 t} + C_2 \end{cases} \tag{3-2}$$

These functions describe a fast initial growth phase before and shortly after birth that is genetically pre-programmed and without retinal feedback, followed by a second, slower growth phase during which the feedback partially modulates the growth rate. Parameters c_i and C_i may be determined by statistically fitting clinical measurements of P_{ax} and P_{eye} as was done in [2] (**Table 3.1**). Although this model is entirely descriptive and assumes no interactions between P_{ax} and P_{eye}, it is able to simulate various refractive development courses by appropriately varying the values of c_i.[47]

Static ODE model

As a first step towards the model, equations (3-2) are rewritten as the following system of *ODEs*:

$$\begin{cases} \dot{P}_{\text{ax}}(t) = a_1 e^{a_2 t} + a_3 e^{a_4 t} \\ \dot{P}_{\text{eye}}(t) = a_5 e^{a_6 t} + a_7 e^{a_8 t} \end{cases} \tag{3-3}$$

where $\dot{P}_{\dots} = dP_{\dots}/dt$ is the derivative of $P_{\dots}$ with respect to time. Rather than describing how the powers change with time, these equations describe how *changes* in power (or the slopes) evolve over time, providing an equivalent description once initial conditions $P_{\text{ax}}(t_0)$ and $P_{\text{eye}}(t_0)$ are known. In this system parameters a_i are given by:

$$\begin{cases} a_1 = c_1 c_2 \\ a_3 = c_3 c_4 \\ a_5 = c_5 c_6 \\ a_7 = c_7 c_8 \end{cases} \tag{3-4}$$

while a_2, a_4, a_6, and a_8 are equal to the c_2, c_4, c_6, and c_8 of system **(3-2)**. As before, the exponential terms in **(3-3)** represent the faster and slower phases of ocular growth. This system's initial conditions at $t_0 = -0.25$ years are:

$$\begin{cases} P_{\text{ax}}(-0.25) = c_1 e^{-0.25 a_2} + c_3 e^{-0.25 a_4} + C_1 \\ P_{\text{eye}}(-0.25) = c_5 e^{-0.25 a_6} + c_7 e^{-0.25 a_8} + C_2 \end{cases} \tag{3-5}$$

The parameters in **(3-4)** and **(3-5)** can be estimated from a direct statistical fit of **(3-2)** to clinical or literature data of P_{ax} and P_{eye}. Model **(3-3)** is also descriptive and is used in the following as a reference for all following models.

Active feedback

Instead of a purely descriptive model that explains how P_{ax} and P_{eye} evolve with age, system **(3-3)** can be modified to include a feedback factor that considers the interactions between both parameters, as well as the impact of external influences. Ideally, this is done by minimizing properties such as the refractive error *SE* or retinal blur diameter. As the real function by which the eye adjusts its growth speed is still unknown, the feedback function F used here is based on the retinal blur diameter of a distant object:

$$F = \left| \frac{P_{\text{eye}}}{P_{\text{ax}}} - 1 \right| \tag{3-6}$$

which is derived in the **Appendix B**. This represents the *closed-loop feedback*.

Although the eye already perceives light before birth,[48] retinal feedback can only start after birth once a clear retinal image is formed. It therefore makes sense that the feedback factor is

linked to the second exponential terms in system **(3-3)**, controlled by factors a_3 and a_7. As the strength of the retinal feedback is more likely to start gradually rather than abruptly, it was modulated using a Gompertz function:[49]

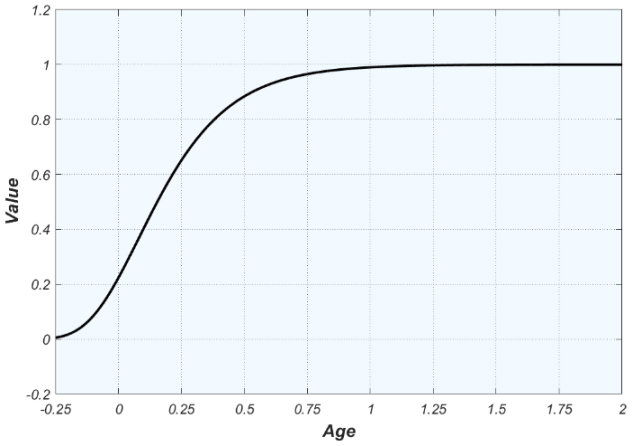

Figure 3.1. Gompertz function (3-7) that gradually switches on the feedback in system (3-8).

$$G(t) = exp\big(g_1 \cdot exp(g_2 \cdot t)\big) \qquad (3\text{-}7)$$

This has an asymmetric sigmoid shape that transitions between *0* and *1* at a rate controlled by the two numerical parameters, so that the transition is completed at *12* months of age (**Figure 3.1**). Using the feedback factor **(3-6)** and Gompertz function **(3-7)**, **(3-3)** can be revised to:

$$\begin{cases} \dot{P}_{\text{ax}}(t) = a_1 e^{a_2 t} + a_3(s_1 + s_2 G \cdot F)e^{a_4 t} \\ \dot{P}_{\text{eye}}(t) = a_5 e^{a_6 t} + a_7(s_3 + s_4 G \cdot F)e^{a_8 t} \end{cases} \qquad (3\text{-}8)$$

Here, s_1 and s_3 may be interpreted as the genetically pre-programmed growth of the eye, while s_2 and s_4 control the strength of the feedback. The relative importance of these two contributions is still unclear from the literature, however. System **(3-8)** forms the basis of the interactive eye growth model and depends on the chosen values of s_i. Choosing $s_1 = s_3 = 1$ and $s_2 = s_4 = 0$ again yields system **(3-3)**.

Myopia

Development

Myopia can easily be introduced into the model by adding an extra term Δ to the feedback function as follows:

$$F = \left|\frac{P_{\text{eye}}}{P_{\text{ax}}} - 1\right| + \Delta(t) \qquad (3\text{-}9)$$

This represents an accelerated power loss for P_{ax} and P_{eye} due to excessive axial growth and

lenticular processes to compensate for this growth,[44-46] respectively. Term Δ essentially turns the closed loop of equation **(3-6)** into an *open loop*, producing runaway growth controlled by genetic,[50] behavioral or environmental factors,[8] and may be affected by accommodation. For the sake of simplicity, in this work Δ is considered constant, with a value of *0* until a moment t_{mo} of myopization onset (i.e., the moment that excessive growth starts rather that the eye becomes myopic). Possible forms of Δ are listed in the Discussion and will be explored in future papers.

Lower limit of P_{eye}

Although myopia is typically associated with excessive axial growth, the crystalline lens also plays an important role. During myopic growth, the crystalline lens initially attempts to match its rate of power loss to compensate for the axial growth, but may eventually reach a point where it is no longer able to lose its power efficiently. This the moment that the eye becomes myopic.[44, 45] In the context of the models, axial power P_{ax} and whole eye power P_{eye} will both quickly reduce during myopization until P_{eye}, which contains the crystalline lens power, slows down or stops its power loss. Based on a recent paper on the Singapore Cohort Study of the Risk Factors for Myopia (SCORM),[45] the critical power threshold at which this occurs can be estimated at $P_{eye,c}$ = *62.2D*. However, as there are large interindividual variations for this parameter, the model uses a more conservative value of *60D* instead. In practice, any P_{eye} value below $P_{eye,c}$ is replaced by $P_{eye,c}$.

Refractive correction

A possible refractive correction $RC(t)$ can also be introduced into the model to assess its influence on refractive development. Since the refractive correction supplements the whole eye power, the change in $RC(t)$ is added to $\dot{P}_{eye}(t)$. This refractive correction must also be added to the critical power threshold, replacing the threshold by $P_{eye,c}$ + $RC(t)$ instead.

Dynamic ODE model

Combining feedback function **(3-9)**, refractive correction $RC(t)$ and critical threshold $P_{eye,c}$ into model **(3-8)** then gives:

$$\begin{cases} \dot{P}_{ax}(t) = a_1 e^{a_2 t} + a_3(s_1 + s_2 G \cdot F) e^{a_4 t} & \\ \dot{P}_{eye}(t) = a_5 e^{a_6 t} + a_7(s_3 + s_4 G \cdot F) e^{a_8 t} + \dot{RC}(t) & \text{if } P_{eye} > P_{eye,c} \\ \qquad\quad = \dot{RC}(t) & \text{if } P_{eye} \le P_{eye,c} \end{cases} \qquad (3\text{-}10)$$

This model is used for all simulations below and represented in the diagram in **Figure 3.2**.

For completeness, note that several simplifications can be made when simulating the refractive development after the age of *2* years. At that age, the first exponential terms of **(3-10)**

have both become *0*, while Gompertz function $G = 1$, so:

$$\begin{cases} \dot{P}_{\text{ax}}(t) = a_3(s_1 + s_2F)e^{a_4t} \\ \dot{P}_{\text{eye}}(t) = a_7(s_3 + s_4F)e^{a_8t} + \dot{RC}(t) & \text{if } P_{eye} > P_{eye,c} \\ \qquad = \dot{RC}(t) & \text{if } P_{eye} \leq P_{eye,c} \end{cases} \tag{3-11}$$

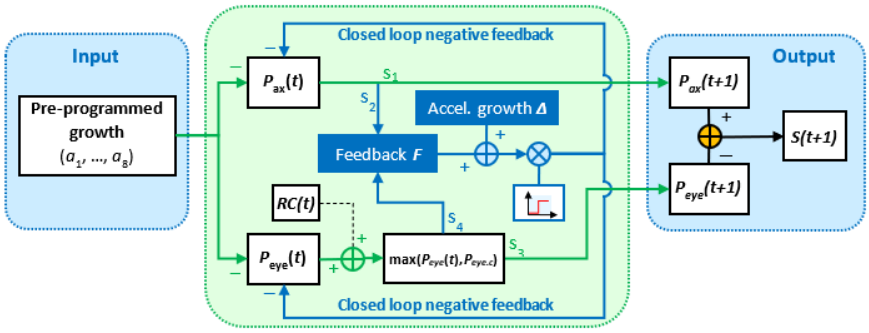

Figure 2: Flow diagram of ODE system (10) describing the influences affecting axial power P*ax* and whole eye power P*eye*. Other symbols are defined in Table 1. Green arrows correspond to the pre-programmed growth, blue arrows to the closed negative feedback loops, ⊕ to a sum of two signals and ⊗ to a multiplication of two signals. Note that feedback function F and accelerated growth term Δ are modular and can be replaced by other functions than the ones used here to account for other influences.

and the initial conditions **(3-5)** at $t_0 = 2$ years change to:

$$\begin{cases} P_{\text{ax}}(2) = c_1e^{-2.a_2} + c_3e^{-2.a_4} + C_1 \\ P_{\text{eye}}(2) = c_5e^{-2.a_6} + c_7e^{-2.a_8} + C_2 \end{cases} \tag{3-12}$$

Calculations

All calculations were performed in MATLAB (R2023b; the MathWorks, Natick, MA, USA) using the parameters values in **Table 3.1** unless stated otherwise.

While some ODE models have an exact solution, such as system **(3-3)** with solution **(3-2)**, this cannot be generalized as systems **(3-8)**, **(3-10)** and **(3-11)** can only be solved numerically due to the inclusion of absolute value in *F* and the critical threshold $P_{\text{eye,c}}$. Here, the forward Euler method was used, which considers the ODE as a series of minute steps starting from the initial conditions **(3-5)**. As the output of this method can vary greatly depending on the step size, calculations were performed using progressively smaller step sizes in system **(3-10)** until the output stopped changing. This was the case for step sizes smaller than *0.0001* years, which provided an output nearly identical to the reference model. Hence, this step size was used.

The output of the forward Euler method was also validated using Matlab's *ode45* solver. Disregarding the conditional threshold $P_{eye,c}$, which cannot be implemented in *ode45*, both methods produced SE values at $t = 25$ years that differed by $\pm 0.01D$. This was considered an acceptable margin of error.

Table 3.1: Parameter values used in the models

Descriptive model (3- 2)				
c_1	$13.29D$	c_5	$11.82D$	Exponential fit parameters
c_2	$-4.98\ yr^{-1}$	c_6	$-5.85\ yr^{-1}$	
c_3	$15.37D$	c_7	$14.96D$	
c_4	$-0.351\ yr^{-1}$	c_8	$-0.399\ yr^{-1}$	
C_1	$63.04D$	C_2	$62.57D$	Offset, targeted value at $t = 25$ years
Static ODE model (3-3)				
a_1	$-66.20\ D/yr$	a_5	$-69.09\ D/yr$	Derived from exponential fit parameters c_i using equation (3-4)
a_2	$-4.98\ yr^{-1}$	a_6	$-5.85\ yr^{-1}$	
a_3	$-5.39\ yr^{-1}$	a_7	$-5.97\ yr^{-1}$	
a_4	$-0.351\ yr^{-1}$	a_8	$-0.399\ yr^{-1}$	
$P_{ax}(t_0)$	$125.987D$	$P_{eye}(t_0)$	$130.059D$	Initial value at $t = -0.25$ years using (3-5)
ODE model with active feedback (3-8)				
g_1	-1.5	g_2	$-5\ yr^{-1}$	Coefficients of feedback Gompertz function
s_1	$Variable \in [0,1]$	s_3	$Variable \in [0,1]$	Amplitude of preprogrammed growth
s_2	$Variable \in [0,73]$	s_4	$Variable \in [0,73]$	Amplitude of feedback
ODE model with active feedback, myopia development and correction (3-10)				
t_{mo}	$Variable$			Time of myopization onset
Δ	$0\ before\ t_{mo}\ ,\ 0.1\ after\ t_{mo}$			Influence of excessive myopic growth
RC	$Variable$			Spherical refractive correction
$P_{eye,c}$	$60D$			Critical threshold of minimum P_{eye}

RESULTS

Model output

The ODE model with active feedback **(3-8)** is able to closely reproduce the reference with only minor differences in refractive error (**Figure 3-3a & b**). Meanwhile, an example of myopization model **(3-10)** shows a gradual start of myopic growth at *4* years when P_{ax} and P_{eye} both begin to decrease faster, until at *6.8* years P_{eye} reaches its minimal value $P_{eye,c}$. Meanwhile, axial power still reduces, leading to a subtle increase in the myopic progression rate (**Figure 3-3c & d**). The eye becomes myopic at *7.9* years and reaches a final refractive error at *24* years of *–3.69D*.

Preprogrammed growth vs. feedback

As the relative contributions of genetically preprogrammed growth and retinal feedback are unclear, one can assess their influence by varying the contributions s1 = s3 of the preprogrammed growth and determining the values of s2 = s4 that make the output of (3-8) match that of reference system (3-3). The values for the emmetropic reference curves are listed

in Table 3-2 and can be fitted by s2 = 0.0787·s12 – 1.0471·s1 + 0.9686 with r2 > 0.99. Note that

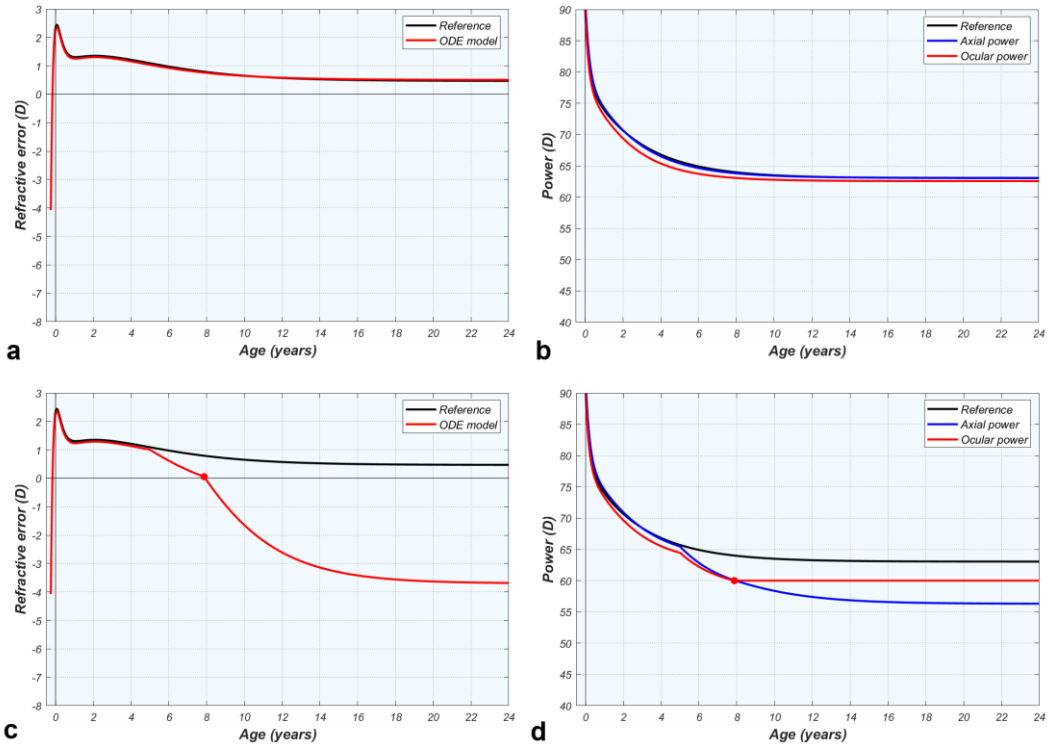

Figure 3.3: Changes in refractive error (a, c) and ocular and axial power (b, d). The top row shows the active feedback model (3-8) using s1 = s3 = 0.5 D/yr, and s2 = s4 = 34.20 D/yr. The bottom row shows the model (3-10) with myopization using s1 = s3 = 0.5 D/yr, s2 = s4 = 34.20 D/yr, Δ = 0.1, tmo = 5 yr, Peye,c = 60D and RC = 0. The round marker indicates when Peye reaches the critical value Peye,c.

choosing s1 ≠ s3 or s2 ≠ s4 produces unrealistic results, which is a limitation of the model.

In practice, the myopia results of model **(3-10)** are rather sensitive to variations in the relative contributions of the preprogrammed and feedback terms. This makes sense as a larger weight for the feedback term increases the sensitivity to myopogenic impulses (**Figure 3-3a**). The following assumes that the coefficients of the preprogrammed growth are $s_1 = s_3 = 0.5\ D/yr$ and the feedback coefficients are $s_2 = s_4 = 34.3\ D/yr$, unless stated otherwise.

Myopia variations

Several parameters affect the progression and end point of myopization in model **(3-8)**.

Table 3.2: Relative contributions of the preprogrammed growth and feedback to match the output of reference system (3-3)

$s_1 = s_3$	$s_2 = s_4$	$s_1 = s_3$	$s_2 = s_4$
0	*72.5*	*0.6*	*27.0*
0.1	*64.5*	*0.7*	*20.0*
0.2	*56.7*	*0.8*	*13.3*
0.3	*48.9*	*0.9*	*6.7*

0.4	*41.5*	*1*	*0.0*
0.5	*34.3*		

The first is the relative contribution of the preprogrammed and feedback terms, described in the previous section (**Figure 3.4a**). Next, an earlier onset of myopization t_{mo} leads to higher levels of myopia, whereas later onsets lead to lower levels (**Figure 3.4b**) as is well-known from the literature. Unsurprisingly, higher values of Δ, representing the influence of the excessive axial growth, lead to a high degree of myopia (**Figure 3.4c**). Finally, a high critical threshold $P_{eye,c}$, indicating an early disruption in homeostasis, leads to more myopia (**Figure 3.4d**). Note that these effects can also interact, reinforcing or attenuating each other to reach higher or lower refractive error values.

Refractive corrections

So far only uncorrected eyes were considered (i.e., $RC(t) = 0D$). If one would add a correction of $-1D$ whenever the uncorrected refractive error exceeds $-1D$, the uncorrected refractive error will vary according to a sawtooth function (**Figure 3.5a**). Considering the refractive correction as part of P_{eye}, the corresponding changes in P_{eye} resemble a stepwise decreasing function that always remains close to P_{ax} (**Figure 3.5b**).

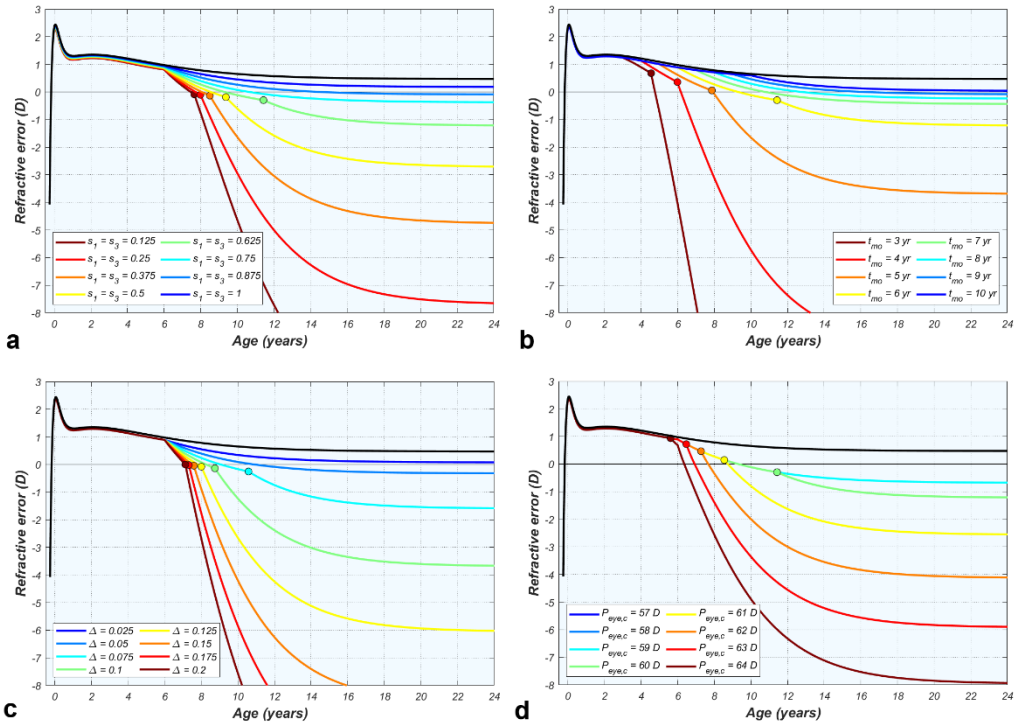

Figure 3.4: Changes in refractive error induced by varying model parameters for s1 = s3 = 0.5 D/yr and s2 = s4 = 34.30 D/yr, tmo = 6 yr, Δ = 0.1, Peye,c = 60D. a). Variations in the relative contributions of the pre-programmed and feedback components s1, …, s4; b). Variations in the time of myopization onset tmo; c). Variations in growth term Δ; d). Variations in critical threshold Peye,c.
The round marker indicates when Peye = Peye,c.

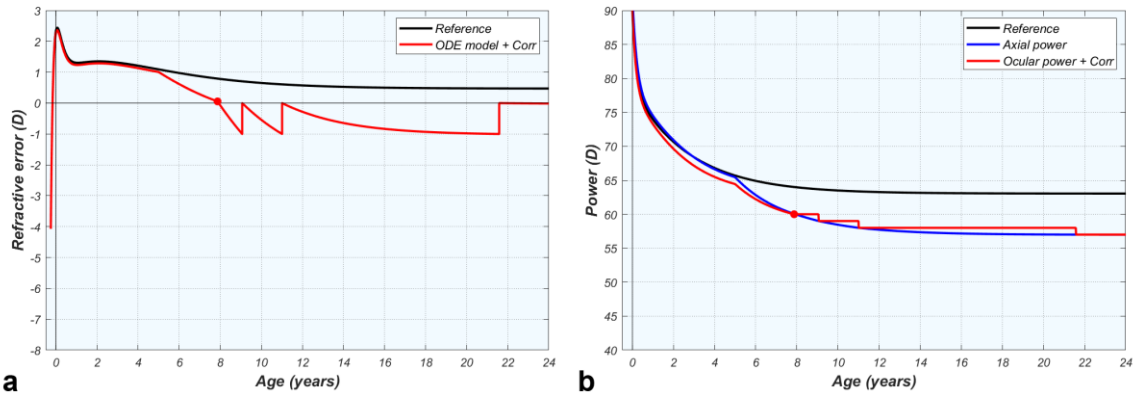

Figure 3.5: Influence of consecutive correction of the refractive error on a). the uncorrected refractive error and b). the axial power Pax and the combination of the ocular power and the refractive correction Peye + RC. Based on model (3-10) using the same parameters as Figure 3.2c&d. Refractive correction steps of –1D were added each time the uncorrected refractive error exceeded –1D.

Note that the model suggests that the final refractive error of the corrected eye was *–3.02D*, which is less myopic than the *–3.69D* produced by the same model without correction. Correcting the eye in larger steps leads to higher degrees of myopia (e.g., *–3.19D* for *–2D* steps), while smaller steps lead to less myopia (e.g., *–2.82D* for *–0.25D* steps). The model therefore predicts that undercorrection leads to higher degrees of myopia.

Imposed lenses

System **(3-8)** allows repeating animal experiments in which a positive or negative lens is fixated temporarily in front of the eye during its early rapid growth phase. In these experiments, imposing a positive lens creates a functional myopia that slows down eye growth, while the functional hypermetropia produced by imposing a negative lens leads to accelerated growth. Provided that the lens was imposed during early development, eye growth is able to compensate for it so that the combined system of lens and eye becomes emmetropic.[25, 36, 51, 52] After lens removal the eye will be severely ametropic, but in some species the growth rate can adjust a second time to compensate for this ametropia, provided the lens was removed during early axial growth.[52, 53] Meanwhile, experiments in human volunteers demonstrated that imposed lenses affect the choroidal thickness,[54-56] and hence the axial length, in the same way in the short term.

To simulate this, lenses of *+1D* and *–1D* were imposed to model **(3-8)** between the ages of *0.5* and *1.5* years. The positive lens led to slower growth (i.e., higher P_{ax} values) and by the end of the imposed lens period, P_{ax} matched the value of the combined power of P_{eye} and the imposed lens (**Figure 3.6a**). After lens removal, axial growth speed increased again so that the refractive error gradually reduced again. For the negative imposed lens, an increase in growth rate was seen

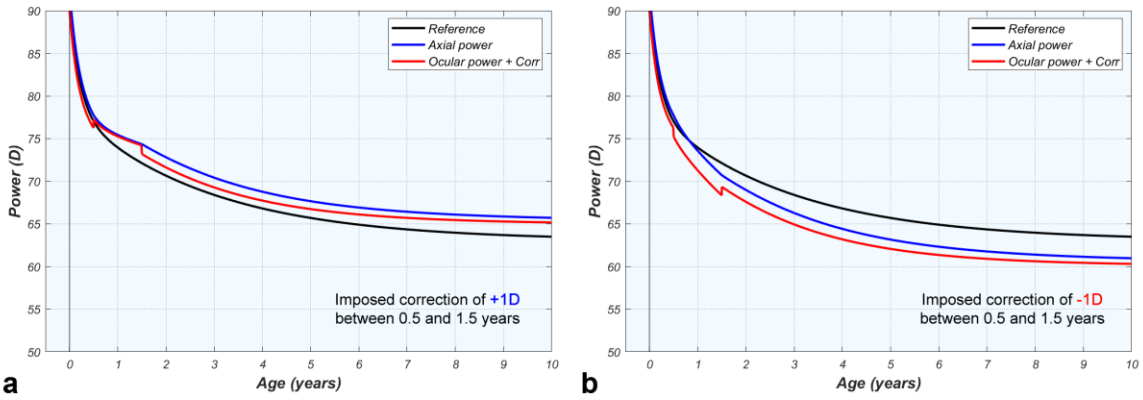

Figure 3.6: Influence of a lens of +1D (a) and -1D (b) imposed on the model between the ages of 0.5 and 1.5 years on the axial power Pax and the combination of the ocular power Peye without accommodation. Based on model (3-8) using s1 = s3 = 0.5 D/yr, s2 = s4 = 34.20 D/yr. Note the reduced age range compared to the other figures.

(i.e., lower P_{ax} values), but P_{ax} did not reach the combined power of P_{eye} and the imposed lens (**Figure 3.6b**). After lens removal, both the growth rate and the refractive error gradually reduce.

Form deprivation by diffusers

In other well-known animal experiments, a diffuser was placed in front of the eye during growth to deprive it of clear vision, eventually leading to myopia.[22] Since a diffuser would produce a blur circle with a fixed diameter, this can be simulated by assuming that feedback factor **(3-8)** has a constant value. Here the value *0.0333* was used, corresponding to the blur caused by an uncorrected refractive error of *±2D*. Doing so in the model from birth onwards leads to a rapid power loss for both P_{ax} and P_{eye} until $P_{eye} = P_{eye,c}$ and the eye becomes myopic with a final value of *–4.97D* (**Figure 3.7**). Higher levels of retinal scatter led to greater myopia. Choosing a large blur diameter, this model can also be used to describe the response to a light blocking filter.

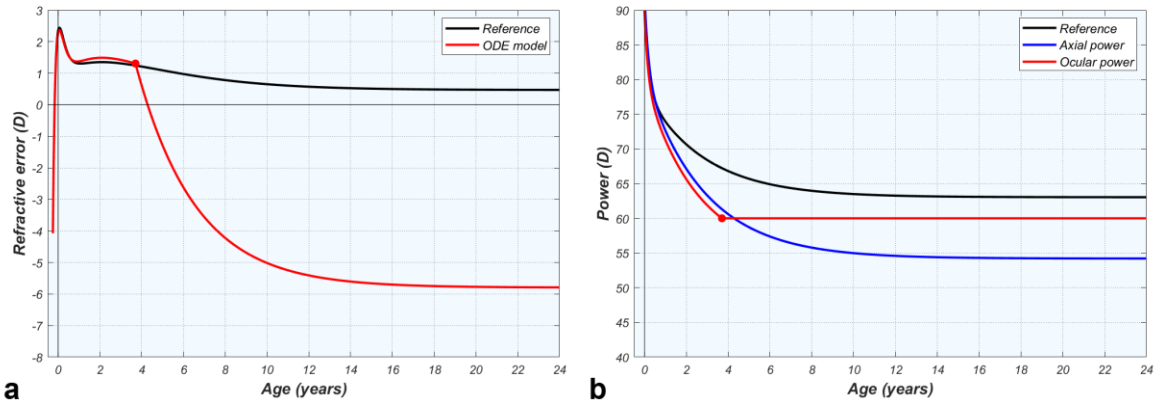

Figure 3.7: Influence of a diffuser with a fixed feedback value of 0.0333. a). uncorrected refractive error and b). axial power P_{ax} and ocular power P_{eye}. Parameters are those of Figure 3.2a&b.

DISCUSSION

To understand the basic principles of emmetropization and myopization, it is essential to

grasp how the regulatory mechanisms controlling eye growth are directed by retinal image blur. The optical, biochemical, and biomechanical interactions between the refractive components (cornea and lens) and posterior structures (retina, choroid, and sclera) play a vital role in this complex process. To this end, this work presented an ordinary differential equation (ODE) model to simulate normal and myopic eye growth with age under various external influences based on the axial power P_{ax} and whole-eye power P_{eye}. The proposed model is the first to account for the influence of the crystalline lens on refractive development, and has a modular architecture for its feedback function F and growth term Δ. These features allow it to reproduce many animal experiments and clinical observations, while remaining flexible to adjust to new observations in the literature once they become available.

The model proposed assumes that pre-programmed growth continues to affect refractive development to some degree for many years after birth, much like the Schaeffel and Howland model.[35] This feature was added to improve the model's robustness using the average growth curves of equations **(3-3)** that guide eye growth to a relatively normal shape, similar to how the rest of the human body finds it final shape through pre-programmed growth. This feature is supported by chicken experiments that could point at a fixed shape factor for healthy eyes,[57, 58] as well as the observation that the growth of the eye seems to slow down near the end of pregnancy (see **Figure 3.2a** of [2]). It is also noteworthy that in the average growth curves a minor phase difference is discernible between the axial and refractive powers (**Figure 3.3a&b**), with the former seemingly leading and the latter following, producing a dampened harmonic behavior(fluctuations) in the refractive error.[1, 2] This observation confirms the presence of active feedback mechanisms operating at the retinal level.

The following will delve deeper into the various aspects of the model.

Comparison with experiments

The proposed model reproduces the observations made in many animal experiments and clinical studies, such as:

1. Myopia is more severe when it has an early onset (**Figure 3.4b**).
2. The myopia progression rate increases at the time of myopia onset[45, 59] when $P_{eye} = P_{eye,c}$ (**Figure 3.3d**)
3. Undercorrection either promotes myopia progression[27] or has no effect (**Figure 3.6**).[60, 61]
4. A positive imposed refractive correction slows the axial growth rate (i.e., higher P_{ax} values), while a negative imposed lens accelerates it (**Figure 3.5**). If the imposed correction is transient, the refractive error returns to emmetropic values.[1, 22] This matches the observation that some infants can emmetropize from myopia.[21, 28, 29]

5. Form deprivation and light blocking leads to myopia (**Figure 3.7**).[1, 22] This is also seen in children with congenital cataract.

The model also makes two predictions:

1. Myopia will be more severe if the critical threshold $P_{eye,c}$ is higher (**Figure 3.4d**).
2. Interindividual variations in the a_i parameters[47] can alter these results, so some individuals will be more susceptible to myopogenic influences and others less susceptible.

Comparison with existing models

Several other models were presented in the literature, each with their own features (**Table 3.3**). Most are based on a combination of refractive error and accommodation, while accommodative lag, near time and illumination levels were used to generate myopia.

Table 3.3: Comparison of the ODE models in the literature

Author(s)	Year	Parameters	Feedback	Myopia using	Remark
Van Alphen[30]	*1961*	*S, Acc.*	Refr. error	–	Concept
Medina[31]	*1980*	*S*	Refr. error	–	Concept
Carroll[32]	*1982*	*S* + biometry	Refr. error	–	Concept
Medina[33, 34]	*1987 +*	*S*	Refr. error	Growth rate, refr. correction	Incl. growth
Schaeffel & Howland[35]	*1988*	*S, Acc., AL*	Refr. error	Imposed lens or form deprivation	Chicken model
Flitcroft[37]	*1998*	*S, Acc.,* near time	Refr. error	Acc. lag, near time	–
Blackie & Howland[41]	*1999*	*S, Acc.*	Retinal blur angle	Acc. lag, near time, illumination	–
Hung & Ciuffreda[42, 43, 62]	*1999 +*	*S, Acc., AL*	Retinal blur diam.	Acc. lag, near time, illumination	Incl. growth
Current	*2024*	P_{ax}, P_{eye}	Retinal blur diam.	Growth term	Incl. growth

Acc: accommodation; AL: axial length; Incl. growth: includes pre-programmed growth; Near time: time spent on near work; P_{ax}: axial power/ dioptric distance; P_{eye}: power of the entire eye; Refr: refractive; S: spherical refractive error.

Although these models were all well-built and presented behaviors closely resembling the observations available at the time, many no longer hold up to the current state of the literature as they either consider accommodation as a contributing factor or would produce myopia while undercorrecting (both of which have been disproven58). Meanwhile, the work closest in structure to the current model is the chicken model by Schaeffel and Howland,35 but it does not consider

the power of the crystalline lens.

Interpretation of parameters

Although most parameters in **Table 3.1** were treated as constants, some of these may be considered as functions in their own right. For example, the parameters controlling the pre-programmed growth in the models (i.e., a_1, a_2, a_5, a_6) are likely controlled by the factors that determine the overall intra-uterine growth, such as genetic predisposition and maternal factors (nutrition, smoking, infection, substance abuse, among others).[63] The same factors may also initialize the parameters of the feedback growth phase (i.e., a_3, a_4, a_7, a_8) before the influences of visual behavior[9, 10] and environment[12] assert themselves. Hence, amplitude parameters a_3 and a_7 were developed further to combine the continued pre-programmed growth (s_1 and s_3) with the feedback function F and accelerated growth term Δ that in turn are each affected by many factors as discussed in the following sections.

Feedback function

It is widely believed that retinal feedback is determined by the relative position of best focus to the retina. But despite many animal and clinical experiments,[1, 22] much remains unclear about how this leads to a growth response as photoreceptors cannot detect refractive error directly. Instead, the level of defocus must be derived by combining the intensity information from groups of photoreceptors through neural processing that takes cues from image contrast, which in turn is affected by the amount of near work,[64] higher order aberrations,[65] peripheral aberrations,[66, 67] chromatic aberrations,[68-70] optical properties of the photoreceptors,[71] as well as the luminance[12] and spatial frequencies[72] found in the environment. This information integrated locally in the retina and over time to create a feedback signal to adjust the axial growth rate. Under ideal circumstances this signal creates a closed loop that guides emmetropization and homeostasis (described by feedback function F), but myopogenic influences could break this cycle into an open loop that produces a runaway myopization (controlled by term Δ).[35, 58] In this initial version of the model only the simplest expressions for F and Δ were considered to allow exploring the influence of each without the complicated relationships that control them. These expressions will be updated in the next iterations of the model.

Besides feedback function (3-9) used in this work, other expressions were considered as well. The first was F = –S = –(Pax – Peye), designed to minimize the refractive error directly. While this option, used in several earlier models,34, 66 was able to reproduce most of the experiments above, its results suggested that a full refractive correction stimulates myopia development and that undercorrection would be beneficial. This idea was popular in the 1990s supported by

numerous animal studies,[22] but has since been proven to promote rather than inhibit myopization in humans.[26, 27, 58, 73] To explain this, Schaeffel and Swiatczak[58] hypothesized that the mechanism of emmetropization may be less sensitive to existing myopic refractive errors.

Another expression considered was based on accommodative lag (see **Appendix B**, **B4**), which has long been thought of as a risk factor as it causes the image of a nearby object to form behind the retina, thus forming trigger for axial growth. However, while this was able to reproduce all results presented above and was used in other models,[37, 41-43] this function was abandoned as the role of accommodative lag in myopia development has been called into question. Although myopes do indeed have more accommodative lag than emmetropes,[74] it could not be confirmed whether this lag was already present before myopia onset[75] or whether it affects the progression rate.[76] Recent work also suggested that the accommodative lag is rather small,[77] so its influence may be small as well and likely more associated with the duration of the lag than the lag itself.[1]

The third expression considered was based on wavefront aberrations as it is known that accommodation not only leads to a desired increase in lens power, but also to larger amounts to higher order aberrations[78, 79] that reduce the retinal image quality.[80, 81] The most notable change occurs in the total spherical aberration of the eye, which begins to reduce at *1D* of accommodation and becomes negative at *3–4D*. Based on this observation, it has been theorized that this negative spherical aberration causes a lower retinal image contrast that could work as a possible trigger for myopic growth.[79, 81] Implementing this into the model would involve adding a constant term *Δ*, exactly as was done in equation **(3-9)**, offering a plausible explanation for that expression.

Limitations

In its current form, the proposed model provides a first-order description guided by average growth curves2 for stability. While this stability permits the description to closely match many observations in the literature, it also imposes a few restrictions. For example, the inclusion of the power loss term alongside the a3 and a7 coefficients may cause an early slowdown of myopic growth due to the exponential factors. As such, the model is not able to describe late-teenage progression or adult-onset myopia. Moreover, it assumes that the weight of the feedback function is the same for both Pax and Peye (i.e., s2 = s4). While this is probably not the case for mechanical reasons, choosing s2 ≠ s4 in the current model leads to unphysiological growth curves and was not explored further for now. Other limitations lie in the form of the feedback function F, which was chosen to be minimalistic in this initial version. One final limitation is the model's behavior at Peye = Peye,c, when Peye becomes a constant. This may be true in some cases, while in others the power loss would slow down and stop later. The latter would reduce the myopic

behavior of the model but would not affect the overall results. This too will be addressed in a future version.

Applications and future directions

Given the modular format of the model, future versions should include alternative feedback functions that are different for axial and refractive powers, to account for the influence of environmental and behavioral factors, temporal integration, as well as the retinal factors controlling axial[53, 65] and lenticular[82] development. By trying different feedback functions and comparing the outcome to clinical and animal experiments, it may be possible to approximate the form of the physiological feedback function. This could help refine our understanding of the interactions between ocular growth and external factors and help develop new avenues for further research into myopia development and myopia control.

The model may also be customized to clinical measurements, but as the outcomes depend greatly on environmental and behavioral circumstances based on individual decisions (e.g., sudden changes in near work or outdoor light exposure), the model may have difficulties with accurately forecasting the refractive error of an individual eye. Instead, it could be used for patient education by presenting parents and children with personalized “what if” scenarios to show the impact of behavioral patterns known to increase myopia.

Conclusions

This work presented a model that describes eye growth and refractive error development as a first order ODE system of the ocular and axial power that reproduces many of the animal and clinical experiments in the literature. This platform contributes to a broader understanding of the origins of refractive errors and may in the future help develop new solutions for myopia control.

REFERENCES

1. Rozema J, Dankert S, Iribarren R. Emmetropization and non-myopic eye growth. Surv Ophthalmol. 2023.
2. Rozema JJ. Refractive development I: Biometric changes during emmetropisation. Ophthal Physiol Opt. 2023;43(3):347-67.
3. Wallman J, Winawer J. Homeostasis of eye growth and the question of myopia. Neuron. 2004;43(4):447-68.
4. Gwiazda J, Thorn F, Bauer J, Held R. Emmetropization and the progression of manifest refraction in children followed from infancy to puberty. Clin Vis Sci. 1993;8(4):337-44.
5. Straub M. Über die Atiologie der Brechungsanomalien des Auges und den Ursprung der Emmetropie. von Graefes Arch Ophthalmol. 1909;70:130-99.
6. Flitcroft D. Emmetropisation and the aetiology of refractive errors. Eye. 2014;28(2):169-79.
7. Flitcroft D. Is myopia a failure of homeostasis? Exp Eye Research. 2013;114:16-24.
8. Morgan IG, Wu P-C, Ostrin LA, Tideman JWL, Yam JC, Lan W, et al. IMI risk factors for myopia. Invest Ophthalmol Vis Sci. 2021;62(5):3-.
9. Huang H-M, Chang DS-T, Wu P-C. The association between near work activities and myopia in children—a systematic review and meta-analysis. PLoS One. 2015;10(10):e0140419.
10. French AN, Ashby RS, Morgan IG, Rose KA. Time outdoors and the prevention of myopia. Exp Eye Research. 2013;114:58-68.
11. Dirani M, Tong L, Gazzard G, Zhang X, Chia A, Young TL, et al. Outdoor activity and myopia in Singapore teenage children. Br J Ophthalmol. 2009;93(8):997-1000.
12. Cohen Y, Iribarren R, Ben-Eli H, Massarwa A, Shama-Bakri N, Chassid O. Light intensity in nursery schools: a possible factor in refractive development. Asia-Pac J Ophthalmol. 2022;11(1):66-71.
13. Smith EL, Hung L-F, Huang J. Protective effects of high ambient lighting on the development of form-deprivation myopia in rhesus monkeys. Invest Ophthalmol Vis Sci. 2012;53(1):421-8.
14. Mutti DO, Sinnott LT, Mitchell GL, Jordan LA, Friedman NE, Frane SL, et al. Ocular component development during infancy and early childhood. Optom Vis Sci. 2018;95(11):976.
15. Jongenelen S, Rozema JJ, Tassignon M-J. Distribution of the crystalline lens power in vivo as a function of age. Invest Ophthalmol Vis Sci. 2015;56(12):7029-35.
16. Iribarren R, Morgan IG, Chan YH, Lin X, Saw S-M. Changes in lens power in Singapore Chinese children during refractive development. Invest Ophthalmol Vis Sci. 2012;53(9):5124-30.
17. Wildsoet C. Active emmetropization—evidence for its existence and ramifications for clinical practice. Ophthal Physiol Opt
1997;17(4):279-90.
18. Gordon RA, Donzis PB. Refractive development of the human eye. Arch Ophthalmol. 1985;103(6):785-9.
19. Ishii K, Yamanari M, Iwata H, Yasuno Y, Oshika T. Relationship between changes in crystalline lens shape and axial elongation in young children. Invest Ophthalmol Vis Sci. 2013;54(1):771-7.
20. Chen Y, Wang W, Wang J, Chen X, Zhu Z, Li J, et al. Normal range of ocular biometry in healthy children: A systemic review and meta-analysis of 33,559 individuals under seven years of age. Ophthal Physiol Opt. 2022;42(6):1264-75.
21. Mutti DO, Mitchell GL, Jones LA, Friedman NE, Frane SL, Lin WK, et al. Axial growth and changes in lenticular and corneal power during emmetropization in infants. Invest Ophthalmol Vis Sci. 2005;46(9):3074-80.
22. Troilo D, Smith EL, Nickla DL, Ashby R, Tkatchenko AV, Ostrin LA, et al. IMI–Report on experimental models of emmetropization and myopia. Invest Ophthalmol Vis Sci. 2019;60(3):M31-M88.
23. Schaeffel F, Feldkaemper M. Animal models in myopia research. Clin Exp Optom. 2015;98(6):507-17.
24. Zadnik K, Mijtti DO. How applicable are animal myopia models to human juvenile onset myopia? Vis Research. 1995;35(9):1283-8.
25. Schaeffel F, Troilo D, Wallman J, Howland HC. Developing eyes that lack accommodation grow to compensate for imposed defocus. Vis Neurosci. 1990;4(2):177-83.
26. Wildsoet CF, Chia A, Cho P, Guggenheim JA, Polling JR, Read S, et al. IMI–interventions for controlling myopia onset and progression report. Invest Ophthalmol Vis Sci. 2019;60(3):M106-M31.
27. Chung K, Mohidin N, O'Leary DJ. Undercorrection of myopia enhances rather than inhibits myopia progression. Vis Research. 2002;42(22):2555-9.
28. Wood I, Hodi S, Morgan L. Longitudinal change of refractive error in infants during the first year of life. Eye. 1995;9(5):551-7.
29. Ehrlich DL, Braddick OJ, Atkinson J, Anker S, Weeks F, Hartley T, et al. Infant emmetropization: longitudinal changes in refraction components from nine to twenty months of age. Optom Vis Sci. 1997;74(10):822-43.
30. Van Alphen G. On emmetropia and ametropia. Basel: Karger; 1961.
31. Medina Puerta A. El origen de las ametropías:¿ Qué es ametropía? Gaceta Óptica. 1980(112):46-8.
32. Carroll JP. On emmetropization. J Theoret Biol. 1982;95(1):135-44.
33. Medina A. A model for emmetropization: predicting the progression of ametropia. Ophthalmologica. 1987;194(2-3):133-9.
34. Medina A, Fariza E. Emmetropization as a first-order feedback system. Vis Research. 1993;33(1):21-6.
35. Schaeffel F, Howland HC. Mathematical model of emmetropization in the chicken. J Opt Soc Am A. 1988;5(12):2080-6.
36. Schaeffel F, Glasser A, Howland HC. Accommodation, refractive error and eye growth in chickens. Vis

Research. 1988;28(5):639-57.
37. Flitcroft D. A model of the contribution of oculomotor and optical factors to emmetropization and myopia. Vis Research. 1998;38(19):2869-79.
38. Hung GK. Linear model of accommodation and vergence can account for discrepancies between AC/A measures using the fixation disparity and phoria methods. Ophthal Physiol Opt 1991;11(3):275-8.
39. Hung GK, Semmlow JL. Static behavior of accommodation and vergence: computer simulation of an interactive dual-feedback system. IEEE Trans Biomed Eng. 1980(8):439-47.
40. Schor CM. Models of mutual interactions between accommodation and convergence. Optom Vis Sci. 1985;62(6):369-74.
41. Blackie C, Howland H. An extension of an accommodation and convergence model of emmetropization to include the effects of illumination intensity. Ophthal Physiol Opt. 1999;19:112-25.
42. Hung GK, Ciuffreda KJ. Model of human refractive error development. Curr Eye Research. 1999;19(1):41-52.
43. Hung GK, Ciuffreda KJ. A unifying theory of refractive error development. Bull Math Biol. 2000;62(6):1087-108.
44. Mutti DO, Mitchell GL, Sinnott LT, Jones-Jordan LA, Moeschberger ML, Cotter SA, et al. Corneal and crystalline lens dimensions before and after myopia onset. Optom Vis Sci. 2012;89(3):251-62.
45. Rozema J, Dankert S, Iribarren R, Lanca C, Saw S-M. Axial growth and lens power loss at myopia onset in Singaporean children. Invest Ophthalmol Vis Sci. 2019;60(8):3091-9.
46. Han X, Xiong R, Jin L, Chang S, Chen Q, Wang D, et al. Role of lens in early refractive development: evidence from a large cohort of Chinese children. Br J Ophthalmol. 2024.
47. Farzanfar A, Rozema JJ. Bi-exponential description for different forms of refractive development J Vision. 2024;(in press).
48. Del Giudice M. Alone in the dark? Modeling the conditions for visual experience in human fetuses. Develop Psychobiol. 2011;53(2):214-9.
49. Gompertz B. XXIV. On the nature of the function expressive of the law of human mortality, and on a new mode of determining the value of life contingencies. In a letter to Francis Baily, Esq. FRS &c. Phil Trans Roy Soc Lon. 1825(115):513-83.
50. Tedja MS, Haarman AE, Meester-Smoor MA, Kaprio J, Mackey DA, Guggenheim JA, et al. IMI–myopia genetics report. Invest Ophthalmol Vis Sci. 2019;60(3):M89-M105.
51. Irving E, Sivak J, Callender M. Refractive plasticity of the developing chick eye. Ophthal Physiol Opt 1992;12(4):448-56.
52. Hung L-F, Crawford ML, Smith EL. Spectacle lenses alter eye growth and the refractive status of young monkeys. Nature medicine. 1995;1(8):761-5.
53. Wallman J, Adams JI. Developmental aspects of experimental myopia in chicks: susceptibility, recovery and relation to emmetropization. Vis Research. 1987;27(7):1139-63.
54. Read SA, Collins MJ, Sander BP. Human optical axial length and defocus. Invest Ophthalmol Vis Sci. 2010;51(12):6262-9.
55. Chiang STH, Phillips JR, Backhouse S. Effect of retinal image defocus on the thickness of the human choroid. Ophthal Physiol Opt 2015;35(4):405-13.
56. Wang D, Chun RKM, Liu M, Lee RPK, Sun Y, Zhang T, et al. Optical defocus rapidly changes choroidal thickness in schoolchildren. PloS One. 2016;11(8):e0161535.
57. Schaeffel F, Howland HC. Properties of the feedback loops controlling eye growth and refractive state in the chicken. Vis Research. 1991;31(4):717-34.
58. Schaeffel F, Swiatczak B. Mechanisms of emmetropization and what might go wrong in myopia. Vis Research. 2024;220:108402.
59. Mutti DO, Hayes JR, Mitchell GL, Jones LA, Moeschberger ML, Cotter SA, et al. Refractive error, axial length, and relative peripheral refractive error before and after the onset of myopia. Invest Ophthalmol Vis Sci. 2007;48(6):2510-9.
60. Lawrenson JG, Shah R, Huntjens B, Downie LE, Virgili G, Dhakal R, et al. Interventions for myopia control in children: a living systematic review and network meta-analysis. Cochrane Database Syst Rev. 2023(2):CD014758.
61. Prousali E, Haidich A-B, Dastiridou A, Tzamalis A, Ziakas N, Mataftsi A. Part-time versus full-time spectacles for myopia control (PARMA study): a randomized clinical trial. Cureus. 2022;14(6).
62. Hung GK, Mahadas K, Mohammad F. Eye growth and myopia development: Unifying theory and Matlab model. Comp Biol Med. 2016;70:106-18.
63. Strauss RS. Effects of the intrauterine environment on childhood growth. Brit Med Bull. 1997;53(1):81-95.
64. Gajjar S, Ostrin LA. A systematic review of near work and myopia: measurement, relationships, mechanisms and clinical corollaries. Acta Ophthalmologica. 2022;100(4):376-87.
65. Hughes RP, Vincent SJ, Read SA, Collins MJ. Higher order aberrations, refractive error development and myopia control: a review. Clin Exp Optom. 2020;103(1):68-85.
66. Romashchenko D, Rosén R, Lundström L. Peripheral refraction and higher order aberrations. Clin Exp Optom. 2020;103(1):86-94.
67. Zheleznyak L. Peripheral blur may provide the eye with a cue for the sign of defocus. J Vision. 2023;23(11):83-.
68. Rucker FJ, Wallman J. Chick eyes compensate for chromatic simulations of hyperopic and myopic defocus:

evidence that the eye uses longitudinal chromatic aberration to guide eye-growth. Vis Research. 2009;49(14):1775-83.
69. Gawne TJ, Grytz R, Norton TT. How chromatic cues can guide human eye growth to achieve good focus. J Vision. 2021;21(5):11-.
70. Swiatczak B, Schaeffel F. Myopia: why the retina stops inhibiting eye growth. Sci Reports. 2022;12(1):21704.
71. Vohnsen B. Geometrical scaling of the developing eye and photoreceptors and a possible relation to emmetropization and myopia. Vis Research. 2021;189:46-53.
72. Flitcroft DI, Harb EN, Wildsoet CF. The spatial frequency content of urban and indoor environments as a potential risk factor for myopia development. Invest Ophthalmol Vis Sci. 2020;61(11):42-.
73. Yazdani N, Sadeghi R, Ehsaei A, Taghipour A, Hasanzadeh S, Zarifmahmoudi L, et al. Under-correction or full correction of myopia? A meta-analysis. Journal of Optometry. 2021;14(1):11-9.
74. Gwiazda J, Thorn F, Bauer J, Held R. Myopic children show insufficient accommodative response to blur. Invest Ophthalmol Vis Sci. 1993;34(3):690-4.
75. Mutti DO, Mitchell GL, Hayes JR, Jones LA, Moeschberger ML, Cotter SA, et al. Accommodative lag before and after the onset of myopia. Invest Ophthalmol Vis Sci. 2006;47(3):837-46.
76. Koomson NY, Amedo AO, Opoku-Baah C, Ampeh PB, Ankamah E, Bonsu K. Relationship between reduced accommodative lag and myopia progression. Optom Vis Sci. 2016;93(7):683-91.
77. Labhishetty V, Cholewiak SA, Roorda A, Banks MS. Lags and leads of accommodation in humans: Fact or fiction? J Vision. 2021;21(3):21-.
78. Li Y-J, Choi JA, Kim H, Yu S-Y, Joo C-K. Changes in ocular wavefront aberrations and retinal image quality with objective accommodation. J Cataract Refr Surg. 2011;37(5):835-41.
79. Del Águila-Carrasco AJ, Kruger PB, Lara F, López-Gil N. Aberrations and accommodation. Clin Exp Optom. 2020;103(1):95-103.
80. López-Gil N, Martin J, Liu T, Bradley A, Díaz-Muñoz D, Thibos LN. Retinal image quality during accommodation. Ophthal Physiol Opt
2013;33(4):497-507.
81. Thibos LN, Bradley A, López-Gil N. Modelling the impact of spherical aberration on accommodation. Ophthal Physiol Opt
2013;33(4):482-96.
82. Linne C, Mon KY, D'souza S, Jeong H, Jiang X, Brown DM, et al. Encephalopsin (OPN3) is required for normal refractive development and the GO/GROW response to induced myopia. Mol Vision. 2023;29:39.

Chapter 5. The influence of color and defocus on contrast sensitivity function

In preparation as:

Arezoo Farzanfar, José Manuel González-Méijome, Rute J. Macedo de Araújo, António Queirós Pereira, Jos J Rozema

The influence of color and defocus on contrast sensitivity function

INTRODUCTION

The variations in retinal image quality caused by defocus are of great interest as they may affect the retinal feedback during emmetropization.[1, 2] Additionally, it is known that accommodation and emmetropization, which influence eye development, are affected by both retinal defocus and the spectral composition of the ambient light.[3-5] Understanding these mechanisms is essential for explaining visual development and developing potential interventions for vision disorders.[6] For instance, deprivation studies in chicks found that intermittent periods of normal vision significantly reduced the progression of myopia, highlighting how characteristics of visual stimuli such as contrast and spatial frequencies affect refractive development.[7, 8] Also, it has been proposed that changes in retinal image brightness and contrast sensitivity (CS) under dim light conditions are crucial factors that can induce refractive changes.[9] As prevalence of myopia grows, understanding visual nuances across refractive conditions is crucial.

Compared to visual acuity (VA), the Contrast Sensitivity Function (CSF) is a metric to comprehensively evaluate the eye's ability to discern differences in contrast across spatial frequencies and colors.[10] Lens-induced defocus affects the quality of the retinal image, and consequently the CSF. Therefore, our study aimed to assess the CSF for different combinations of light colors and defocus levels.

Several studies explored how defocus leads to a decrease in CSF,[11, 12] alters the shape of the CSF in large pupils,[13, 14] and varies between individuals. For instance, Radhakrishnan et al.[15] examined contrast sensitivity under cycloplegia for different levels of positive and negative defocus in individuals with and without myopia, and reported notable differences in contrast sensitivity between both groups.[15] Non-myopic eyes experience a reduction in CSF at higher spatial frequencies as defocus increases, regardless of whether positive or negative lenses are used, while myopes show a more pronounced decrease in CSF with positive defocus compared to

negative defocus due to latent accommodation.[7] Other studies explored how defocus affects CSF at different ages in healthy individuals, and found that this influence diminishes with age due to changes in the optical properties of the eye.[16, 17] Furthermore, analyses of CSF in people with various degrees of myopia wearing spectacle or contact lens corrections found that low to moderate myopes exhibit normal levels of contrast sensitivity, whereas high myopes experienced significant reductions, particularly when wearing spectacles.[4] This suggests that, while contact lenses can address optical errors better compared to spectacles, they may not fully compensate for contrast sensitivity losses due to myopic retinal changes.[4, 18-20]

Although the achromatic CSF has been extensively studied and was comprehensively discussed in Barten's review,[21, 22] there were also studies on chromatic CSF across different ranges of luminance levels. Granger and Heurtley (1973) observed low-pass characteristics for red-green CSFs on a yellow background, noting high-frequency patterns appeared achromatic.[23] Green (1985) conducted experiments with colored sine-gratings without isoluminant patterns, yielding data resembling achromatic CSFs under controlled but atypical conditions.[24] Mullen (1985) focused on data that excluded chromatic aberration effects and was limited to a single luminance level.[25] In 1975, Cavonius et al.[24, 26] assessed the contrast sensitivity for individual color filters using Wratten filters for spatial frequencies ranging from 0 to 32 cycles per degree (cpd). Red and green filters had similar contrast sensitivity functions, while it was reduced for the blue filter, which may be associated with the inherent chromatic aberrations of the eye.[26] Furthermore, contrast sensitivity is found to be lower for chromatic than for achromatic stimuli.[22, 27]

For this study, the focus was on young adults aged 20-35 years. Moreover, achromatic sensitivity decreases with age, which is more pronounced at higher luminance levels and for higher spatial frequencies. Chromatic sensitivity also shows consistent age effects.[28-30]

This study examines how different lens-induced defocus levels and colors impact CSF in emmetropic and myopic individuals. While previous research focused on either the influence of positive and negative defocus effects or the influence of light color, this work simultaneously considered both as the interaction between these factors remains unclear. Additionally, the potential causes for the reduction in CSF for blue light compared to other colors are discussed.

METHODS

Participants

In this prospective study, a total of thirty volunteers (30 eyes) were recruited, including emmetropes (19) and myopes (11), to assess their contrast sensitivity functions (CSF). These

measurements were performed for four color bands (white, green, red, and blue) and a range of defocuses between ±1.50D in 0.50 D steps by placing trial lenses as close as possible to participants' eyes. This study was approved by the Ethics Committee of the University of Minho, Braga, Portugal, and all participants gave informed consent before the measurements.

Participants were recruited from the optometry students at the University of Minho and were young adults (20–35 years old) in good ocular health. All had visual acuity of at least 0.02 LogMar with their habitual correction. Prior to measurements, two drops of Tropicamide 0.5% (Tropicil, Laboratórios Davi, Portugal) were instilled with a 5 min interval in one eye. This was usually the left eye, unless the left eye had to be excluded, and the right eyes met the inclusion criteria instead. Thirty minutes after the second drop, the refractive error was determined with an open-field auto-refraction using the WAM-5500 (Grand Seiko, Hiroshima, Japan), followed by the axial length and corneal keratometry using the IOLMaster 500 (Zeiss, Wetzlar, Germany), and the whole-eye aberrations of the eye were measured the IRX3 Hartmann-Shack aberrometer (ImagineEyes, Orsay, France).

Participants with a spherical refractive error of -1.25D or more under cycloplegia were included in the myopic group and all others were considered emmetropic, while participants with a refractive astigmatism over –2.50D were excluded. During the experiment, the refractive error of all participants was corrected using trial lenses. Their biometric information is given in **Table 4.1**.

Dichroic filters

We used the red (FD1R), green (FD1G), and blue (FD1B) dichroic filters by Thorlabs (Newton, NJ, USA) to produce colored light for the experiment. The filters were mounted onto a spectacle frame designed for contrast sensitivity testing consisting of a closed opaque mask sealed against the face that only allowed light to enter through the filters. Filters were tested in a random order.

Contrast sensitivity

The contrast sensitivity was examined under photopic conditions (85 cd/m^2) and without glare using the Functional Vision Analyzer (FVA, Optec, Stereo Optical Co., Inc., Chicago, IL, USA), a closed system testing device (**Figure 4.1**). The testing environment was prepared beforehand, ensuring adequate ambient lighting and proper equipment calibration.

The FVA shows gratings in three orientations (vertical, tilted 15° to the right, and tilted 15° to the left) as a series static, grayscale sinusoidal patterns in 9 contrast levels. These pattern

series are presented sequentially for spatial frequencies of 1.5, 3, 6, and 18 cycles per degree (cpd). Participants were asked to identify the orientation of each grating and the threshold for each spatial frequency was determined as the last correctly identified contrast patch. All results were converted to logarithmic values. CSF testing lasted approximately 75 minutes, with brief resting times between tests.

Fig. 4.1. The Functional Vision Analyzer

Table 4.1. Biometrics of the participants included in measurements

Parti-cipant	Age	Sex	Eye	LogMAR	Sphere	Cylinder	Axis	Spherical Equivalent	Axial length	Keratometry (R1/R2)
Emmetropes										
E1	31	F	Right		-0.25			-0.25	23.60	8.20/8.10
E2	32	F	Right	-0.12	0.50			0.50	23.35	7.87/7.63
E3	22	F	Right	-0.08	0.50			0.50	23.31	8.04/7.81
E4	20	F	Right	-0.08	0.50			0.50	22.57	7.58/7.30
E5	20	F	Right	-0.12	0.25			0.25	23.12	7.88/7.74
E6	34	M	Right	-0.12	-0.25			-0.25	24.20	7.63/7.56
E7	18	M	Right	-0.10	0.25	-1.25	10	-0.38	24.24	8.09/7.77
E8	28	M	Right	-0.10	0.75			0.75	24.05	8.27/8.10
E9	25	F	Right	-0.10	0.50			0.50	23.43	8.07/7.93
E10	19	F	Right	-0.04	0.25			0.25	24.16	8.41/8.23
E11	29	F	Right	0.00	-0.25			-0.25	23.42	7.96/7.85
E12	19	F	Right	-0.02	0.00			0.00	23.77	7.86/7.65
E13	20	F	Right	-0.06	0.00			0.00	23.03	7.60/7.44
E14	20	F	Right	-0.04	0.00			0.00	23.69	8.08/8.06
E15	21	F	Left	0.00	-0.25			-0.25	23.57	8.14/8.03
E16	18	F	Right	0.02	0.25			0.25	22.40	7.86/7.72
E17	18	F	Right	-0.06	0.75			0.75	23.53	8.05/7.88
E18	31	F	Right	0.00	0.25			0.25	23.03	7.70/7.44
E19	20	M	Right	-0.04	0.00			0.00	24.30	8.11/8.03
Mean ± STD	23.42 ± 5.52			-0.06 ± 0.05	0.20 ± 0.33			0.16 ± 0.35	23.51 ± 0.56	R1: 7.96 ± 0.23 R2: 7.79 ± 0.25
Myopes										
M1	24	M	Right	-0.10	-2.50			-2.50		
M2	35	F	Right	0.00	-5.00			-5.00	25.21	7.63/7.49
M3	25	F	Right	-0.10	-4.50	-1.00	165	-5.00	24.81	7.38/7.19
M4	22	F	Right	-0.02	-2.25	-1.25	90	-2.88	24.53	7.84/7.74
M5	19	F	Right	-0.10	-1.75	-1.00	180	-2.25	24.14	7.71/7.48
M6	19	F	Left	-0.02	-2.25			-2.25	23.89	7.44/7.41
M7	20	F	Right	-0.02	-3.50	-2.50	10	-4.75	24.92	7.97/7.56
M8	20	F	Right	0.00	-1.50			-1.50	24.60	8.00/7.77
M9	19	F	Right	0.00	-2.25	1.25	10	-1.63	24.72	8.10/7.77
M10	20	F	Right	-0.02	-4.50	-0.75	160	-4.88	25.51	7.97/7.84
M11	19	F	Right	0.00	-3.50	-1.00	110	-4.00	24.34	7.58/7.46
Mean ± STD	22.00 ± 4.80			-0.03 ± 0.04	-3.10 ± 1.20	-0.90 ± 1.11	103.6 ± 71.3	-3.33 ± 1.41	24.70 ± 0.48	R1:7.76 ± 0.25 R2:7.57 ± 0.21

Statistical Analysis

The statistical analysis consisted of t-tests and ANOVAs to compare the CSF between groups. To investigate the influence of multiple independent variables on CSF, a multiple linear regression was performed. Statistical analysis was performed using SPSS software (Windows version 29.0.2.0; SPSS, Inc., Chicago, IL, USA), and statistical significance was defined as $P < 0.05$.

RESULTS

Influence of defocus

The mean in-focus white light CSF of myopes was slightly lower than that of non-myopes, especially at high spatial frequencies (**Figure 4.2**). T-test analysis of the in-focus contrast sensitivity for white color per refractive group (emmetropic and myopic group) shows that there is a significant difference between both groups for spatial frequencies of 3 and 6 cpd (two-tailed t-test; $p = 0.032$ and $p = 0.024$, respectively; **Table 4.2**).

The white light CSF decreased significantly with increasing amounts of positive or negative defocus as indicated by the ANOVA results in **Table 4.2**. Emmetropes showed a significant difference between all levels of defocus (positive and negative), while for myopes no differences were seen for high spatial frequencies (12 and 18 cpd). Overall, the CSF values in both groups are higher for negative defocus than for positive defocus (**Figure 4.2**).

Table 4.2. Significance of the influence of refractive error and level of imposed defocus on CSF

	Emmetropes vs. myopes, in focus (t-test)		Between defocus groups (ANOVA) Emmetropes		Myopes	
Spatial frequency	**t**	**P value***	**F**	**P value***	**F**	**P value***
1.5 cpd	0.933	0.359	13.246	**0.000**	11.645	**0.000**
3 cpd	2.258	**0.032**	20.976	**0.000**	8.764	**0.000**
6 cpd	2.385	**0.024**	10.518	**0.000**	4.220	**0.002**
12 cpd	1.038	0.309	5.082	**0.000**	1.653	0.168
18 cpd	1.830	0.079	2.861	**0.020**	1.631	0.178

* Significant if $P < 0.05$

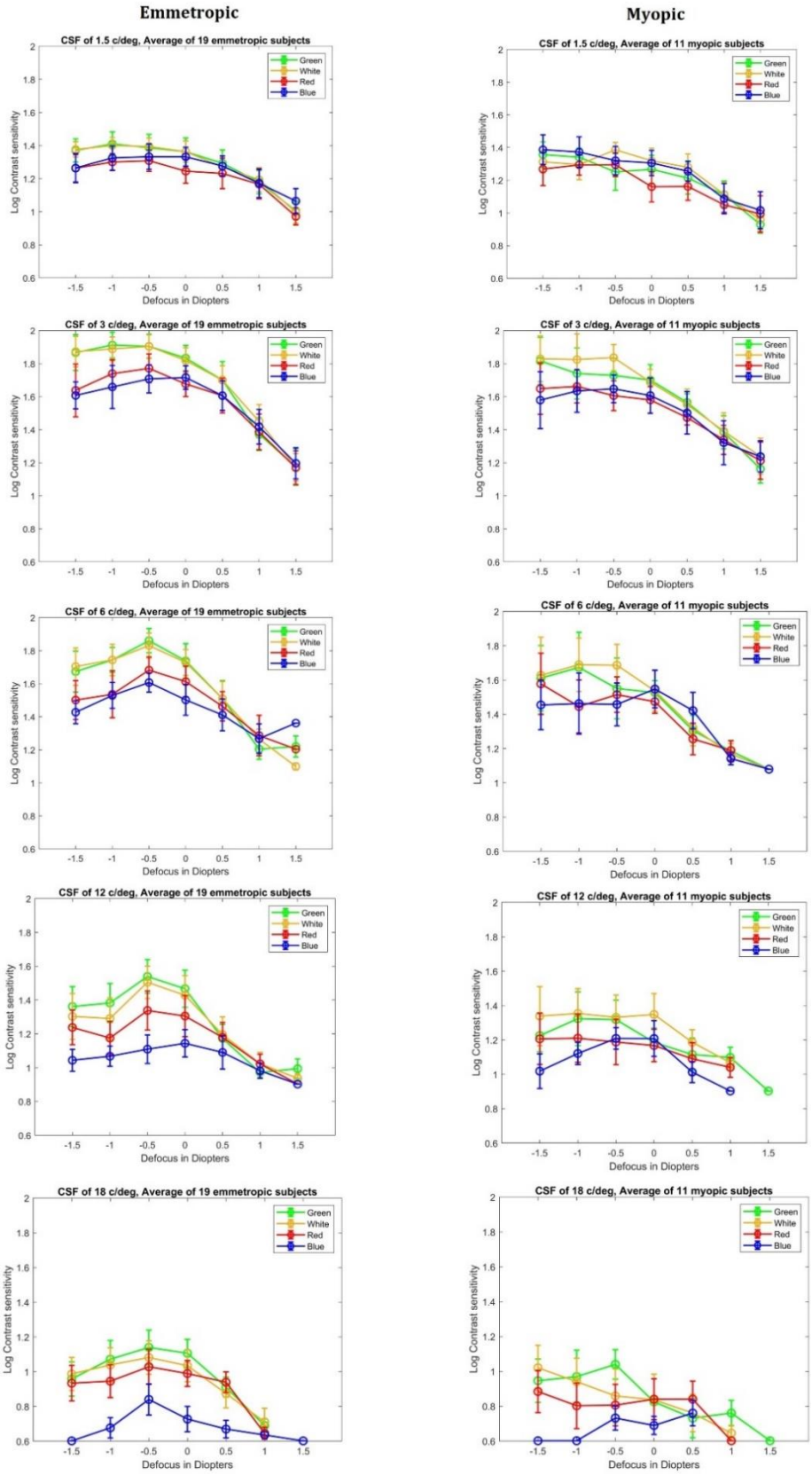

Fig. 4.2. Effect of defocus on log contrast sensitivity, average values (n = 19) in emmetropes, and average values in myopes (n = 11) for four colors (white, green, red, and blue). Error bars represent the 95% confidence intervals of the mean.

Influence of light color

The values of CSF decreased with increasing spatial frequencies for all colors (**Figure 4.3)**. The mean in-focus contrast sensitivity function was almost the same for white and green light, while blue light saw the lowest values at spatial frequencies above 3 cycles per degree (cpd). Measurements with the green filter yielded higher CSF values in emmetropes than in myopes. For myopes, white and green filters had the same value for CSF at spatial frequencies lower than 6 cpd and the lower value of CSF was found for the blue color at the highest spatial frequency (18 cpd).

Emmetropes saw significant differences between all colors (white, green, red, and blue) for each spatial frequency higher than 1.5 (ANOVA, **Table 4.3**), while for myopes no differences were seen between the colors at any spatial frequency.

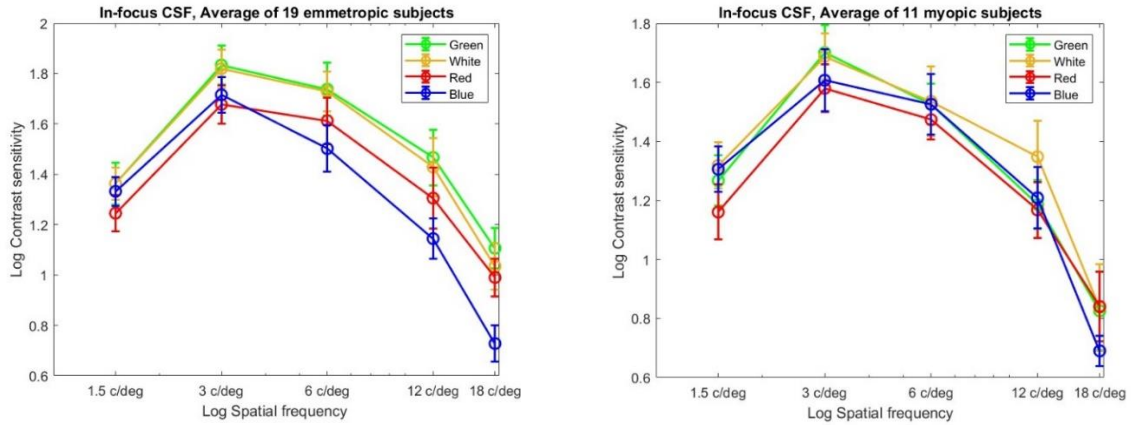

Fig. 4 3. Comparison between contrast sensitivity of four colors as a function of spatial frequency, average values in emmetropes (n = 19), and average values in myopes (n = 11). Error bars represent the 95% confidence interval of the mean.

Table 4.3. Significance of the influence of color on CSF in emmetropes and myopes separately

	Emmetropes		Myopes	
Spatial frequency	**F**	**P value***	**F**	**P value***
1.5 cpd	1.471	0.230	2.710	0.058
3 cpd	4.309	**0.007**	1.374	0.265
6 cpd	4.833	**0.004**	0.650	0.588
12 cpd	5.651	**0.002**	2.326	0.096
18 cpd	7.254	**0.000**	0.528	0.667

* Significant if P < 0.05

Joint influence of defocus and light color

To assess the possible interaction between defocus level and light color, a multiple linear regression analysis was performed for each spatial frequency. Based on this analysis, spherical refractive error, color, and defocus are significant predictors of spatial frequency. The findings in this multiple linear regression model are presented in **Table 4.4**. While the results indicate that both defocus and color have a significant impact on contrast sensitivity function, there are no significant cross-terms between ametropia, color, and defocus at any spatial frequency.

Table 4.4. Association between Contrast Sensitivity and Possible Determinants Tested with Multiple Linear Regression (a) coefficients and b) model summary

		Spatial frequency				
		1.5	**3**	**6**	**12**	**18**
Ametropia	β_1	0.082	0.127	-0.164	0.140	0.191
	t_1	2.591	4.424	4.740	3.525	4.061
	p_1	0.010	<0.001	<0.001	0.001	<0.001
Color	B_2	-0.066	-0.217	-0.232	-0.271	-0.225
	t_2	-2.071	-7.576	-6.686	-6.868	-4.794
	p_2	0.039	<0.001	<0.001	<0.001	<0.001
Defocus	β_3	-0.432	-0.527	-0.380	-0.246	-0.209
	t_3	-13.582	-18.364	-10.949	-6.210	-4.448
	p_3	<0.001	<0.001	<0.001	<0.001	<0.001
Model Summary						
F value		64.699	136.609	60.915	30.950	19.322
P-value		<0.001	<0.001	<0.001	<0.001	<0.001
R^2		0.196	0.337	0.219	0.144	0.127
Regression*		21.234 + 0.382 A - 0.518 C - 3.919 D	67.886 + 2.161 A - 6.268 C - 17.405 D	54.988 + 2.391 A - 5.721 C - 12.346 D	28.966 + 1.116 A - 3.608 C - 4.275 D	12.476 + 0.599 A - 1.282 A - 1.633 D

** A: ametropia in diopters; C: color (0 = White 1 = Green, 2 = Red, 3= Blue); D: defocus in diopters.*

Luminance

Given the importance of luminance in the contrast sensitivity function, we estimated the luminance transmitted through the stimuli for each colored filter. It is evident that after applying the dichroic filters, the luminance transmitted through the colored filters decreases compared to white light. Using the transmission spectrum of the dichroic filters, along with the transmission spectrum of white light through the Functional vision analyzer and the spectral sensitivity of the human eye (Appendix C), we calculated the transmission luminance to be 43% for green, 24% for red, and 5% for blue. The reduction in luminance was found to be significantly higher for blue light compared to the other colors.

Furthermore, inspired by the luminance CSF model (Appendix C),[40] the CSF values were

calculated for green, red and blue, demonstrating a substantial reduction in CSF for blue light (87.09 for green, 68.56 for red, 28.07 for blue).

DISCUSSION

In the late 1970s, researchers found that low-quality retinal images, particularly those with reduced contrast, could trigger excessive eye growth, leading to myopia. This phenomenon is known as "deprivation myopia", and the severity of myopia increases as the quality of the retinal image decrease. Studies conducted on chickens and guinea pigs revealed that both low image contrast and high spatial frequency components play significant roles in the onset of myopia. Furthermore, exposing chickens to low pass filtered movies induced myopia, with the severity of the condition closely linked to changes in their CSF. These findings highlight the crucial role of CS adaptation in the development of myopia.[31,32,33,34]

Meanwhile, the role of chromatic cues in emmetropization and myopization was explored in other studies, suggesting that limiting the spectral bandwidth of light produces varying effects in different animal species due to distinct underlying mechanisms. For instance, red light induces myopia in chickens, while blue light leads to hyperopia.[35] However, similar experiments in humans have produced mixed results. In humans, blue light has been associated with slight eye shortening, whereas red and green lights have been linked to eye elongation.[36] Therefore, in order to investigate the effect of external factors like color and defocus on eye growth, this paper explored the joint effect of defocus and light color on CSF in emmetropic and myopic participants. Also, the interaction between these two factors (color and defocus) with each other was assessed.

It was found that the value of CSF is reduced for positive defocuses and blue color for spatial frequencies of 1.5 cpd, 3 cpd 6 cpd, and 12 cpd rather than negative defocus. The effect of positive and negative defocus on CSF has been studied and found that CS is reduced by increasing the spatial frequency for both positive and negative defocus in emmetropes, and for myopic ones, the CS was decreased more for positive defocus rather than negative defocus for all the spatial frequencies. Our results suggest that the value of CSF is higher for negative defocuses rather than positive defocuses for all the spatial frequencies, which is likely due to accommodation. Spatial frequency influenced the extent of CS loss, with higher frequencies showing more pronounced reductions. Blue light consistently resulted in lower CSF values compared to other colors in both emmetropic and myopic eyes. Also, in other studies, chromatic CSF was investigated separately[37], but the combined effect of defocus and color on CSF was not studied simultaneously.

A question that arises is why CSF for blue light appears to be significantly lower compared to other colors. Several hypothesis contribute to the decreased CS observed for blue light rather

than green and red ones have been proposed to explain this decrease in CSF observed for blue light, as opposed to green and red light. Firstly, due to longitudinal chromatic aberration of the eye, different wavelengths of light are refracted by varying amounts as they pass through the lens. Blue light, with its shorter wavelength, is refracted more than green and red light, resulting in an average defocus of -1.26D for blue light.[38] This defocus contributes to the reduction in CSF for blue light. In our study, we applied a correction of -1D for blue light to compensate for this chromatic aberration. On the other hand, the chromatic aberration for red light is much smaller (-0.15 D), so we did not apply any compensation for red in our experiment. Secondly, the number of blue-sensitive cones in the retina is lower compared to red and green ones, resulting in reduced sensitivity to blue light.[39] Thirdly, blue cones have inherently lower sensitivity and are less effective at detecting contrast, especially at low spatial frequencies. This decreased sensitivity can be attributed to the unique properties of blue cones and their response to light, which does not match the efficiency of red and green cones.[39] The final hypothesis that may contribute to the reduction in CSF for blue is the impact of luminance on CSF. In our work, we estimated the luminance transmitted through the stimulus for the color filters, which was 43% for green, 23% for red, and 5% for blue. This represents an 88% reduction in luminance from green to blue light. Such a decrease in luminance may significantly contribute to the reduction in CSF for blue light compared to other colors. Additionally, we calculated the CSF value at a higher spatial frequency (18cpd) for three color filters using the luminance CSF model from previous literature.[40] The calculated values were 87.09 for green, 68.60 for red and 28.07 for blue light, indicating a 68% reduction in CSF for blue light compared to green one. However, the exact cause of the significant reduction in blue CSF compared to other colors remains unclear.

Consistent with the literature, CS was significantly lower for myopes than for emmetropes.[15] This difference suggests that there may be early disruptions in retinal function within myopes that trigger signal an acceleration of axial growth. This growth stretches the retina and disrupts the balance between the scleral shell and choroid-retina.[41] These changes can cause reduced acuity and reduced CS. Besides those subjective and psychophysical evidences, previous studies using objective techniques as electroretinogram showed that the retinal function is altered even in low-to-moderate myopes.[42]

In conclusion, this work demonstrated the significant, but independent influence of various levels of defocus and color bands on CSF. Additionally, the considerable reduction in CSF for blue light may be linked to a combination of chromatic aberrations and reduced luminance in the blue of the spectrum. Studying the impact of lens-induced defocus and wavelength on CS may be investigated further in the context of the regulation of eye growth.

REFERENCES

1. Hung L-F, Crawford ML, Smith EL. Spectacle lenses alter eye growth and the refractive status of young monkeys. Nat. Med. 1995;1(8):761-5.
2. Schaeffel F, Glasser A, Howland HC. Accommodation, refractive error and eye growth in chickens. Vis Res. 1988;28(5):639-57.
3. Diether S, Schaeffel F. Local changes in eye growth induced by imposed local refractive error despite active accommodation. Vis Res. 1997;37(6):659-68.
4. Liou S-W, Chiu C-J. Myopia and contrast sensitivity function. Curr. Eye Res. 2001;22(2):81-4.
5. Kraft C, Leube A, Ohlendorf A, Wahl S. Contrast adaptation appears independent of the longitudinal chromatic aberration of the human eye. JOSA A. 2019;36(4):B77-B84.
6. Rucker FJ. The role of luminance and chromatic cues in emmetropisation. Ophthalmic Physiol. Opt. 2013;33(3):196-214.
7. Schmid KL, Wildsoet CF. Contrast and spatial-frequency requirements for emmetropization in chicks. Vis Res. 1997;37(15):2011-21.
8. Diether S, Gekeler F, Schaeffel F. Changes in contrast sensitivity induced by defocus and their possible relations to emmetropization in the chicken. Invest. Ophthalmol. Vis. Sci.2001;42(12):3072-9.
9. Feldkaemper M, Diether S, Kleine G, Schaeffel F. Interactions of spatial and luminance information in the retina of chickens during myopia development. Exp. Eye Res.1999;68(1):105-15.
10. Arden G. The importance of measuring contrast sensitivity in cases of visual disturbance. Br. J. Ophthalmol. 1978;62(4):198-209.
11. Charman W. Effect of refractive error in visual tests with sinusoidal gratings. Br. J. Physiological Opt. 1979;33(2):10-20.
12. Kay C, Morrison JD. A quantitative investigation into the effects of pupil diameter and defocus on contrast sensitivity for an extended range of spatial frequencies in natural and homatropinized eyes. Ophthalmic Physiol. Opt.1987;7(1):21-30.
13. Bour LJ, Apkarian P. Selective broad-band spatial frequency loss in contrast sensitivity functions. Comparison with a model based on optical transfer functions. Invest. Ophthalmol. Vis. Sci. 1996;37(12):2475-84.
14. Strang NC, Atchison DA, Woods RL. Effects of defocus and pupil size on human contrast sensitivity. Ophthalmic Physiol. Opt. 1999;19(5):415-26.
15. Radhakrishnan H, Pardhan S, Calver RI, O'Leary DJ. Effect of positive and negative defocus on contrast sensitivity in myopes and non-myopes.Vis Res. 2004;44(16):1869-78.
16. Nio Y, Jansonius N, Fidler V, Geraghty E, Norrby S, Kooijman A. Age-related changes of defocus-specific contrast sensitivity in healthy subjects. Ophthalmic Physiol. Opt. 2000;20(4):323-34.
17. Yan F-F, Hou F, Lu Z-L, Hu X, Huang C-B. Efficient characterization and classification of contrast sensitivity functions in aging. Sci. Rep. 2017;7(1):5045.
18. Stoimenova BD. The effect of myopia on contrast thresholds. Invest. Ophthalmol. Vis. Sci.2007;48(5):2371-4.
19. Bradley A, Hook J, Haeseker J. A comparison of clinical acuity and contrast sensitivity charts: effect of uncorrected myopia. Ophthalmic Physiol. Opt. 1991;11(3):218-26.
20. Collins JW, Carney LG. Visual performance in high myopia. Curr. Eye Res. 1990;9(3):217-24.
21. Barten PG. Contrast sensitivity of the human eye and its effects on image quality: SPIE press; 1999.
22. Westland S, Owens H, Cheung V, Paterson-Stephens I. Model of luminance contrast-sensitivity function for application to image assessment. Color Res. Appl.2006;31(4):315-9.
23. Granger E, Heurtley J. Visual chromaticity-modulation transfer function. JOSA. 1973;63(9):1173-4.
24. Green DG. The contrast sensitivity of the colour mechanisms of the human eye. J. Physiol.1968;196(2):415-29.
25. Mullen KT. The contrast sensitivity of human colour vision to red-green and blue-yellow chromatic gratings. J. Physiol. 1985;359(1):381-400.
26. Cavonius C, Estévez O. Contrast sensitivity of individual colour mechanisms of human vision. J. Physiol. 1975;248(3):649-62.
27. Kim KJ, Mantiuk R, Lee KH, editors. Measurements of achromatic and chromatic contrast sensitivity functions for an extended range of adaptation luminance. Hum. Vis. Electron. Imaging XVIII; 2013: SPIE.
28. Ashraf M, Wuerger S, Kim M, Martinovic J, Mantiuk RK, editors. Spatio-chromatic contrast sensitivity across the lifespan: interactions between age and light level in high dynamic range. 28th Color Imaging Conf. 2020, CIC 2020; 2020: Society for Imaging Science and Technology.
29. Kutas G, Kwak Y, Bodrogi P, Park D-S, Lee S-D, Choh H-K, et al. Luminance contrast and chromaticity contrast preference on the colour display for young and elderly users. Displays. 2008;29(3):297-307.
30. Kim YJ, Reynaud A, Hess RF, Mullen KT. A normative data set for the clinical assessment of achromatic and chromatic contrast sensitivity using a qCSF approach.Invest. Ophthalmol. Vis. Sci.2017;58(9):3628-36.
31. Bartmann M, Schaeffel F. A simple mechanism for emmetropization without cues from accommodation or colour. Vis Res. 1994 Apr 1;34(7):873-6.
32. Smith III EL, Hung LF. Form-deprivation myopia in monkeys is a graded phenomenon. Vis Res. 2000 Feb 1;40(4):371-81.
33. Schmid KL, Wildsoet CF. Assessment of visual acuity and contrast sensitivity in the chick using an optokinetic

nystagmus paradigm. Vis Res. 1998 Sep 1;38(17):2629-34.
34. Diether S, Gekeler F, Schaeffel F. Changes in contrast sensitivity induced by defocus and their possible relations to emmetropization in the chicken. Invest. Ophthalmol. Vis. Sci. 2001 Nov 1;42(12):3072-9.
35. Rucker FJ, Wallman J. Chick eyes compensate for chromatic simulations of hyperopic and myopic defocus: evidence that the eye uses longitudinal chromatic aberration to guide eye-growth. Vis Res. 2009 Jul 1;49(14):1775-83.
36. Gawne TJ, She Z, Norton TT. Chromatically simulated myopic blur counteracts a myopiagenic environment. Exp. Eye Res. 2022 Sep 1;222:109187.
37. Thorn F, Cameron L, Arnel J, Thorn S, editors. Myopia adults see through defocus better than emmetropes. Proc. 6th Int. Conf. on Myopia; 1998: Springer.
38. Marcos S, Burns SA, Moreno-Barriusop E, Navarro R. A new approach to the study of ocular chromatic aberrations. Vis Res. 1999 Dec 1;39(26):4309-23.
39. Kelly DH. Lateral inhibition in human colour mechanisms. J. Physiol. 1973 Jan 1;228(1):55-72.
40Westland S, Owens H, Cheung V, Paterson-Stephens I. Model of luminance contrast-sensitivity function for application to image assessment. Color Res. Appl. 2006 Aug;31(4):315-9.
41. Chui TY, Yap MK, Chan HH, Thibos LN. Retinal stretching limits peripheral visual acuity in myopia. Vis Res. 2005;45(5):593-605.
42. Amorim-de-Sousa A, Schilling T, Fernandes P, Seshadri Y, Bahmani H, González-Méijome JM. Blue light blind-spot stimulation upregulates b-wave and pattern ERG activity in myopes. Sci Rep. 2021;11(1):9273.

Chapter 6. The influence of variations in ocular biometric and optical parameters on differences in refractive error

Previously published as:

Farzanfar, Veronica Lockett-Ruiz, Rafael Navarro, Carina Koppen, Jos J Rozema
The influence of variations in ocular biometric and optical parameters on differences in refractive error

Ophthalmic and Physiological Optics, 2024 Jul 44(5):1000-9.

INTRODUCTION

Early studies[1–4] established that ocular biometric parameters can vary widely between individuals and that strong correlations exist between these parameters, in both emmetropes and ametropes. However, as refractive errors are caused by a mismatch between these parameters, different correlations are found in each refractive group.[5] In particular, the influence of variations in axial length on refractive error has been clearly established,[6–8] but the importance of differences in corneal power, for example, is less clear, with some studies confirming [9–11] and others [12, 13] not showing a significant influence. Similarly, while some reports have shown that the anterior chamber depth (*ACD*) is generally deeper in myopes than in hypermetropes,[10, 11, 14] other authors were unable to confirm this finding.[15, 16] Though seemingly contradictory, this discrepancy between studies arises from differences in the range of refractive error being considered. Consequently, to understand the variations within a population's refractive error, one must know the variability of its ocular biometry.

Although these observations are for adult eyes, they are especially important in developing or pathological eyes, where the relative contributions of the biometric components will be somewhat different from those found in adults. The newborn eye, for example, undergoes marked biometric changes during eye growth[17, 18] that are interconnected in a complex way that has to be just right to achieve emmetropia.[19] One example is the dynamic adaptation of crystalline lens power to axial length during homeostatic eye growth, the failure of which may lead to the development of myopia.[20, 21] But just as there are large variations in biometry between individuals of any age,[22, 23] the method by which the adult refractive error is reached is unique for each eye.[22-24] In other words, the refractive state of an eye at any time is the result of its growth history, which is typically not known during clinical examination. It is therefore more practical to study the origins of refractive error at a population level, while keeping in mind the specific biometric variability.

To this end, we propose an alternative approach to investigate the contributions of and interactions between ocular biometric parameters to the variations in refractive error using the principles of error propagation. Similar methods have been used to identify successfully sources

affecting the outcome of cataract surgery[25–27] and to determine how minor changes in ocular biometry affect the overall refractive error.[28] This analysis is implemented as either a set of two lenses, representing the cornea and the lens, or as ray transfer matrices.[29] After an initial assessment of the method using synthetic test data, the method was applied to biometric data derived from the literature to determine how the ocular components contribute to the refractive errors of children at different ages, as well as adults, full-term infants, premature infants with or without retinopathy of prematurity (ROP) and adults with diabetes.[30-35]

METHODS

Error propagation

Error propagation is a well-known method used in engineering to estimate the compounded uncertainty of a parameter f that is calculated from several other parameters X_1, …, X_N, each with an uncertainty ΔX_1, …, ΔX_N. Typically, these uncertainties are measurement errors or the standard deviation of the population. The magnitude by which each parameter X_k influences $f(X_1, \ldots, X_N)$ is then given by its uncertainty multiplied by the derivatives as follows[36]:

$$\Delta f(x_1, \ldots, x_N) = \sqrt{\sum_{k=1}^{N} \left(\frac{\partial f}{\partial x_k}\right)^2 (\Delta x_k)^2} \qquad (5\text{-}1)$$

In the context of eye models, parameters X_k refer to axial length, corneal power, *ACD*, corneal thickness, lens thickness, lens power, etc., while the function f represents the spherical refractive error S. Uncertainties ΔX_k represent the standard deviations of parameter x_k.

Note that the compounded uncertainty calculated using Equation (5-1) will likely be larger than one would find if the values for f were measured directly.[37] This is not a problem for the current analysis, because we are interested in the relative contributions of each X_k and ΔX_k to Δf rather than the value of Δf itself. These were estimated as follows:

$$100 \times \left(\frac{\partial f}{\partial x_\mathrm{i}}\right)^2 (\Delta x_\mathrm{i})^2 \Big/ \sum_{k=1}^{N} \left(\frac{\partial f}{\partial x_\mathrm{k}}\right)^2 (\Delta x_\mathrm{k})^2 \qquad (5\text{-}2)$$

All partial derivatives were calculated manually and validated using the MATLAB symbolic toolbox (R2022a, mathworks.com).

Simple method

Error propagation is a well-known method used in engineering to estimate the compounded uncertainty of a parameter f that is calculated from several other parameters X_1,

The first paraxial method to determine refractive error from ocular biometry starts from the observation that spherical refractive error S is the difference between the axial power P_{ax} and whole

eye power P_{eye}. Both powers can be expanded as follows[38]:

$$S = P_{\text{ax}} - P_{\text{eye}} = \left(\frac{n}{L - pp_{\text{eye2}}}\right) - \left(P_{\text{c}} + P_{\text{l}} - P_{\text{c}} \cdot P_{\text{l}} \cdot \frac{pp_{\text{c2}} + ACD_{\text{tot}} + pp_{\text{l1}}}{n}\right) \qquad (5\text{-}3)$$

for which the definitions of all parameters are provided in Table 5.1 and Figure 5.1. These include clinically available parameters, such as axial length L, total corneal power P_{c} and total anterior chamber depth ACD_{tot}, as well as the estimated refractive index of the humors n. The principal plane positions (pp_{eye2}, pp_{c2}, pp_{l1}) are more difficult to determine clinically; so instead, age-based regressions were used.[38] Because age is not a variable in the error propagation, these age-based principal plane positions will behave as constants in the analysis. The refractive index n, determined by the salt and protein concentrations in the humors, presents little variation between individuals.[39, 40]

Table 5.1: Overview of the biometric parameters and paraxial calculations used, derived from the Navarro eye model[29]and age-based regressions.[38]

Symbol	Unit	Calculation/value	Description
CCT	mm	*0.540*	Central corneal thickness
ACD	mm	*Measured/Taken from eye model*	Anterior chamber depth (excl. corneal thickness)
ACD_{tot}	mm	*Measured/Taken from eye model*	Anterior chamber depth (incl. corneal thickness)
LT	mm	*Measured/Taken from eye model*	Lens thickness
L	mm	*Measured/Taken from eye model*	Axial length
n_{air}	$-$	*1.000*	Refractive index of air
n_{c}	$-$	*1.376*	Refractive index of the cornea
n_{s}	$-$	*1.3726*	Refractive index of the lens surface
n_{l}	$-$	*Measured/Taken from eye model*	Equivalent refractive index of the lens
n	$-$	*1.336*	Refractive index of the ocular humours
r_{ca}	mm	*Measured/Taken from eye model*	Anterior on-axis corneal radius of curvature
r_{cp}	mm	$0.821.r_{\text{ca}}$	Posterior on-axis corneal radius of curvature
P_{ca}	D	$(n_{\text{c}} - n_{\text{air}})/r_{\text{ca}}$	Anterior corneal curvature
P_{cp}	D	$(n - n_{\text{c}})/r_{\text{cp}}$	Posterior corneal curvature
P_{c}	D	$P_{\text{ca}} + P_{\text{cp}} - 0.001.P_{\text{ca}}.P_{\text{cp}}.CCT/n_{\text{c}}$	Total corneal power
r_{la}	mm	*Measured/Taken from eye model*	Anterior on-axis lens radius of curvature
r_{lp}	mm	*Measured/Taken from eye model*	Posterior on-axis lens radius of curvature
P_{la}	D	$(n_{\text{l}} - n)/r_{\text{la}}$	Anterior lens power
P_{lp}	D	$(n - n_{\text{l}})/r_{\text{lp}}$	Posterior lens power
P_{l}	D	$P_{\text{la}} + P_{\text{lp}} - 0.001.P_{\text{la}}.P_{\text{lp}}.LT/n_{\text{l}}$	Total lens power
P_{s}	D	$P_{\text{la}} + P_{\text{lp}} - 0.001.P_{\text{la}}.P_{\text{lp}}.LT/n_{\text{s}}$	Surface power of the lens
P_{G}	D	$P_{\text{l}} - P_{\text{s}}$	Contribution of gradient-index (GRIN) structure to lens power
pp_{c2}	mm	*–0.057*	Position of second corneal principal point*
pp_{l1}	mm	*5.809 – 0.697·exp(–0.211·Age)*	Position of first corneal principal point*
pp_{eye2}	mm	*0.392·exp(–0.181·Age) – 2.4·10⁻³·Age + 2.093*	Position of second ocular principal point*

Note: Age in years.
Abbreviations: ACD, anterior chamber depth; D, diopters.

*With respect to the anterior corneal apex

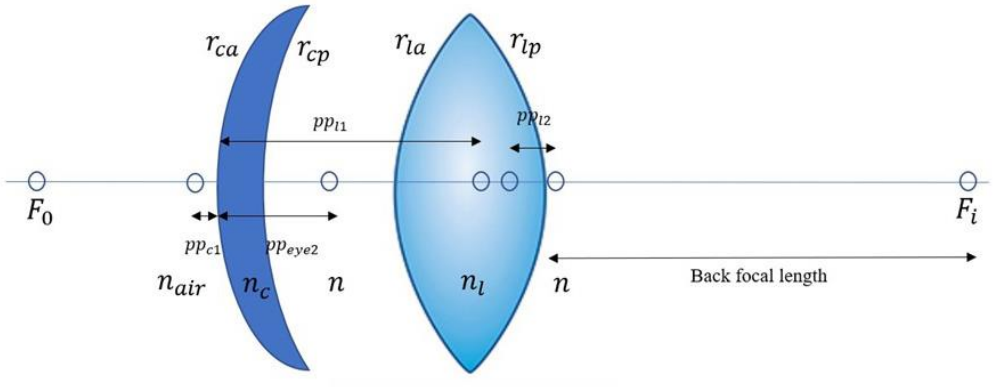

Figure 5 .1 Principal planes and focal lengths, with rca and rcp the anterior and posterior corneal radii of curvature, rla and rlp the anterior and posterior lenticular radii of curvature, nair, nc, n and nl the refractive indices of the air, cornea, ocular humors and the lens, and ppc1, ppl1 and ppeye2, the positions of the first cornea, first lenticular and second ocular principal points with respect to the corneal apex.

The formulas needed to calculate the error propagation can be derived by applying equation (5.1) to the parameters in Equation (5-3). Considering the three principal points as constants, this gives the following:

$$\Delta S = \sqrt{\left(\frac{\partial S}{\partial L}\right)^2 (\Delta L)^2 + \left(\frac{\partial S}{\partial P_c}\right)^2 (\Delta P_c)^2 + \left(\frac{\partial S}{\partial P_l}\right)^2 (\Delta P_l)^2 + \left(\frac{\partial S}{\partial ACD_{tot}}\right)^2 (\Delta ACD_{tot})^2 + \left(\frac{\partial S}{\partial n}\right)^2 (\Delta n)^2} \quad (5\text{-}4)$$

with

$$\frac{\partial S}{\partial L} = -\frac{n}{\left(L - pp_{eye2}\right)^2}$$

$$\frac{\partial S}{\partial P_l} = -1 + P_c \cdot \frac{pp_{c2} + ACD_{tot} + pp_{l1}}{n}$$

$$\frac{\partial S}{\partial P_c} = -1 + P_l \cdot \frac{pp_{c2} + ACD_{tot} + pp_{l1}}{n}$$

$$\frac{\partial S}{\partial ACD_{tot}} = P_c \cdot P_l / n$$

$$\frac{\partial S}{\partial n} = \frac{1}{L - pp_{eye2}} - \frac{P_l P_c (ACD_{tot} + pp_{c2} + pp_{l1})}{n^2}$$

These expressions are used for the simple method estimate of the influence of biometric variations on the changes in *S*.

Matrix method

One can also describe the eye in the form of a paraxial ray transfer matrix M_{eye},[29] of which the constituent equations can be filled into an error propagation analysis. This method is more accurate than the previous one but requires more parameters, such as the corneal and lenticular radii of curvature, the gradient index power of the lens, the refractive indices and the thicknesses of all the

optical media (Table 5.1). Matrix M_{eye} consists of four elements ABCD that represent how the position and angle of a light ray is altered when passing through the optical system, calculated through a series of matrix multiplications representing the ray's refractions and translations. Here, the contributions of the cornea and anterior chamber are incorporated in matrix M, while the gradient index of the crystalline lens requires a special matrix L_{GRIN}. Hence, the eye can be described as follows:

$$M_{eye} = L_{GRIN} \cdot M = \begin{pmatrix} L_{11} & L_{12} \\ L_{21} & L_{22} \end{pmatrix} \begin{pmatrix} M_{11} & M_{12} \\ M_{21} & M_{22} \end{pmatrix}$$

$$= \begin{pmatrix} L_{11}M_{11} + L_{12}M_{21} & L_{11}M_{12} + L_{12}M_{22} \\ L_{21}M_{11} + L_{22}M_{21} & L_{21}M_{12} + L_{22}M_{22} \end{pmatrix} = \begin{pmatrix} A & B \\ C & D \end{pmatrix} \qquad (5\text{-}5)$$

with A the dilation, B the disjugacy, C the divergence and D the divarication; each a 2 × 2 submatrix that alters a different aspect of the passing beams of light. A and D do not have units, while B is in units of length and C is in diopters.[41] The components of L_{GRIN} are given by the following:

$$L_{11} = 1 - LT\frac{n_{\mathrm{s}} - n}{n_{\mathrm{s}} r_{\mathrm{la}}}$$

$$L_{12} = -LT\frac{n}{n_{\mathrm{s}}}$$

$$L_{21} = \frac{n_{\mathrm{s}} - n}{n}\left(\frac{1}{r_{\mathrm{la}}} - \frac{1}{r_{\mathrm{lp}}}\right) + \left(\frac{(n - n_{\mathrm{s}})^2}{n \cdot n_s r_{\mathrm{la}} r_{\mathrm{lp}}} LT\right) + P_G$$

$$L_{22} = 1 - LT\frac{n - n_{\mathrm{s}}}{n_s r_{\mathrm{lp}}}$$

with PG the contribution of the gradient index to the lens power, calculated as the difference between the total lens power P_{l} and the lens surface power P_s (Table 5.1). The components of M are as follows:

$$M_{11} = \left(1 - \frac{CCT(n_{\mathrm{c}} - 1)}{n_{\mathrm{c}} r_{\mathrm{ca}}}\right)\left(1 - \frac{ACD(n - n_{\mathrm{c}})}{n r_{\mathrm{cp}}}\right) - \frac{ACD(n_{\mathrm{c}} - 1)}{n r_{\mathrm{ca}}}$$

$$M_{12} = -\frac{CCT}{n_{\mathrm{c}}}\left(1 - \frac{ACD(n - n_{\mathrm{c}})}{n r_{\mathrm{cp}}}\right) - \frac{ACD}{n}$$

$$M_{21} = \frac{n_{\mathrm{c}} - 1}{n r_{\mathrm{ca}}}\left(1 - \frac{CCT(n - n_{\mathrm{c}})}{n_{\mathrm{c}} r_{\mathrm{cp}}}\right) + \frac{n - n_{\mathrm{c}}}{n r_{\mathrm{cp}}}$$

$$M_{22} = \frac{1}{n}\left(1 - \frac{CCT(n - n_{\mathrm{c}})}{n_{\mathrm{c}} r_{\mathrm{cp}}}\right)$$

Matrix elements A and C in equation (5-4) can then be used to estimate the position of the principal plane on the image side with respect to the anterior corneal apex as follows:

$$pp_{\mathrm{eye2}} = CCT + ACD + LT + (A - 1)/C \qquad (5\text{-}6)$$

Meanwhile, the power of the entire eye is given by the following:

$$P_{\mathrm{eye}} = \frac{n}{f_{\mathrm{eye2}}} = n \cdot C \qquad (5\text{-}7)$$

with f_{eye2} the focal distance on the image side. The full expressions for A and C are provided in Appendix D (Supplement A).From this, the refractive error can be calculated as follows:

$$S = P_{\text{ax}} - P_{\text{eye}} = \frac{n}{L - pp_{\text{eye2}}} - n \cdot C = \frac{n}{L - CCT - ACD - LT + (A-1)/C} - n \cdot C \qquad (5\text{-}8)$$

Error propagation for this method can be achieved by filling equation (5-7) into (5-1), resulting in the following:

$$\Delta S = \sqrt{\begin{array}{c} \left(\frac{\partial S}{\partial L}\right)^2 (\Delta L)^2 + \left(\frac{\partial S}{\partial P_G}\right)^2 (\Delta P_G)^2 + \left(\frac{\partial S}{\partial r_{ca}}\right)^2 (\Delta r_{ca})^2 + \left(\frac{\partial S}{\partial ACD}\right)^2 (\Delta ACD)^2 + \left(\frac{\partial S}{\partial LT}\right)^2 (\Delta LT)^2 \\ + \left(\frac{\partial S}{\partial r_{\text{lp}}}\right)^2 (\Delta r_{\text{lp}})^2 + \left(\frac{\partial S}{\partial r_{\text{la}}}\right)^2 (\Delta r_{\text{la}})^2 + \left(\frac{\partial S}{\partial n_s}\right)^2 (\Delta n_s)^2 + \left(\frac{\partial S}{\partial r_{\text{cp}}}\right)^2 (\Delta r_{\text{cp}})^2 \\ + \left(\frac{\partial S}{\partial n}\right)^2 (\Delta n)^2 + \left(\frac{\partial S}{\partial n_{\text{c}}}\right)^2 (\Delta n_{\text{c}})^2 + \left(\frac{\partial S}{\partial CCT}\right)^2 (\Delta CCT)^2 \end{array}} \qquad (5\text{-}9)$$

The resulting expressions of the 12 partial derivatives are length and provided in Appendix D (Supplement A). Expression (9) will be used for the error propagation analysis of the matrix method.

Data

To test both methods on a realistic and complete dataset, a set of 1000 SyntEyes was first used; stochastically generated biometric datasets of the eye with average values and variations that match those in the general population between 20 – 60 years of age.[30] Since SyntEyes provides all parameters required for either error propagation method, they form an ideal demonstration platform for these methods before applying them to clinical data.

Next, several datasets from the literature were considered. The first, from Mutti et al.,[31] provides longitudinal biometry data for a group of children between 3 months and 6.5 years of age, allowing to understand changes in the contributions during emmetropization and early homeostasis. As this dataset provides information for both the lenticular radii of curvature and refractive index, both error propagation methods may be applied. A second dataset, by Twelker et al.,[32] is a cross-sectional cohort of schoolchildren between 6 to 14 years of age, with an increasing prevalence of myopia. This allows the assessment of how developing myopia is reflected in the biometric changes. Here, the biometric data was averaged over the separated values for boys and girls that were provided.

An additional analysis compared the biometric contributions to refractive error in premature infants with or without retinopathy of prematurity (ROP), examined longitudinally between 32 and 52 weeks of postmenstrual age.[34] Premature eyes have shorter axial lengths, shallower anterior chambers and more highly curved corneas than those of full-term infants,[42] differences that become more considerable as the severity of ROP increases. As the number of participants was relatively small, no analysis by ROP stage could be performed. Here, lens power was estimated using Bennett's method.[43,

[44] The data of full-term infants between 0 – 3 days of age, presented by Axer-Siegel et al.,[33, 45] was also considered.

Finally, since the lenticular biometry of diabetic eyes is considerably different from that of healthy eyes,[35] the contributions of the ocular parameters to the refractive error of 74 participants with Type 1 diabetes were compared to those in 64 age-matched controls.

The values of all required parameters and their standard deviations are given in Appendix F for all datasets. Since real datasets are often incomplete and typically lack the necessary information about the refractive indices of the ocular media, the indices of the Navarro eye model[46] were used to supplement the real data where needed.

RESULTS

Test data

Applying both methods to 10 sets of 1000 SyntEyes leads to the contribution percentages shown in Table 5.2. The largest contributions are given by the variations in axial length L, lens power PL, and corneal power P_c for the simple method (56.87%, 31.51% and 10.30%, respectively), and by L, the contribution of gradient-index (GRIN) structure to lens power (P_G) and the anterior corneal curvature r_{ca} for the matrix method (63.62%, 16.30%, 12.94%, respectively). The contributions of the variations in the principal plane positions using the simple method (i. e. , the position of second ocular principal point (pp_{eye2}), the position of the second corneal principal point (pp_{c2}) and the position of the first corneal principal point (pp_{l1})) were very small (0.50%, 0.22% and 6.79 ·10−5%, respectively).

Children

The contributions of the biometric components shown in Figure 5.2 were obtained by applying both error propagation methods to the children's data from Mutti et al.[31] Again, the largest contributions were given by the variations in axial length, lenticular and corneal power for the simple method (*67%*, *23%* and 9%, respectively), and by the axial length, gradient lens power and the anterior corneal curvature for the matrix method (*55%*, *21%* and *14%*, respectively). The percentage estimates provided by the matrix method agreed overall with the equivalent parameters in the simple method, albeit with higher contributions from the variations in corneal power and anterior chamber depth at the expense of the contribution from axial length.

Table 5.2: Average contribution of the variations in the individual parameters to changes in refractive error for both methods based on 10 runs of 1000 SyntEyes (symbols defined in Table 5.1).

Parameter	Simple method	Parameters	Matrix method
L	56.87%	L	63.62%
P_{l}	31.51%	P_{G}	16.30%
P_{c}	10.30%	r_{ca}	12.94%
ACD_{tot}	0.65%	ACD	3.63 %
pp_{eye2}	0.50%	pp_{eye2}	
pp_{l1}	0.22%	pp_{l1}	
pp_{c2}	$6.79{\cdot}10^{-}$%	pp_{c2}	
n	0.04%	n	0.04%
LT		LT	1.30%
r_{lp}		r_{la}	0.67%
r_{la}		r_{lp}	0.65%
n_{s}		n_{s}	0.63%
r_{cp}		r_{cp}	0.30%
n_{c}		n_{c}	0.015%
CCT		CCT	0.01%

Note: Standard deviations over the 10 runs were all <0.01%

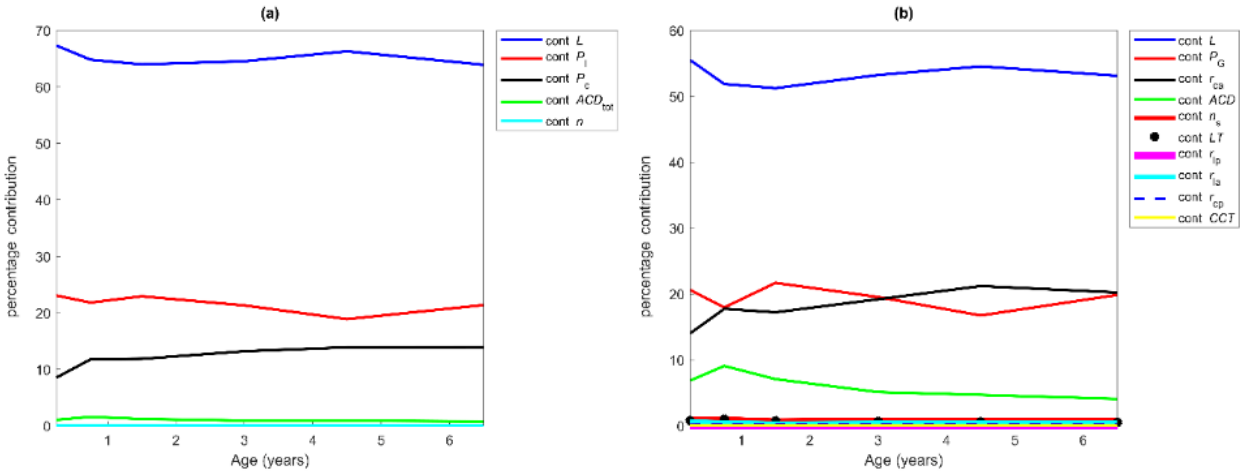

Figure 5.2: Contributions of the variations in ocular biometry to the changes in refractive error using the Mutti et al.[31] data for: (a) the simple method and (b) the matrix method.
Symbols are defined in Table 5.1.

Influence of myopia

In the children's data from Twelker et al.,[32] myopization caused the contribution of axial length to increase from *54.5 %* to *73.4%*, while the contribution from the changes in lens and corneal power decreased from *35.2%* to *19.94%* and from 9.82*%* to *6.32%*, respectively (Figure 5.3). This suggests that during normal refractive development, the percentage contributions from the variations in ocular biometry to the changes in *S* are generally stable, but this is disrupted by myopization.

Full-term and pre-term infants

The contributions from the variations in ocular biometry in pre-term infants, both with and without ROP, using the simple method are shown in Figure 5.4. The curves seen in children without ROP fluctuated considerably, while the contributions from axial length and lens power were about equal. The full-term children tested by Axer-Siegel showed very similar results. The fluctuations in Figure 5.4a are likely due to the large standard deviations resulting from the relatively small population size and the fact that the lens power was calculated rather than measured, leading to compounded uncertainty.

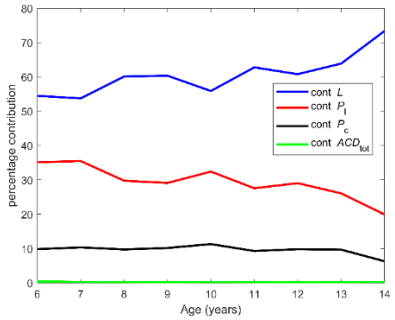

Figure 5.3: Biometric contributions to variations in refractive error from the Twelker et al.[32] data using the simple method. Symbols are defined in Table 5.1.

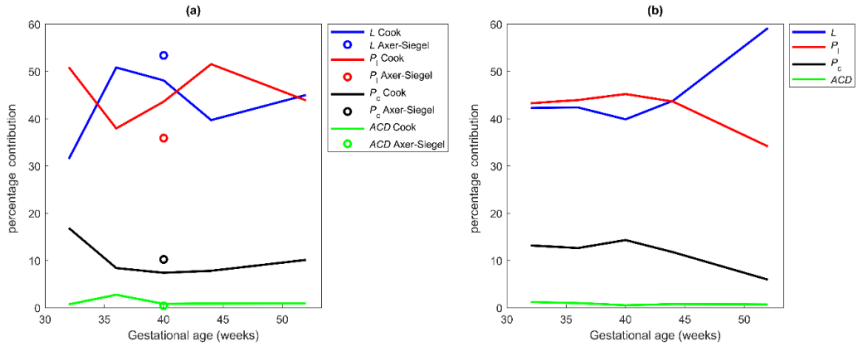

Figure 5.4: Contributions of the variations in ocular biometric components using the simple method to the changes in refractive error from the Cook et al.[34] data for: (a) pre-term infants without retinopathy of prematurity (ROP) and the full-term data by Axer-Siegel; (b) the Cook data for pre-term infants with ROP. Symbols are defined in Table 5.1.

Diabetes

Applying the simple method to the data of healthy adults and adults with diabetes,[35] clear differences are seen (Figure 5.5). Unlike the healthy adults, for the diabetic group, lens power made a considerably larger contribution to the refractive error than the cornea. Regardless, axial length variations still provided the greatest contribution to refractive error for both groups.

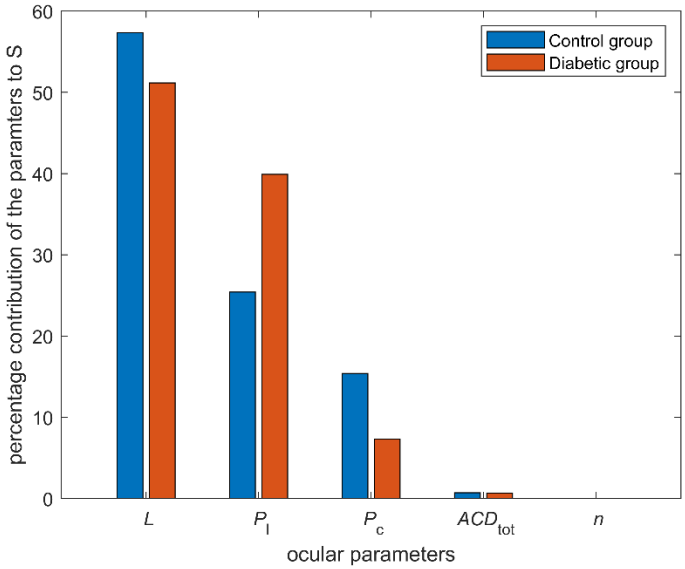

Figure 5.5: Contributions of ocular biometric components to the change in refractive error using the simple method for normal and diabetic adult groups. L is the axial length, PL the lens power, Pc the corneal power, ACDtot the total anterior chamber depth (incl. corneal thickness), and n the refractive index of the ocular humors.

DISCUSSION

This work applied error propagation analysis to simple and matrix representations of the eye to determine how ocular biometric differences affect the distribution of the refractive error. The SyntEyes data showed that both methods assess different but related aspects of ocular biometry (Table 5.1), with axial length variations being responsible for about two-thirds of the differences in refractive error, followed by changes in the lens power (16 – 31%) and anterior corneal radius of curvature (10 - 12%). This is comparable to the data for the control group of healthy adults [35] seen in Figure 5.5, which had corresponding values of 57.3%, 25.4% and 15.4%, respectively. However, the relative importance of corneal and lens powers differs between populations and datasets. To this end, both methods were applied to several datasets, including SyntEyes, which contained every parameter required, as well as clinical datasets for children and adults of different ages having a range of ocular conditions.

Applying the simple method to the longitudinal biometric data of children between the ages of 3 months and 6.5 years from Mutti et al.[31] showed that during emmetropisation and early homeostasis, the contributions from variability in axial length, lens power and corneal curvature were comparable to those found using the simple method in adults (Figure 5.2a). For the matrix method, the contribution from variations in axial length was lower than for adults (±53% instead of 64%), while the variations in the anterior corneal radius of curvature in young children were higher

than corneal power in adults (±20% vs. 8.5%). Similar differences were seen for anterior chamber depth (5 – 9% vs. 3%; Figure 5.2b). Considered longitudinally, only very mild increases in the corneal contributions and mild decreases in the lenticular (simple method) and ACD contributions (matrix method) could be observed. This stability of the contributions is especially remarkable considering the large biometric changes that occur during this period. Myopia disrupts this stability, however, as can be seen in the longitudinal data of school age children by Twelker et al.[32] With increasing myopia prevalence, the contribution of lens power gradually decreased from 35% to 20%, while that of axial length increased from 54% to 73%. This is to be expected as myopia is typically associated with excessive axial growth.

Another group exhibiting altered refractive development are premature infants, many of whom develop ROP. Overall, pre-term infants tend to have shorter axial lengths with a shallower anterior chamber compared with full-term infants at the same gestational age.[47] In pre-term infants, this could result in high degrees of myopia later on, often driven by the cornea and lens rather than axial length, as would likely be the case in full-term individuals[48] and ROP tends to exacerbate these effects.[49] A previous study[34] reported that as ROP progresses, consistent decreases in axial length and anterior chamber depth are observed. The occurrence of myopia varies across different stages of ROP, suggesting a potential link. These findings highlight the complex nature of refractive development in premature infants and emphasize the need for management strategies specific to different ROP stages. Regarding the pre-term data presented by Cook et al.[34] changes in axial length and lens power seemed to contribute equally to the refractive error (Figure 5.4). However, this result may not be reliable as the differences in ocular biometry between pre-term and full-term eyes become more manifest with age, coupled with the fact that the lens power was calculated from average data for a relatively small population compared with previous cohorts. So, while a greater contribution from lens power variations is plausible in pre-term children,[49] this observation to be confirmed with additional data.

Finally, the biometric variations in the diabetic group different substantially from those in the control group, most notably with regard to the dimensions and power of the crystalline lens[35] and especially in those having an early onset of the disease.[50] This difference is reflected in the relative effects of variations in lens and corneal power, with a considerably larger contribution from lens power changes in diabetic eyes (Figure 5.5). These lenticular changes are induced, in part, by the aqueous, which undergoes a rapid drop in glucose concentration during hypoglycemia. As the aqueous and lens interact through osmosis, an exchange of water occurs between them, depending on the patient's glycemic state, which in turn affects the refractive index of the lens, and thus the refraction of the eye.[51]

Similar error propagation methods have been used in previous studies, but mostly to assess how measurement errors from biometry devices affect intraocular lens (IOL) calculations and surgical outcomes.[25-27] In that study, the uncertainty regarding corneal power measurements formed the greatest source of error, along with estimates of the postoperative IOL position,[25, 27, 28] depending on the power calculation formula being used. In a similar context, Ribeiro et al.[28] varied the individual dimensions of the Liou and Brennan eye model to determine corresponding changes in overall refractive error using ray tracing software. For phakic eyes measured with an optical biometer and considering the Monte Carlo process using the measurement errors of the device, variations in anterior corneal asphericity most affected refractive error (36.1%), followed by the anterior radius of curvature (28.0%), corneal thickness (11.0%) and lens thickness (8.9%). Meanwhile, in pseudophakic eyes, the most important contributor by far was the postoperative anterior chamber depth (76.8%). While interesting, the Ribeiro et al. analysis did not consider the existing correlations between the biometric parameters, which would have overestimated the resulting refractive errors. [52]Moreover, as the Monte Carlo process was considered over the range of measurement errors of an optical biometer, these percentage contributions should not be compared with the current results. Finally, in a classic study Hirsch and Weymouth[53] attempted to predict refractive error using multiple regression analysis, reporting a contribution of approximately 47% from changes in axial length, while some 24% and 7% were due to variations in corneal radius of curvature and anterior chamber depth, respectively. The remaining 22% were assumed to be variations in crystalline lens curvature, refractive indices of the media and measurement errors. [53]These values are somewhat different from the current findings, probably because they do not include the lens power. Also, Olsen et al. used a strict statistical approach to investigate the correlation between refractive error and ocular refractive components. Their findings revealed a significant correlation between ocular refraction and not only axial length but also lens and cornea power.[1]

This analysis has some limitations. The most important is the sensitivity to large variability in standard deviations, which in turn is determined by the number of participants and as for the IOL power analyses described above, by the measurement errors of the biometer being used. This is especially evident in the fluctuating values for calculated lens powers from the Cook et al.[34] and Axer-Siegel et al.[33, 45] data sets (Figure 5.4a), compared with the lens power values measured with a custom phakometer for a much larger dataset by Mutti et al.[31] (Figure 5.2). In practice, however, there are only a limited number of biometry systems on the market, having about the same level of repeatability, so using a sufficiently large dataset (e.g., 50 eyes per data point) should minimize this issue. Another limitation is the unavailability of the posterior corneal radius in most of the datasets considered here, necessitating the estimate of r_{cp} = 0.821.rca given in Table 5.1, which was previously

derived[38] from Oculus Pentacam (pentacam.com) data of 4,953 Iranian school children with a mean age of 9.74±1.68 years that included both the anterior and posterior corneal radii. This method is preferred over the use of a keratometry index, as most indices tend to overestimate the actual total power,[54, 55] and it allows more accurate thick-lens calculations. Another limitation of the present study is the use of age-based regressions to estimate the position of the principal planes with the simple method, rather than their full calculation. This choice was motivated by the fact that calculation and inclusion would have led to far more complicated equations for the simple method than strictly necessary. On the other hand, the matrix method is more accurate and mathematically complete as it considers all relevant parameters, and unlike the simple method, does not make any assumptions about the principal plane position at the expense of increased complexity. Here too, a simplification with fixed principal points was considered using pp_{eye2} as a variable instead of equation (6), but while this simplified the refractive error formula, it did not do much to simplify the partial derivatives and therefore was abandoned. Hence, as the matrix method was more accurate and complete, it was preferred over the simple method. Although it may be limited by the need for parameters that are currently difficult to obtain, such as the lens radii of curvature, new technologies are continuously being introduced that will help to overcome these issues. In the meantime, the simple method can provide a reliable first-order estimate.

Diabetes can affect the ocular components, particularly the aqueous humor and the lens, thereby producing changes in refractive error. In poorly controlled diabetes, fluctuations in the properties of the aqueous humor can rapidly impact internal refraction, leading to variations in vision. Additionally, diabetes can gradually affect the lens, potentially causing longer-term changes in lens curvature.

In conclusion, this work proposed two methods for estimating the contribution of variations in ocular biometric components to the resulting refracting error within a population. About 50 - 65% of these refractive error changes are determined by variations in axial length, and to a lesser degree by variations in lens and corneal power. The latter two appear to vary in importance, depending on the measuring equipment being used and the population being considered.

REFERENCES

1. Olsen T, Arnarsson A, Sasaki H, Sasaki K, Jonasson F. On the ocular refractive components: the Reykjavik Eye Study. Acta Ophthalmol. 2007;85(4):361-6.
2. Berg F. Über Variabilität und Korrelation bei den verschiedenen Abmessungen des Auges.Graefe Arch Clin Exp Ophthalmol. 1931;127:606-39.
3. Strömberg E. XXXIV: Über Refraktion und Achsenlänge des menschlichen Auges: (Vorläufige Mitteilung). Acta Ophthalmol. 1936;14(1-2):281-97.
4. Stenstrom S. Variations and correlations of the optical components of the eye. Mod trends ophthalmol. 1948;2:87-102.
5. Benjamin B, Davey J, Sheridan M, Sorsby A, Tanner J. Emmetropia and its aberrations; a study in the correlation of the optical components of the eye. Spec Rep Series (Med Research Council (GB)). 1957;11(293):1-69.
6. Fieß A, Nickels S, Schulz A, Münzel T, Wild PS, Beutel ME, et al. The relationship of ocular geometry with refractive error in normal and low birth weight adults. J Optom. 2021;14(1):50-7.
7. Hou W, Norton TT, Hyman L, Gwiazda J, Group C. Axial elongation in myopic children and its association with myopia progression in the Correction of Myopia Evaluation Trial (COMET). Eye Cont Lens. 2018;44(4):248.
8. Meng W, Butterworth J, Malecaze F, Calvas P. Axial length of myopia: a review of current research. Ophthalmologica. 2011;225(3):127-34.
9. Shufelt C, Fraser-Bell S, Ying-Lai M, Torres M, Varma R. Refractive error, ocular biometry, and lens opalescence in an adult population: the Los Angeles Latino Eye Study. Invest Ophthalmol Vis Sci. 2005;46(12):4450-60.
10. Mallen EA, Gammoh Y, Al-Bdour M, Sayegh FN. Refractive error and ocular biometry in Jordanian adults. Ophthal Physiol Opt. 2005;25(4):302-9.
11. Hashemi H, Khabazkhoob M, Emamian MH, Shariati M, Miraftab M, Yekta A, et al. Association between refractive errors and ocular biometry in Iranian adults. J Ophthal Vis Res. 2015;10(3):214.
12. McBrien NA, Adams DW. A longitudinal investigation of adult-onset and adult-progression of myopia in an occupational group. Refractive and biometric findings. Invest Ophthalmol Vis Sci. 1997;38(2):321-33.
13. Yekta A, Fotouhi A, Hashemi H, Ostadi MH, Heravian J, Heydarian S, et al. Relationship between refractive errors and ocular biometry components in carpet weavers. Iran J Ophthalmol. 2010;22(2);45-54
14. Ojaimi E, Rose KA, Morgan IG, Smith W, Martin FJ, Kifley A, et al. Distribution of ocular biometric parameters and refraction in a population-based study of Australian children. Invest Ophthalmol Vis Sci. 2005;46(8):2748-54.
15. Warrier SK, Wu HM, Newland HS, Muecke JS, Selva D, Aung T, et al. Ocular biometry and determinants of refractive error in rural Myanmar: the Meiktila Eye Study. Br J Ophthalmol. 2008;92(12):1591-4
16. Wickremasinghe S, Foster PJ, Uranchimeg D, Lee PS, Devereux JG, Alsbirk PH, et al. Ocular biometry and refraction in Mongolian adults. Invest Ophthalmol Vis Sci. 2004;45(3):776-83.
17. Rozema J, Dankert S, Iribarren R. Emmetropization and non-myopic eye growth. Surv Ophthalmol. 2023.
18. Straub M. Über die Aetiologie der Brechungsanomalien des Auges und den Ursprung der Emmetropie. Graefes Arch Ophthalmol. 1909;70:130-99.
19. Rozema JJ. Refractive development I: Biometric changes during emmetropisation. Ophthal Physiol Opt. 2023;43(3):347-67.
20. Mutti DO, Mitchell GL, Sinnott LT, Jones-Jordan LA, Moeschberger ML, Cotter SA, et al. Corneal and crystalline lens dimensions before and after myopia onset. Optom Vis Sci. 2012;89(3):251-62.
21. Rozema J, Dankert S, Iribarren R, Lanca C, Saw S-M. Axial growth and lens power loss at myopia onset in Singaporean children. Invest Ophthalmol Vis Sci. 2019;60(8):3091-9.
22. Rozema JJ, Tassignon M-J. The Bigaussian nature of ocular biometry. Optom Vis Sci. 2014;91(7):713-22.
23. Steiger A. Die Entstehung der spharischen Refraktionen des menschlichen Auges: S. Karger; 1913.
24. Flitcroft D. Emmetropisation and the aetiology of refractive errors. Eye. 2014;28(2):169-79.
25. Norrby S. Sources of error in intraocular lens power calculation. J Cataract Refr Surg. 2008;34(3):368-76.
26. Olsen T. Sources of error in intraocular lens power calculation. J Cataract Refr Surg. 1992;18(2):125-9.
27. Hirnschall N, Findl O, Bayer N, Leisser C, Norrby S, Zimper E, et al. Sources of error in toric intraocular lens power calculation. J Refr Surg. 2020;36(10):646-52.
28. Ribeiro F, Castanheira-Dinis A, Dias JM. Refractive error assessment: influence of different optical elements and current limits of biometric techniques. J Refr Surg. 2013;29(3):206-12.
29. Navarro R, Lockett-Ruiz V, López JL. Analytical ray transfer matrix for the crystalline lens. Biomed Opt Express. 2022;13(11):5836-48.
30. Rozema JJ, Rodriguez P, Navarro R, Tassignon M-J. SyntEyes: a higher-order statistical eye model for healthy eyes. Invest Ophthalmol Vis Sci. 2016;57(2):683-91.
31. Mutti DO, Sinnott LT, Mitchell GL, Jordan LA, Friedman NE, Frane SL, et al. Ocular component development during infancy and early childhood. Optom Vis Sci 2018;95(11):976.
32. Twelker JD, Mitchell GL, Messer DH, Bhakta R, Jones LA, Mutti DO, et al. Children's ocular components and age, gender, and ethnicity. Optometry and vision science: official publication of the American Academy of Optometry. 2009;86(8):918.
33. Rozema JJ, Herscovici Z, Snir M, Axer-Siegel R. Analysing the ocular biometry of new-born infants. Ophthal Physiol Opt. 2018;38(2):119-28.
34. Cook A, White S, Batterbury M, Clark D. Ocular growth and refractive error development in premature infants

with or without retinopathy of prematurity. Invest Ophthalmol Vis Sci. 2008;49(12):5199-207.
35. Suheimat M, Efron N, Edwards K, Pritchard N, Mathur A, Mallen EA, et al. Biometry of eyes in type 1 diabetes. Biomed Opt Express. 2015;6(3):702-15.
36. Gertsbakh I, Gertsbakh I. Measurement uncertainty: error propagation formula. Measurement Theory for Engineers. Berlin: Springer.2003:87-94.
37. Kuo W, Uppuluri V. A review of error propagation analysis in systems. Microelectronics Reliability. 1983;23(2):235-48.
38. Rozema JJ. Estimating principal plane positions for ocular power calculations in children and adults. Ophthal Physiol Opt. 2021;41(2):409-13.
39. Yudkin AM. The formation of the aqueous humor: its relation to intra-ocular and vascular pressures. Arch Ophthalmol. 1929;1(4):435-46.
40. Yudkin AM. Theaqueous humor: a critical and experimental study. J Am Med Assoc. 1926;87(23):1910-6.
41. Evans T, Rubin A. Linear optics of the eye and optical systems: a review of methods and applications. BMJ Open Ophthalmol. 2022;7(1).
42. O'Brien C, Clark D. Ocular biometry in pre-term infants without retinopathy of prematurity. Eye. 1994;8(6):662-5.
43. Beenett A. A method of determining the equivalent powers of the eye and its crystalline lens without resort to phakometry. Ophthal Physiol Opt. 1988;8(1):53-9.
44. Rozema JJ, Atchison DA, Tassignon M-J. Comparing methods to estimate the human lens power. Invest Ophthalmol Vis Sci. 2011;52(11):7937-42.
45. Axer-Siegel R, Bourla D, Sirota L, Weinberger D, Snir M. Ocular growth in premature infants conceived by in vitro fertilization versus natural conception. Invest Ophthalmol Vis Sci. 2005;46(4):1163-9.
46. Navarro R, Santamaria J, Bescós J. Accommodation-dependent model of the human eye with aspherics. JOSA A. 1985;2(8):1273-80.
47. Fledelius HC, Fledelius C. Eye size in threshold retinopathy of prematurity, based on a Danish preterm infant series: early axial eye growth, pre-and postnatal aspects. Invest Ophthalmol Vis Sci. 2012;53(7):4177-84.
48. Bhatti S, Paysse EA, Weikert MP, Kong L. Evaluation of structural contributors in myopic eyes of preterm and full-term children. Graefe's Arch Clin Exp Ophthalmol. 2016;254:957-62.
49. Kaur S, Dogra M, Sukhija J, Samanta R, Singh SR, Grover S, et al. Preterm refraction and ocular biometry in children with and without retinopathy of prematurity in the first year of life. J Am Assoc Pediat Ophthalmol Strabi. 2021;25(5):271. e1-. e6.50. Rozema JJ, Khan A, Atchison DA. Modelling ocular ageing in adults with well-controlled type I diabetes. Advanc Ophthalmol Pract Research. 2022;2(2):100048.
51. Kaštelan S, Gverović-Antunica A, Pelčić G, Gotovac M, Marković I, Kasun B, editors. Refractive changes associated with diabetes mellitus. Seminars in Ophthalmol; 2018: Taylor & Francis.
52. Sorsby A, Benjamin B, Bennett AG. Steiger on refraction: a reappraisal. Br J Ophthalmol. 1981;65(12):805.
53. Hirsch MJ, Weymouth FW. Notes on ametropia—a further analysis of Stenström's data. Opt Vis Sci. 1947;24(12):601-8.
54. Olsen T. On the calculation of power from curvature of the cornea. Br J Ophthalmol. 1986;70(2):152.
55. Ho J-D, Tsai C-Y, Tsai RJ-F, Kuo L-L, Tsai I-L, Liou S-W. Validity of the keratometric index: evaluation by the Pentacam rotating Scheimpflug camera. J Cataract Refr Surg. 2008;34(1):137-45.

Chapter 7. Discussion

Addressing myopia (nearsightedness) has become a crucial challenge due to its rapidly rising rates, especially in countries with high educational demands and indoor lifestyles.[1] Myopia occurs when the axial and optical powers of the eye are mismatched, causing blurry retinal images. Approximately 28% of people in Europe have myopia, and this number is projected to exceed 50% by 2050. While myopia involves over 500 genes, recent rises are mainly due to lifestyle changes, not genetics.[2] In areas with little education, only 1-2% have myopia, showing genetics matter less there. We still need to understand what visual factors are necessary for normal eye growth. Myopia represents a deviation from normal ocular growth patterns that typically occur during school age, making it a key area of interest for studying normal eye growth. Modeling refractive development provides foundational knowledge of normal eye growth and refractive changes. This understanding helps in predicting myopia risk factors, such as lack of outdoor lighting and extended near work, understanding its underlying mechanisms, and developing effective interventions and treatments to prevent or control its progression.

A significant amount of foundational experimental work has been conducted on animals with two primary aims: understanding the factors affecting eye growth and investigating the necessity of a feedback mechanism in eye development. These animal experiments involve placing animals under specific conditions to observe their growth responses and explore how retinal signals control eye growth. First, we explained some of the previous experimental studies that have examined the factors affecting eye growth and myopia.

FACTORS AFFECTING EYE GROWTH

Early experimental studies in the late 1970s showed that myopia can be experimentally induced in young animals through visual deprivation, a condition driven by reduced contrast and image blurring.[3, 4] The more degraded the image, the more severe the resulting myopia.[5] However, these early studies largely overlooked the temporal dynamics of image degradation. Understanding both the duration and severity of image degradation needed to trigger abnormal eye growth during form-deprivation remains critical. Subsequent research on chickens and guinea pigs revealed that both low and high spatial frequencies contribute to myopia. Additionally, exposing chickens to blurred movies caused myopia, with changes in contrast sensitivity playing a key role.[5, 6, 7, 8 ,9] Interestingly, it was also discovered that fluctuations in daily dopamine levels are associated with eye growth and myopia development.[10] When deprivation myopia is induced, dopamine levels drop in the affected retinal areas[11] and this drop in dopamine is caused by changes in image contrast and spatial frequency, not just reduced light.[12]

Moreover, earlier studies have demonstrated that the human eye can respond to changes in focus when exposed to various light colors. This has led to the hypothesis that chromatic cues are essential for detecting defocus and regulating eye growth.[13] By employing software to simulate focus adjustments in red, green, and blue light, scientists observed that only emmetropic eyes altered their length in response to these simulations. In contrast, myopic eyes showed minimal change, and the "red in focus" filter unexpectedly caused the eyes to lengthen instead of shortening. These findings suggest that while emmetropic eyes can use color cues to control eye growth, the response differs significantly between emmetropic and myopic eyes.[13] Previous research using simulated longitudinal chromatic aberration has led to two key findings: (1) the human retina is able to detect chromatic defocus and make appropriate adjustments to axial length, and (2) myopic retinas do not exhibit this response, at least not during short-term exposure.[13] These results highlight the importance of color cues in understanding visual processing, which could have significant implications for vision correction and eye development studies.[13]

A recent simulation has further revealed that the interaction between monochromatic and chromatic aberrations creates a unique signal called chromatic optical anisotropy, which helps the retina differentiate between positive and negative defocus. This signal varies among myopes, emmetropes, and hyperopes.[14] Studies by Rucker (2013) explored how the eye uses chromatic aberration signals to distinguish between different types of defocus.[15] Additionally, studies on peripheral defocus suggest that the retina's ability to interpret these signals plays a role in refractive development. Smith et al. (2010) demonstrated that peripheral hyperopic defocus could induce myopia, leading to the development of optical interventions like peripheral defocus contact lenses designed to slow myopia progression. These findings highlight the importance of peripheral retinal signals in guiding refractive development.[16]

While these studies advanced our understanding of how various optical signals contribute to refractive development, several limitations remain. Many studies highlight significant variability in how individuals respond to defocus signals, influenced by factors such as genetic, environmental conditions (e.g., near work or outdoor exposure), and age. This variability complicates the generalization of results across diverse populations. Also, studies simulating retinal image quality, such as those using wavefront analysis, often rely on idealized conditions that may not account for real-world factors like eye movement, natural lighting, and variability in ocular structures. Long-term studies across diverse populations, while challenging in terms of sample size and duration, would provide valuable insights into how genetic, environmental, and behavioral factors interact with optical defocus. Therefore, a key future objective could be developing computational models that integrate multiple optical cues, such as chromatic aberrations, peripheral defocus, and contrast sensitivity, to predict how the eye interprets these signals in dynamic visual environments.

Additionally, combining optical studies with biomechanical analyses of ocular structures like the sclera and choroid could provide a deeper understanding of how these elements interact with defocus signals. Table 6.1 gives an overview of the factors that can affect the development of refraction according to previous studies.

Experimental studies demonstrated that myopia deprivation is associated with retinal image degradation in animals. However, these studies alone do not fully explain the process of emmetropization. Without a mechanism to halt eye growth, the system remains open loop, potentially leading to increased myopia. For instance, in young animals, wearing positive lenses induces functional myopia, which subsequently halts eye growth and triggers choroidal thickening, thus gradually correcting the myopia. In contrast, adult human myopic eyes do not naturally undergo axial shortening but can still achieve choroidal thickening when exposed to positive defocus.

The potential of choroidal thickening as a mechanism for myopia control has obtained significant interest. Early theories suggested that choroidal thickening could serve as an additional method of focusing the eye by repositioning the retina closer to the focal plane.[28] Introduced by Wallman and colleagues in the 1990s, this concept posited that choroidal thickening acts as a supplementary response to visual defocus, complementing adjustments made by lens changes and axial length alterations. Animal studies and various interventions—such as positive lens wear, flickering light, and atropine—have supported this hypothesis by demonstrating associated choroidal thickening.[29]

Nonetheless, several limitations in these studies must be acknowledged. The extent of choroidal thickening observed in animals, which can compensate for significant myopic shifts, does not directly translate to humans. For example, while chicken models show sufficient thickening to counter up to 7 diopters of myopia, human choroidal thickening is much less, approximately 40 micrometers—only enough to counter about one-tenth of a diopter.[30] This discrepancy suggests that choroidal thickening may be less effective in humans compared to animal models. Furthermore, the long-term efficacy of choroidal thickening in consistently preventing eye growth remains uncertain.[31]

Recent research has also proposed that metabolic factors and oxygen demand might play a more crucial role in choroidal changes, challenging the earlier "third mechanism" theory.[32, 33] Given these complexities and ongoing uncertainties, further research is essential to evaluate the reliability of choroidal thickening in predicting long-term inhibition of eye growth and to explain the underlying metabolic mechanisms.[34]

Table 6.1: Factors affecting eye growth

Study objective	Key findings	Future recommendations
Investigating the role of longitudinal chromatic aberrations (LCA) in emmetropization of the chick eye (Rucker, 2009 and Gawne, 2021)[17,18]	1)LCA provides visual cues for eye growth adjustments in response to defocus.	1)Explore the role of spatial frequency in a wider range 2)Testing real-world conditions 3) Investigating the effects of TCA
Detecting of defocus sign using peripheral blur orientation (human eyes) (Zheleznyak, 2023 and Zheleznyak, 2024)[19,20]	1)Investigating the orientation of anisotropic peripheral blur as a cue for emmetropization 2)Interaction of monochromatic and polychromatic aberrations distinguishes positive from negative defocus. 3)Myopic eyes show vertically elongated blur; emmetropes and hyperopes show horizontally elongated blur. 4)Peripheral blur orientation is influenced by longitudinal chromatic aberration and off-axis astigmatism.	1)Limited to the nasal visual field (so, expanding analysis to the entire visual field) 2)Assumes uniform peripheral aberrations 3)Real-world variability in peripheral aberrations not fully addressed.
Temporal properties of positive and negative defocus on Marmoset monkeys on emmetropization (Zhu, 2022)[21]	1)Positive lenses (+5D): Continuous wear caused hyperopia; interruptions enhance compensation. 2)Negative lenses (-5D): Continuous wear caused myopia; interruptions reduce myopia.	1)Explore different interruption durations and frequencies. 2)Assess long-term effects of interruptions 3)Apply findings to lens design and human trials.
Impact of Peripheral Refraction on myopia progression (human eyes) (Romashchenko, 2020) [22]	1)Differences between peripheral and central vision 2)Increased optical errors with off-axis angles affecting peripheral image quality	1)Limited data access, variability in measurement techniques 2)More research needed on peripheral aberrations in myopia control
The role of higher order aberrations on myopia (HOAs) (Hughes, 2020) [23]	1)HOA changes affect retinal image quality and axial growth	1)Long-term studies on HOAs change
Role of spatial frequency content of urban and indoor environments on myopia development (Flitcroft, 2020) [24,25]	1)Indoor environments have a steeper spatial frequency slope, similar to conditions that induce myopia in animal models	1)Explore dynamic visual content and varying light conditions 2)Study interaction with optical defocus and dynamic visual content
Role of ambient light on myopia control (Smith, 2021) [26]	High light levels mitigate myopia in animals	1)Conduct long-term studies across diverse populations 2)Explore combined effects of light intensity and spectral composition
Relationship between light levels and dopamine dynamics (Cohen, 2012) [27]	U-shaped relationship with ambient light levels and dopamine dynamics	1)Address Longitudinal data gaps 2)Apply findings to human studies 3) Study long-term effects of varying light on dopamine dynamics and refractive development

The effectiveness of optical interventions for myopia management may also depend on the functional state of retinal inhibitory pathways, which differ between individuals with normal vision (emmetropes) and those with myopia. Research into treatments like peripheral defocus lenses, multifocal designs, and DIMS lenses has shown promise in controlling myopia, although the exact mechanisms remain unclear. For instance, DIMS lenses, which use hexagonal or ring patterns to create secondary focal planes, have been effective in slowing myopia progression. However, questions persist regarding why positive defocus and spatial filtering lose effectiveness in myopic retinas and whether these changes precede or follow myopia onset.

THE NEED FOR ADVANCED MODELING OF RETINAL FEEDBACK

The above-mentioned findings suggest the presence of an active feedback mechanism during eye growth in humans. The process by which the retina provides feedback to regulate eye growth is complex and not entirely understood. It has been shown that the retina processes a substantial amount of visual information by analyzing changes in light intensity rather than exact brightness levels. This process utilizes an ON-OFF system to analyze groups of photoreceptors. By comparing the relative responses of central and surrounding cells, ON and OFF cells are identified. Stimulation of the ON pathway has been shown to influence choroidal thickness, affecting eye growth and myopia development. Specifically, in chickens, increased light exposure via the ON pathway enhances retinal dopamine release, which inhibits myopia progression, while the OFF pathway exhibits opposite effects.[35, 36] The combined activity of the ON-OFF system allows the retina to transmit spatial contrast information from various factors such as near work, higher-order aberrations, chromatic aberrations, luminance, and spatial frequencies. Therefore, the ON and OFF pathways play critical roles in processing visual information and potentially influencing eye growth and myopia development.[37]

Despite these experimental efforts, several critical questions remain unanswered, such as why active feedback mechanisms fail to control myopia. One possible explanation is that, in myopic eyes, positive defocus does not generate the usual inhibitory signal to prevent eye elongation.[38] This failure in feedback response could account for the continued progression of myopia and the ineffectiveness of under-correction strategies. Additionally, results from animal studies may not directly translate to humans. Conducting experimental studies would require a large number of animal subjects or a substantial cohort of young children for extensive measurements, involving significant time, financial investment, participant discomfort, and ethical concerns related to animal use. Thus, there is a growing need for mathematical modeling based on retinal feedback mechanisms.

Several models have been introduced in the literature to investigate the control mechanisms behind eye refraction, focusing on both open-loop and closed-loop systems, each incorporating distinct characteristics. The advantage of closed-loop control models is their ability to account for

environmental variations. This approach allows emmetropization to occur in a more dynamic manner, guiding the eye toward a clear and focused retinal image while offering better control over refractive development.[39-49]

Previous research on retinal feedback and its role in refractive error development has provided valuable insights into the mechanisms underlying ocular growth regulation. One key theory is the Incremental Retinal-Defocus Theory, which suggests that changes in retinal defocus during genetically driven ocular growth serve as cues for adjusting environmentally-induced growth rates.[48] This theory has been explored through various experimental paradigms, including lens imposition, diffusers, occlusion, crystalline lens removal, and prolonged near work, all of which consistently highlight the critical influence of retinal defocus on axial growth. Computational simulations using MATLAB/SIMULINK have further validated this theory by demonstrating directional changes in eye growth that align with defocus cues.[48] Nevertheless, significant limitations remain in understanding the precise mechanisms. A key challenge involves explaining the role of neuromodulators, such as dopamine, in mediating scleral growth in response to defocus signals. Existing studies indicate that these neuromodulators contribute to feedback loops that regulate contrast sensitivity, ultimately affecting structural changes in the sclera. However, specific pathways and interactions, particularly in later stages of development when genetically programmed growth stabilizes, are still not fully understood. Further research is needed to investigate these feedback processes across different age groups and visual conditions.[48]

Another area requiring deeper exploration is the complexity of retinal signal processing. Current models often oversimplify retinal feedback, overlooking critical factors such as chromatic aberration, spatial frequency, and environmental conditions. Incorporating these elements into more sophisticated models would improve the precision and generalizability of predictions for diverse visual environments and refractive errors. Additionally, examining the interactions between retinal layers, neuromodulators, and external factors could provide a more comprehensive understanding of how defocus signals are interpreted and translated into growth adjustments.

Future research should prioritize integrating environmental variables—such as lighting conditions, viewing distances, and visual tasks—into predictive models. Moreover, validating these models with longitudinal data will be crucial for developing more effective interventions for refractive error management, particularly for conditions like myopia and hyperopia.

OUR PROPOSED EYE GROWTH MODELING

This thesis aimed to develop a mathematical model that simulates the outcomes of previous eye growth studies by considering the interaction between axial and optical power to achieve a sharp

image on the retina (i.e., reduce refractive error). Our proposed differential model includes two phases: the first phase for genetically preprogrammed factors and the second phase for retinal feedback mechanisms that work to reduce refractive error. Refractive error is determined by the difference between axial power (the power needed for a sharp retinal image) and the eye power (total refractive power of the eye). These powers are described by two bi-exponential functions inspired by previous literature (Chapter 3). We rewrite these relationships as ordinary differential equations (ODEs) and incorporate a retinal feedback system that combines retinal blur with a term for excessive axial elongation. This proposed ODE system can describe normal and abnormal ocular growth from before birth until adulthood. While excessive axial growth plays a significant role in myopia development, crystalline lens is also important. Although Hung's model is more advanced and comprehensive than earlier retinal feedback models—incorporating both genetically pre-programmed growth and retinal blur and successfully simulating normal eye growth and observations from animal experiments involving imposed lenses and diffusers—it overlooked the role of the crystalline lens. Therefore, our proposed model attempts to account for lens power as a key factor in the eye growth mechanism. An advantage of the proposed ODE model is its ability to assess the relative contributions of genetically preprogrammed growth and retinal feedback by varying the amplitude of preprogrammed growth and feedback.

In the future, we aim to extend this basic model to a more complex one that considers the interactions of ocular components and environmental factors affecting eye growth, such as light, defocus, and color. Due to the modular architecture of its feedback function F and growth term Δ, the proposed ODE model is adaptable for incorporating additional factors. While including more interactions between parameters may lead to a more realistic model of eye growth, it cannot replace actual clinical trials. Nevertheless, researchers can use the model to test and refine hypotheses about eye growth in a more efficient, safe, and cost-effective manner.

In short, our goal was to develop an active emmetropization model using a first-order ODE system to evaluate the relative significance of active versus passive growth. We validated our proposed model by successfully replicating numerous animal and clinical experiments documented in existing literature. For example, our model demonstrated that positive lens-induced defocus slows the rate of axial length increase, while negative defocus accelerates it. Additionally, form deprivation was shown to lead to myopia. Moving forward, this validated model could be instrumental in exploring new methods to prevent or slow the progression of myopia.

In its initial form, the proposed model employed a basic feedback function and external term. However, by developing a more comprehensive model that incorporates interactions among ocular components, we aim to identify specific combinations of growth parameters that contribute to

excessive axial elongation and myopia. Understanding these mechanisms will enable us to propose and test targeted interventions to prevent the progression of myopia.

To enhance our model, we designed an experiment, as described in Chapter 5, to investigate how the contrast sensitivity function (CSF) is affected by different wavelengths of light—green, red, and blue—and how this impacts image quality. We also tested contrast sensitivity across a range of spatial frequencies (1.5, 3, 6, 12, 18 cpd) under varying levels of defocus to understand how different detail levels influence contrast sensitivity and defocus perception. The next step involves updating our basic model to incorporate these factors, adjusting the model's equations to account for the combined effects of defocus and color on eye growth.

A key challenge for the next iteration of our ODE system is to refine the retinal feedback function by integrating more external and environmental factors, ensuring that the model's results align with existing experimental studies. Initially, we will focus on incorporating the effects of color and defocus on CSF into our basic model. We plan to generalize the luminance CSF model by including color, defocus, and refractive error, and then explore how this generalized function can enhance our proposed retinal feedback mechanisms. Alternatively, these factors may be incorporated into the retinal feedback system through parameters such as a_3 and a_7 in the ODEs system. By treating these parameters as functions rather than constants, we can allow for dynamic adjustments based on spatial frequency, color, defocus, luminance level, and refractive error. Furthermore, Hung's quantitative model of local retinal circuitry developed in MATLAB/SIMULINK can be used as an example of how to integrate additional external factors through connections within our model.

Expanding our model to include spatial frequency, color, defocus, and refractive error will bring us closer to developing a complex retinal feedback function that accurately reflects physiological feedback mechanisms for regulating eye growth. Ultimately, our goal is to create precise models of refractive error development that consider both genetic and environmental influences, as well as biochemical factors. Existing models have limitations, such as not incorporating certain feedback mechanisms and failing to fully account for individual genetic susceptibility. Therefore, in the future, we aim to address these gaps by integrating all relevant variables affecting refractive error.

REFERENCES

1. *Morgan I, Rose K. How genetic is school myopia? Prog. Retin. Eye Res. 2005 Jan 1;24(1):1-38.*
2. *Hysi PG, Choquet H, Khawaja AP, Wojciechowski R, Tedja MS, Yin J, Simcoe MJ, Patasova K, Mahroo OA, Thai KK, Cumberland PM. Meta-analysis of 542,934 subjects of European ancestry identifies new genes and mechanisms predisposing to refractive error and myopia. Nat. Genet. 2020 Apr;52(4):401-7.*
3. *Wiesel TN, Raviola E. Myopia and eye enlargement after neonatal lid fusion in monkeys. Nature. 1977;266(5597):66-8.*
4. *Sherman SM, Norton TT, Casagrande VA. Myopia in the lid-sutured tree shrew (Tupaia glis). Brain Res. 1977 Mar 18;124(1):154-7.*
5. *Bartmann M, Schaeffel F. A simple mechanism for emmetropization without cues from accommodation or colour. Vis Res. 1994 Apr 1;34(7):873-6.*
6. *Diether S, Gekeler F, Schaeffel F. Changes in contrast sensitivity induced by defocus and their possible relations to emmetropization in the chicken. Invest. Ophthalmol. Vis. Sci. 2001 Nov 1;42(12):3072-9.*
7. *Schmid KL, Wildsoet CF. Assessment of visual acuity and contrast sensitivity in the chick using an optokinetic nystagmus paradigm. Vis Res. 1998 Sep 1;38(17):2629-34.*
8. *Diether S, Gekeler F, Schaeffel F. Changes in contrast sensitivity induced by defocus and their possible relations to emmetropization in the chicken. Invest. Ophthalmol. Vis. Sci. 2001 Nov 1;42(12):3072-9.*
9. *Weiss S, Schaeffel F. Diurnal growth rhythms in the chicken eye: relation to myopia development and retinal dopamine levels. J. Com. Physiol. A. 1993 Apr;172:263-70.*
10. *Ohngemach S, Hagel G, Schaeffel F. Concentrations of biogenic amines in fundal layers in chickens with normal visual experience, deprivation, and after reserpine application. Vis. Neurosci. 1997 May;14(3):493-505.*
11. *Feldkaemper M, Diether S, Kleine G, Schaeffel F. Interactions of spatial and luminance information in the retina of chickens during myopia development. Exp. Eye Res. 1999 Jan 1;68(1):105-15.*
12. *Seidemann A, Schaeffel F. Effects of longitudinal chromatic aberration on accommodation and emmetropization. Vis Res. 2002 Sep 1;42(21):2409-17.*
13. *Swiatczak B, Schaeffel F. Myopia: why the retina stops inhibiting eye growth. Sci. Rep. 2022 Dec 15;12(1):21704.*
14. *Zheleznyak L, Liu C, Winter S. Chromatic cues for the sign of defocus in the peripheral retina. Biomed. Opt. Express. 2024 Aug 8;15(9):5098-114.*
15. *Rucker FJ. The role of luminance and chromatic cues in emmetropisation. Ophthalmic Physiol. Opt. 2013 May;33(3):196-214.*
16. *Smith EL, Hung LF, Huang J, Blasdel TL, Humbird TL, Bockhorst KH. Effects of optical defocus on refractive development in monkeys: evidence for local, regionally selective mechanisms. Invest. Ophthalmol. Vis. Sci. 2010 Aug 1;51(8):3864-73.*
17. *Rucker FJ, Wallman J. Chick eyes compensate for chromatic simulations of hyperopic and myopic defocus: evidence that the eye uses longitudinal chromatic aberration to guide eye-growth. Vis. Res. 2009 Jul 1;49(14):1775-83.*
18. *Gawne TJ, Grytz R, Norton TT. How chromatic cues can guide human eye growth to achieve good focus. J. Vis. 2021 May 3;21(5):11-.*
19. *Zheleznyak L. Peripheral blur may provide the eye with a cue for the sign of defocus. J. Vis. 2023 Sep 1;23(11):83-.*
20. *Zheleznyak L, Liu C, Winter S. Chromatic cues for the sign of defocus in the peripheral retina. Biomed. Opt. Express. 2024 Aug 8;15(9):5098-114.*
21. *Zhu X, Kang P, Troilo D, Benavente-Perez A. Temporal properties of positive and negative defocus on emmetropization. Sci. Rep. 2022 Mar 4;12(1):3582.*
22. *Romashchenko D, Rosén R, Lundström L. Peripheral refraction and higher order aberrations. Clin. Exp. Optom. 2020 Jan 1;103(1):86-94.*
23. *Hughes RP, Vincent SJ, Read SA, Collins MJ. Higher order aberrations, refractive error development and myopia control: a review. Clin. Exp. Optom. 2020 Jan 1;103(1):68-85.*
24. *Flitcroft DI, Harb EN, Wildsoet CF. The spatial frequency content of urban and indoor environments as a potential risk factor for myopia development. Invest. Ophthalmol. Vis. Sci. 2020 Sep 1;61(11):42-.*
25. *Li DL, Dong XX, Lanca C, Grzybowski A, Pan CW. Lower indoor spatial frequency increases the risk of myopia in children. Br. J. Ophthalmol. 2024 Aug 8.*
26. *Smith EL, Hung LF, Huang J. Protective effects of high ambient lighting on the development of form-deprivation myopia in rhesus monkeys. Invest. Ophthalmol. Vis. Sci. 2012 Jan 1;53(1):421-8.*
27. *Cohen Y, Peleg E, Belkin M, Polat U, Solomon AS. Ambient illuminance, retinal dopamine release and refractive development in chicks. Exp. Eye Res. 2012 Oct 1;103:33-40.*
28. *Wildsoet C, Wallman J. Choroidal and scleral mechanisms of compensation for spectacle lenses in chicks. Vis. Res. 1995 May 1;35(9):1175-94.*
29. *Read SA, Collins MJ, Vincent SJ. Light exposure and eye growth in childhood. Invest. Ophthalmol. Vis. Sci. 2015 Oct 1;56(11):6779-87.*
30. *Mathis U, Ziemssen F, Schaeffel F. Effects of a human VEGF antibody (Bevacizumab) on deprivation myopia and choroidal thickness in the chicken. Exp. Eye Res. 2014 Oct 1;127:161-9.*

31. *Ostrin LA, Harb E, Nickla DL, Read SA, Alonso-Caneiro D, Schroedl F, Kaser-Eichberger A, Zhou X, Wildsoet CF. IMI—the dynamic choroid: new insights, challenges, and potential significance for human myopia. Invest. Ophthalmol. Vis. Sci. 2023 May 1;64(6):4-.*
32. *Wu H, Chen W, Zhao F, Zhou Q, Reinach PS, Deng L, Ma L, Luo S, Srinivasalu N, Pan M, Hu Y. Scleral hypoxia is a target for myopia control. Proc. Natl. Acad. Sci. 2018 Jul 24;115(30):E7091-100.*
33. *Nickla DL, Wildsoet CF. The effect of the nonspecific nitric oxide synthase inhibitor NG-nitro-L-arginine methyl ester on the choroidal compensatory response to myopic defocus in chickens. Optom. Vis. Sci. 2004 Feb 1;81(2):111-8.*
34. *Wang D, Chun RK, Liu M, Lee RP, Sun Y, Zhang T, Lam C, Liu Q, To CH. Optical defocus rapidly changes choroidal thickness in schoolchildren. PLoS ONE. 2016 Aug 18;11(8):e0161535.*
35. *Aung MH, Hogan K, Mazade RE, na Park H, Sidhu CS, Iuvone PM, Pardue MT. ON than OFF pathway disruption leads to greater deficits in visual function and retinal dopamine signaling. Exp. Eye. Res. 2022 Jul 1;220:109091.*
36. *Wang M, Aleman AC, Schaeffel F. Probing the potency of artificial dynamic ON or OFF stimuli to inhibit myopia development. Invest. Ophthalmol. Vis. Sci. 2019 Jun 3;60(7):2599-611.*
37. *Aleman AC, Wang M, Schaeffel F. Reading and myopia: contrast polarity matters. Sci Rep. 2018 Jul 18;8(1):1-8*
38. *Swiatczak B, Schaeffel F. Emmetropic, but not myopic human eyes distinguish positive defocus from calculated blur. Invest. Ophthalmol. Vis. Sci. 2021 Mar 1;62(3):14-*
39. *Van Alphen G. On emmetropia and ametropia. Basel: Karger; 1961.*
40. *Medina Puerta A. El origen de las ametropías:¿ Qué es ametropía? Gac. Ópt. 1980(112):46-8.*
41. *Carroll JP. On emmetropization. J Theoret Biol. 1982;95(1):135-44.*
42. *Medina A. A model for emmetropization: predicting the progression of ametropia. Ophthalmologica. 1987;194(2-3):133-9.*
43. *Medina A, Fariza E. Emmetropization as a first-order feedback system. Vis Research. 1993;33(1):21-6.*
44. *Schaeffel F, Howland HC. Mathematical model of emmetropization in the chicken. J Opt Soc Am A. 1988;5(12):2080-6.*
45. *Flitcroft D. A model of the contribution of oculomotor and optical factors to emmetropization and myopia. Vis. Res. 1998;38(19):2869-79.*
46. *Blackie C, Howland H. An extension of an accommodation and convergence model of emmetropization to include the effects of illumination intensity. Ophthal Physiol Opt. 1999;19:112-25.*
47. *Hung GK, Ciuffreda KJ. Model of human refractive error development. Curr. Eye Res. 1999;19(1):41-52.*
48. *Hung GK, Ciuffreda KJ. A unifying theory of refractive error development. Bull Math Biol. 2000;62(6):1087-108.*
49. *Hung GK, Mahadas K, Mohammad F. Eye growth and myopia development: Unifying theory and Matlab model. Comp Biol Med. 2016;70:106-18.*

APPENDICES

Appendix A. Regressions by Jones et al. (2005)

Ocular Component	Models	
Lens power	E:	$21.850 + 133.590 \cdot age^{-2}$
	PH:	$22.501 + 158.168 \cdot age^{-2}$
	M:	$21.244 + 149.618 \cdot age^{-2}$
	EH:	$22.251 + 129.020 \cdot age^{-2}$
Anterior chamber depth	E:	$1.817 - 0.265 \cdot \ln(age)^{2} + 1.441 \cdot \ln(age)$
	PH:	$2.773 - 0.062 \cdot \ln(age)^{2} + 0.447 \cdot \ln(age)$
	M:	$1.425 - 0.311 \cdot \ln(age)^{2} + 1.749 \cdot \ln(age)$
	EH:	$1.381 - 0.349 \cdot \ln(age)^{2} + 1.787 \cdot \ln(age)$
Axial length	E:	Age ≤ 10.5 years: $20.189 + 1.258 \cdot \ln(age)$
		Age > 10.5 years: $21.353 + 0759 \cdot \ln(age)$
	PH	Age≤10.5 years: $19.926 + 0.970 \cdot \ln(age)$
		Age > 10.5 years: $19.825 + 1.010 \cdot \ln(age)$
	M:	Age≤10.5 years: $18.144 + 2.391 \cdot \ln(age)$
		Age > 10.5 years: $17.808 + 2.560 \cdot \ln(age)$
	EH:	Age≤10.5 years: $19.660 + 1.366 \cdot \ln(age)$
		Age > 10.5 years: $21.180 + 0.715 \cdot \ln(age)$
Corneal power	E:	$42.131 - 0.566 \cdot \ln(age)^{2} + 2.033 \cdot \ln(age)$
	PH:	$45.061 + 0.161 \cdot \ln(age)^{2} - 1.033 \cdot \ln(age)$
	M:	$44.253 - 0.009 \cdot \ln(age)^{2} + 0.008 \cdot \ln(age)$
	EH:	$44.525 + 0.163 \cdot \ln(age)^{2} - 0.704 \cdot \ln(age)$

E: Emmetropes; PH : Persistent hypermetropes ; M : Myopes ; EH: Emmetropizing hypermetropes.

Appendix B. Blur circle calculation

The axial power (dioptric distance) and whole eye power may be described as:

$$\begin{cases} P_{\text{ax}} = n/(f+z) \\ P_{\text{eye}} = n/f \end{cases} \qquad \text{(B1)}$$

with f the focal distance and z the distance between the focal point and the retina (**Figure B1**, top). Suppose a point at infinity and a pupil diameter D. In presence of ametropia, this will produce a blur circle of height d that can found through:

$$\frac{D}{f} = \frac{d}{z}$$

Which can be revised as:

$$\frac{d}{D} = \frac{z}{f} = \frac{(f+z)-f}{f}$$

Using equations **(B1)** this becomes:

$$\frac{d}{D} = \frac{n/P_{\text{ax}} - n/P_{\text{eye}}}{n/P_{\text{eye}}} = \frac{P_{\text{eye}}}{P_{\text{ax}}} - 1 = \frac{-S}{P_{\text{ax}}}$$

as refractive error $S = P_{\text{ax}} - P_{\text{eye}}$. Hence:

$$d = \left(\frac{P_{\text{eye}}}{P_{\text{ax}}} - 1\right) = \frac{-S \cdot D}{P_{\text{ax}}} \qquad \text{(B2)}$$

The retinal blur size therefore scales with the $P_{\text{eye}}/P_{\text{ax}}$ or the S/P_{ax} ratios. This is *0* for emmetropia and different from *0* for ametropia. The sign of d is associated with the orientation of the retinal image of the pupil, which in turn depends on the sign of the ametropia. In practice,

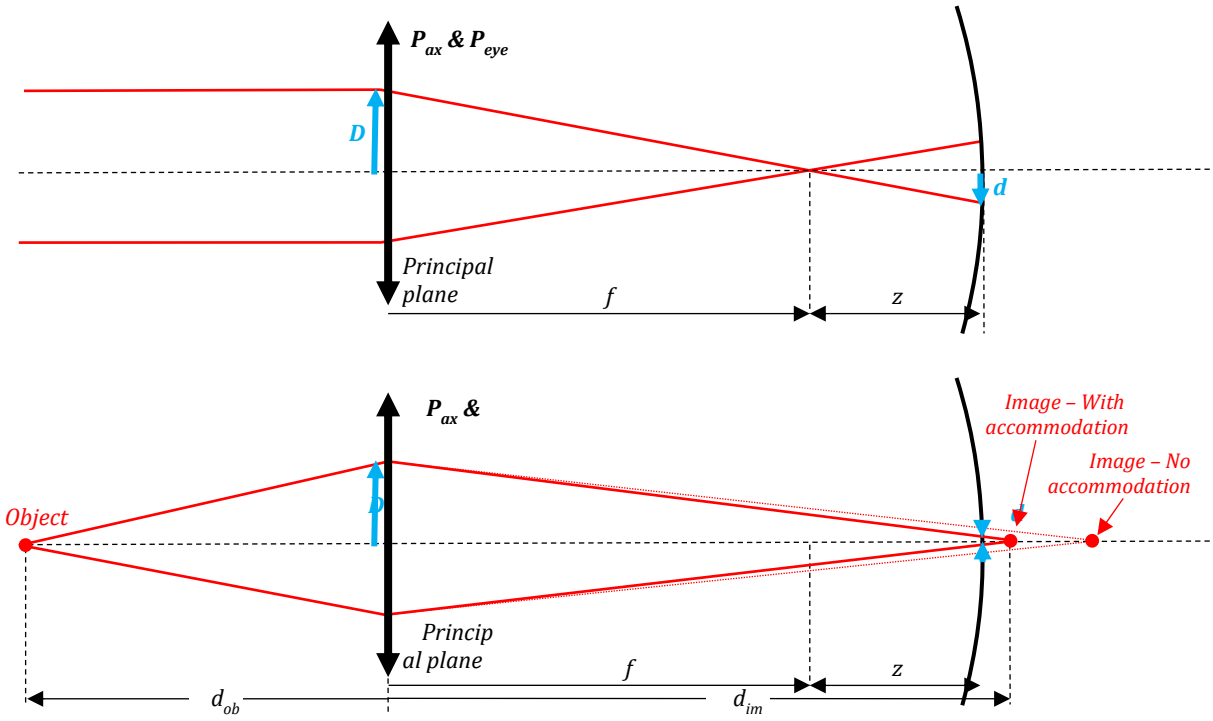

Figure B1: Schematic overview of the parameters for an object at infinity (top) and nearby (bottom).

however, this sign is unimportant as, based on defocus alone, the same amount of myopia or hypermetropia would produce the same retinal blur. Assuming a fixed pupil size of size *1*, the retinal blur portion of the feedback function can finally be written as:

$$F = \left| \frac{P_{\text{eye}}}{P_{\text{ax}}} - 1 \right|$$

where the |...| represent the absolute value.

Near object without accommodation

Suppose an object at distance d_{ob} in front of an eye, then an image is formed at a distance d_{im}, determined by the thin lens equation (**Figure B1**, bottom):

$$P_{\text{eye}} = \frac{1}{d_{\text{ob}}} + \frac{n}{d_{\text{im}}}$$

In this case:

$$\frac{D}{d_{\text{im}}} = \frac{d}{d_{\text{im}} - (f + z)}$$

and

$$d = \frac{d_{\text{im}} - (f + z)}{d_{\text{im}}} D = \left(1 - \frac{n(f + z)}{n \cdot d_{\text{im}}}\right) D = \left(1 - \frac{P_{\text{eye}} - 1/d_{\text{ob}}}{P_{\text{ax}}}\right) D$$

So

$$d = \left(1 - \frac{P_{\text{eye}} - V_{\text{ob}}}{P_{\text{ax}}}\right) D$$

with V_{ob} the vergence of the object. Here too the retinal blur size scales with $P_{\text{eye}}/P_{\text{ax}}$. $V_{\text{ob}} = 0$ returns equation **(B2)** with an inverted sign, but this is again of no importance.

Near object with accommodation

If in the previous case the eye would accommodate by a power P_{acc} (**Figure B1**, bottom), the thin lens equation gives:

$$P_{\text{eye}} + P_{\text{acc}} = \frac{1}{d_{\text{ob}}} + \frac{n}{d_{\text{im}}}$$

From this follows:

$$d = \left(1 - \frac{n(f+z)}{n \cdot d_{\text{im}}}\right) D = \left(1 - \frac{P_{\text{eye}}}{P_{\text{ax}}} - \frac{V_{\text{ob}} - P_{\text{acc}}}{P_{\text{ax}}}\right) D \qquad \text{(B3)}$$

where $V_{\text{ob}} - P_{\text{acc}}$ corresponds with the accommodative lag. $V_{\text{ob}} = P_{\text{acc}} = 0$ returns equation **(B2)** with an inverted sign. For the special case where the eye is able to fully move the sharp image to the retina through accommodation (i.e., $d_{\text{im}} = f + z$) equation **(B3)** yields $d = 0$, corresponding with an image in focus. Assuming a fixed pupil size of size *1*, the retinal blur portion of the feedback function is then:

$$F = \left|1 - \frac{P_{\text{eye}}}{P_{\text{ax}}} - \frac{V_{\text{ob}} - P_{\text{acc}}}{P_{\text{ax}}}\right| \quad \text{(B4)}$$

which combines the image blur from ametropia and accommodative lag.

Appendix C. Spectral transmission of Dichroic filters

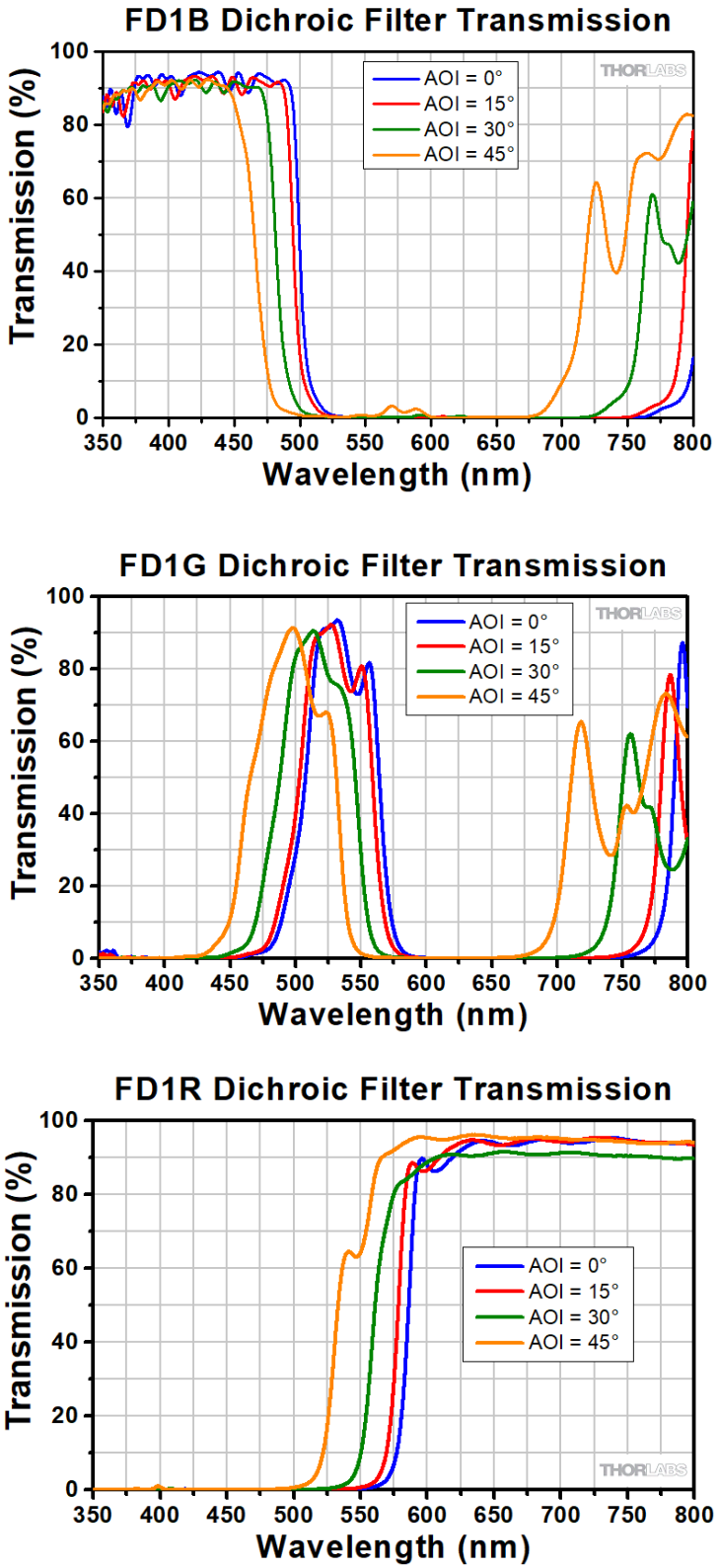

Figure C1. the percent transmission versus wavelength of dichroic filters for four different angles of incidence (AOI)

Luminance contrast sensitivity function model [47]

$$CSF(f) = afe^{-bf}(1 + ce^{bf})^{0.5}$$

$$a = \left[540\left(1 + \frac{0.7}{L}\right)^{-0.2}\right] / [1 + \frac{12\left(1 + \frac{f}{3}\right)^{-2}}{w}]$$

$$b = 0.3\left(1 + \frac{100}{L}\right)^{0.15}$$

$$c = 0.06$$

Where f is the spatial frequency of the stimulus, w is the stimulus size in degree of visual angle, and L is the mean luminance of the stimulus in cd/m2 .

Appendix D.

SUPPLEMENTARY A: Additional Equations

1. Full expressions of A and C in Equation (4):

$$A = -\frac{n \cdot LT}{n_s}\left[\frac{n_c - 1}{n_c r_{ca}}\left(\frac{n_c}{n} - \frac{CCT(n - n_c)}{n \cdot r_{cp}}\right) + \frac{n - n_c}{n \cdot r_{cp}}\right] + \left(1 - \frac{LT(n_s - n)}{n_s r_{la}}\right)\left[1 - \frac{ACD(n - n_c)}{n \cdot r_{cp}} - \frac{n - 1}{n \cdot r_{ca}}\left(CCT\left(1 - \frac{ACD(n - n_c)}{n \cdot r_{pc}}\right) + \frac{n_c ACD}{n}\right)\right]$$

$$C = \left(1 - \frac{LT(n - n_s)}{n_s r_{lp}}\right)\left[\frac{n_c - 1}{n \cdot r_{ca}}\left(1 - \frac{CCT(n - n_c)}{n \cdot r_{cp}}\right) + \frac{n - n_c}{n \cdot r_{cp}}\right] + \left[1 - \frac{ACD(n - n_c)}{n \cdot r_{cp}} - \frac{n_c - 1}{n_c r_{ca}}\left(CCT\left(1 - \frac{ACD(n - n_c)}{n \cdot r_{cp}}\right) + \frac{n_c ACD}{n}\right)\right] \cdot \left[P_G + \frac{n_s - n}{n}\left(\frac{1}{r_{la}} - \frac{1}{r_{lp}}\right) + \frac{LT(n - n_s)^2}{n \cdot n_s r_{la} r_{lp}}\right]$$

2. Partial derivatives for the matrix method:

Axial length (L)

$$\frac{\partial SE}{\partial L} = -\frac{n}{\left(L - (CCT + LT + ACD) + \frac{A - 1}{C}\right)^2}$$

GRIN structure to the lens power (P_G)

$$\frac{\partial SE}{\partial P_G} = \frac{n\frac{(A - 1)\frac{\partial C}{\partial P_G}}{C^2}}{\left(L - CCT - ACD - LT + \frac{A - 1}{C}\right)^2} - n\left(\frac{\partial C}{\partial P_G}\right)$$

with

$$\frac{\partial C}{\partial P_G} = \frac{(n_c - 1).\left(CCT\left(\frac{ACD(n - n_c)}{n r_{cp}} - 1\right) - \frac{n_c ACD}{n}\right)}{n_c r_{ca}} - \frac{ACD(n - n_c)}{n.r_{cp}} + 1$$

Anterior cornea radius of curvature (r_{ca})

$$\frac{\partial SE}{\partial r_{ca}} = \frac{-n\left(\dfrac{C\dfrac{\partial A}{\partial r_{ca}} - (A-1)\dfrac{\partial C}{\partial r_{ca}}}{C^2}\right)}{\left(L - CCT - ACD - LT + \dfrac{A-1}{C}\right)^2} - n\frac{\partial C}{\partial r_{ca}}$$

with

$$\frac{\partial A}{\partial r_{ca}} = \frac{LT\left(n_c - \dfrac{CCT.(n\ -\ n_c)}{nr_{pc}}\right)(n_c\ -\ 1)}{n_c n_s {r_{ca}}^2} - \frac{1}{n_c {r_{ca}}^2}.\left(\frac{LT(n-n_s)}{n_s r_a} + 1\right).\left(CCT\left(\frac{ACD.(n\ -\ n_c)}{nr_{pc}} - 1\right) - \left(\frac{n_c ACD}{n^2}\right)(n_c - 1)\left(\frac{ACD(n\ -\ n_c)}{r_{pc}} - 1\right)\right)$$

$$\frac{\partial C}{\partial r_{ca}} = \left(\frac{n_c}{n} - \frac{CCT(n-n_c)}{n.r_{cp}}\right)\left(\frac{LT(n-n_s)}{n_s r_p} - 1\right).\frac{(n_c-1)}{n_c {r_{ca}}^2} - \frac{1}{n_c {r_{ca}}^2}\left[\frac{(n_c-1).CCT}{n}.\left(\left(\frac{ACD(n-n_c)}{n.r_{cp}} - 1\right) - \frac{n_c ACD}{n}\right).\left(P_G - (\frac{1}{r_{la}} - \frac{1}{r_{lp}})(n - n_s)\right) + \frac{LLT(n-n_s)^2}{n.n_s r_{la} r_{lp}}\right]$$

Anterior chamber depth (ACD)

$$\frac{\partial SE}{\partial ACD} = \frac{-n\left(-1 + \left(\dfrac{\partial A}{\partial ACD}C - (A-1)\dfrac{\partial C}{\partial ACD}\right)/C^2\right)}{\left(L - CCT - ACD - LT + \dfrac{A-1}{C}\right)^2} - n\frac{\partial C}{\partial ACD}$$

with

$$\frac{\partial A}{\partial ACD} = L_{11}\frac{\partial C_{11}}{\partial ACD} + L_{12}\frac{\partial C_{21}}{\partial ACD} = \left(1 - LT\frac{n_s - n}{n_s r_{la}}\right)\left[\left(1 - \frac{CCT(n_c-1)}{n_c \cdot r_{ca}}\right)\left(-\frac{n-n_c}{n \cdot r_{cp}}\right) - \frac{(n_c-1)}{n \cdot r_{ca}}\right]$$

$$\frac{\partial C}{\partial ACD} = \left[\frac{n_s - n}{n}\left(\frac{1}{r_{la}} - \frac{1}{r_{lp}}\right) + \frac{(n-n_s)^2}{n \cdot n_s r_{la} r_{lp}}t + P_G\right] \cdot \left[\left(1 - \frac{CCT(n_c-1)}{n_c r_{ca}}\right)\left(\frac{n_c - n}{n \cdot r_{cp}}\right) - \frac{n_c - 1}{n \cdot r_{ca}}\right]$$

Refractive index of the ocular humours (n)

$$\frac{\partial SE}{\partial n} = \frac{\left(L - CCT - ACD - LT + \dfrac{A-1}{C}\right) - n\left(\dfrac{\partial A}{\partial n}C - (A-1)\dfrac{\partial C}{\partial n}\right)/C^2}{\left(L - CCT - ACD - LT + \dfrac{A-1}{C}\right)^2} - C - n\frac{\partial C}{\partial n}$$

with

$$\frac{\partial A}{\partial n} = \left(\frac{LT(n-n_s)}{n_s r_{la}} + 1\right)\left(\frac{ACD(n-n_c)}{n^2 r_{cp}} - \frac{ACD}{n.r_{cp}} + \frac{CCT(n_c-1)}{n_c r_{ca}}\right)$$
$$\cdot\left(-\frac{LT}{n_s}\left(\frac{n-n_c}{n\cdot r_{cp}} + \frac{1}{n_c r_{ca}}\left(\frac{n_c}{n} - \frac{CCT(n-n_c)}{n\cdot r_{cp}}\right)(n_c - 1)\right)\right.$$
$$+\frac{n\cdot LT}{n_s}\left(\frac{n-n_c}{n^2 r_{cp}} - \frac{1}{n\cdot r_{cp}} + \frac{(n_c-1)}{n_c r_{ca}}\left(\frac{n_c}{n^2} + \frac{CCT}{n\cdot r_{cp}} - \frac{CCT(n-n_c)}{n^2 r_{cp}}\right)\right)$$
$$\left.+\frac{LT}{n_s r_{la}}\left(\frac{1}{n_c r_{ca}}\left(CCT\left(\frac{ACD(n-n_c)}{n\cdot r_{cp}} - 1\right) - \frac{n_c ACD}{n}\right)(n_c-1) - \frac{ACD(n-n_c)}{n\cdot r_{cp}} + 1\right)\right)$$

$$\frac{\partial C}{\partial n} = \left(\frac{LT(n-n_s)}{n_s r_p} - 1\right)\left(\frac{n-n_c}{n^2 r_{cp}} - \frac{1}{n\cdot r_{cp}} + \frac{n_c-1}{n_c r_{ca}}\left(\frac{n_c}{n^2} + \frac{CCT}{n\cdot r_{cp}} - \frac{CCT(n-n_c)}{n^2 r_{cp}}\right)\right)$$
$$+\left(\frac{ACD(n-n_c)}{n^2 r_{cp}} - \frac{ACD}{n\cdot r_{cp}} + \frac{n_c - 1}{n_c r_{ca}}\left(CCT\left(\frac{ACD}{n\cdot r_{cp}} - \frac{ACD(n-n_c)}{n^2 r_{cp}}\right) + \frac{n_c ACD}{n^2}\right)\right)$$
$$\cdot\left(P_G - \frac{n-n_s}{n}\left(\frac{1}{r_{la}} - \frac{1}{r_{lp}}\right) + \frac{LT(n-n_s)^2}{n\cdot n_s r_{la} r_{lp}}\right)$$
$$-\left(\frac{n_c - 1}{n_c r_{ca}}\left(CCT\left(\frac{ACD(n-n_c)}{n\cdot r_{cp}} - 1\right) - \frac{n_c ACD}{n}\right) - \frac{ACD(n-n_c)}{n\cdot r_{cp}} + 1\right)$$
$$\cdot\left(\frac{n_s}{n^2}\left(\frac{1}{r_{la}} - \frac{1}{r_{lp}}\right) - \frac{2\cdot LT(n-n_s)}{n\cdot n_s r_{la} r_{lp}} + \frac{LT(n-n_s)^2}{n^2 n_s r_{la} r_{lp}}\right)$$
$$-\frac{LT}{n_s r_{lp}}\left(\frac{n-n_c}{n\cdot r_{cp}} + \frac{n_c - 1}{n\cdot n_c r_{ca}}\left(n_c - \frac{CCT(n-n_c)}{r_{cp}}\right)\right)$$

Lens thickness (LT):

$$\frac{\partial SE}{\partial LT} = \frac{-\left(1 + \left(\frac{\partial A}{\partial LT}C - (A-1)\frac{\partial C}{\partial LT}\right)/C^2\right)n}{\left(L - CCT - ACD - LT + \frac{A-1}{C}\right)^2} - n\frac{\partial C}{\partial LT}$$

with

$$\frac{\partial A}{\partial LT} = \frac{1}{n_c r_{ca}}.(n-n_s).(n_c-1).\left[\left(\left(\frac{CCT.ACD(n-n_c)}{n.r_{cp}}\right) - 1\right) - \frac{ACD.n_c}{n}\right]$$
$$-\left(\frac{ACD(n-n_c)}{n r_{cp}} + \frac{1}{n_s r_a}\right) - \left(\frac{CCT(n_c-1)}{n_c r_{ca}}\right)$$
$$\cdot\left(-\frac{LT}{n_s}\left(\frac{n-n_c}{n\cdot r_{cp}} + \frac{1}{n_c r_{ca}}\left(\frac{n_c}{n} - \frac{CCT(n-n_c)}{n\cdot r_{cp}}\right)(n_c - 1)\right)\right.$$
$$+\frac{n\cdot LT}{n_s}\left(\frac{n-n_c}{n^2 r_{cp}} - \frac{1}{n\cdot r_{cp}} + \frac{(n_c-1)}{n_c r_{ca}}\left(\frac{n_c}{n^2} + \frac{CCT}{n\cdot r_{cp}} - \frac{CCT(n-n_c)}{n^2 r_{cp}}\right)\right)$$
$$+\frac{LT}{n_s r_{la}}\left(\frac{1}{n_c r_{ca}}\left(CCT\left(\frac{ACD(n-n_c)}{n\cdot r_{cp}} - 1\right) - \frac{n_c ACD}{n}\right)(n_c-1) - \frac{ACD(n-n_c)}{n\cdot r_{cp}}\right.$$
$$\left.\left.+1\right)\right)$$

$$\frac{\partial C}{\partial LT} = \frac{(n - n_s)^2}{n\, n_s r_{la}} \cdot \left[\frac{(n_c - 1).}{n_c r_{ca}} \left(LT \left(\frac{ACD(n - n_c)}{n.r_{cp}} - 1 \right) - \frac{n_c ACD}{n} \right) - \frac{ACD(n - n_c)}{n.r_{cp}} + 1 \right] - \frac{(n - n_s)}{n_s r_{lp}} \cdot \left[\frac{(n - n_c)}{n.r_{cp}} + \left(\frac{n_c}{n} - \frac{LT(n - n_c)}{n.r_{cp}} \right) \left(\frac{(n_c - 1)}{n_c r_{ca}} \right) \right]$$

Posterior lens radius of curvature (r_{lp}):

$$\frac{\partial SE}{\partial r_{lp}} = \frac{n \frac{\partial C}{\partial r_{lp}} (A - 1)/C^2}{\left(L - CCT - ACD - LT + \frac{A - 1}{C} \right)^2} - n. \frac{\partial C}{\partial r_{lp}}$$

with

$$\frac{\partial C}{\partial r_{lp}} = LT \frac{(n - n_s)}{n_s {r_{lp}}^2} \cdot \left(\frac{n - n_c}{n.r_{cp}} + \frac{(n_c - 1)}{n_c r_{ca}} \cdot \left(\frac{n_c}{n} - \frac{CCT(n - n_c)}{n.r_{cp}} \right) \right) - \left(\frac{(n - n_s)}{n.{r_{lp}}^2} + \frac{LT(n - n_s)^2}{n.n_s r_{la} {r_{lp}}^2} \right). \left[\frac{\left(CCT.(n_c - 1) \left(\frac{ACD(n - n_c)}{n r_{cp}} - 1 \right) - \frac{n_c ACD}{n} \right)}{n_c r_{ca}} - \frac{ACD(n - n_c)}{n r_{cp}} + 1 \right]$$

Anterior lens radius of curvature (r_{la})

$$\frac{\partial SE}{\partial r_{la}} = \frac{-n \left(\frac{\partial A}{\partial r_{la}} C - (A - 1) \frac{\partial C}{\partial r_{la}} \right)/C^2}{\left(L - t_c - ACD - t + \frac{A - 1}{C} \right)^2} - n. \frac{\partial C}{\partial r_{la}}$$

with

$$\frac{\partial A}{\partial r_{la}} = \frac{-LT\,(n - n_s)}{n_s {r_{la}}^2} \left(\left[\frac{CCT}{n_c r_{ca}} \cdot \left(\frac{ACD(n - n_c)}{n.r_{cp}} - 1 \right) - \frac{n_c.ACD(n_c - 1)}{n} \right] - \frac{ACD(n - n_c)}{n.r_{cp}} + 1 \right)$$

$$\frac{\partial C}{\partial r_{la}} = \left(\frac{(n - n_s)}{n.{r_{la}}^2} - \frac{LT(n - n_s)^2}{n n_s {r_{la}}^2 r_{lp}} \right). \left(\left(\left(CCT. \left(\frac{ACD(n - n_c)}{n.r_{cp}} - 1 \right) - \frac{n_c.ACD}{n} \right). \frac{(n_c - 1)}{n_c r_{ca}} \right) - \frac{ACD(n - n_c)}{n.r_{cp}} + 1 \right)$$

Refractive index of the lens surface (n_s):

$$\frac{\partial SE}{\partial n_s} = \frac{-n \left(\frac{\partial A}{\partial n_s} C - (A - 1) \frac{\partial C}{\partial n_s} \right)/C^2}{\left(L - CCT - ACD - LT + \frac{A - 1}{C} \right)^2} - n \frac{\partial C}{\partial n_s}$$

with

$$\frac{\partial A}{\partial n_s} = \frac{n \cdot LT}{n_s^2} \left(\frac{n - n_c}{n \cdot r_{cp}} + \frac{n_c - 1}{n_c r_{ca}} \left(\frac{n_c}{n} - \frac{CCT(n - n_c)}{n \cdot r_{cp}} \right) \right) - \left(\frac{LT}{n_s r_{la}} + \frac{LT(n - n_s)}{n_s^2 r_{la}} \right) \left(\frac{n_c - 1}{n_c r_{ca}} \left(CCT \left(\frac{ACD(n - n_c)}{n \cdot r_{cp}} - 1 \right) - \frac{n_c ACD}{n} \right) - \frac{ACD(n - n_c)}{n \cdot r_{cp}} + 1 \right)$$

$$\frac{\partial C}{\partial n_s} = \left(\frac{n-n_c}{n\cdot r_{cp}} + \frac{n_c-1}{n_c r_{ca}}\left(\frac{n_c}{n} - \frac{CCT(n-n_c)}{n\cdot r_{cp}}\right)\right)\left(\frac{LT}{n_s r_{lp}} + \frac{LT(n-n_s)}{n_s^2 r_{lp}}\right) - \left(\frac{2\cdot LT(n-n_s)}{n\cdot n_s r_{la} r_{lp}} - \frac{1}{n}\left(\frac{1}{r_{la}} - \frac{1}{r_{lp}}\right) + \frac{LT(n-n_s)^2}{n\cdot n_s^2 r_{la} r_{lp}}\right) \cdot \left(\frac{n_c-1}{n_c r_{ca}}\left(CCT\left(\frac{ACD(n-n_c)}{n\cdot r_{cp}} - 1\right) - \frac{n_c ACD}{n}\right) - \frac{ACD(n-n_c)}{n\cdot r_{cp}} + 1\right)$$

Posterior cornea radius of curvature (r_{cp})

$$\frac{\partial SE}{\partial r_{cp}} = \frac{-\frac{n}{C^2}\left(C\frac{\partial A}{\partial r_{cp}} - (A-1)\frac{\partial C}{\partial r_{cp}}\right)}{\left(L - CCT - ACD - LT + \frac{A-1}{C}\right)^2} - n\frac{\partial C}{\partial r_{cp}}$$

where

$$\frac{\partial A}{\partial r_{cp}} = \left(\frac{ACD(n-n_c)}{n r_{cp}^2} - \frac{ACD.CCT.(n-n_c)(n_c-1)}{n n_c r_{ca} r_{cp}^2}\right)\left(\frac{t(n-n_s)}{n_s r_{la}} + 1\right) + \frac{n.CCT}{n_s}\left(\frac{n-n_c}{n r_{cp}^2} - \frac{CCT(n-n_c)(n_c-1)}{n n_c r_{ca} r_{cp}^2}\right)$$

$$\frac{\partial C}{\partial r_{cp}} = \left(\frac{LT(n-n_s)}{n_s r_{cp}} - 1\right)\left(\frac{(n-n_c)}{n.r_{cp}^2} - \frac{CCT(n-n_c)(n_c-1)}{n.n_c r_{ca} r_{cp}^2}\right) + \left(\frac{ACD(n-n_c)}{n.r_{cp}^2} - \frac{\left(ACD.CCT(n-n_c)(n_c-1)\right)}{n.n_c\, r_{ca} r_{cp}^2}\right)$$

Refractive index of the cornea (n_c):

$$\frac{\partial SE}{\partial n_c} = \frac{-n\left(\frac{\partial A}{\partial n_c}C - (A-1)\frac{\partial C}{\partial n_c}\right)/C^2}{\left(L - CCT - ACD - LT + \frac{A-1}{C}\right)^2} - n\frac{\partial C}{\partial n_c}$$

with

$$\frac{\partial A}{\partial n_c} = \left(\frac{LT(n-n_s)}{n_s r_{la}} + 1\right) \cdot \left(\frac{ACD}{n\cdot r_{cp}} + \frac{CCT}{n_c r_{ca}}\left(\frac{ACD(n-n_c)}{n\cdot r_{cp}} - 1\right) - \frac{n_c ACD}{n\cdot n_c r_{ca}} - \frac{n_c-1}{n_c^2 r_{ca}}\left(CCT\left(\frac{ACD(n-n_c)}{n\cdot r_{cp}} - 1\right) - \frac{n_c ACD}{n}\right) - \frac{n_c-1}{n_c r_{ca}}\left(\frac{ACD}{n} + \frac{ACD\cdot CCT}{n\cdot r_{cp}}\right)\right) + \frac{n\cdot LT}{n_s}\left(\frac{1}{n\cdot r_{cp}} - \frac{\frac{n_c}{n} - \frac{CCT(n-n_c)}{n\cdot r_{cp}}}{n_c\cdot r_{ca}} - \frac{n_c-1}{n_c r_{ca}}\left(\frac{1}{n} + \frac{CCT}{n\cdot r_{cp}}\right) + \frac{n_c-1}{n_c^2 r_{ca}}\left(\frac{n_c}{n} - \frac{CCT(n-n_c)}{n\cdot r_{cp}}\right)\right)$$

$$\frac{\partial C}{\partial n_c} = \left(\frac{LT(n-n_s)}{n_s r_{lp}} - 1\right)\left(\frac{1}{nr_{cp}} - \frac{n_c}{n \cdot n_c r_{ca}} + \frac{CCT(n-n_c)}{n_c r_{ca} n r_{cp}} - \frac{(n_c-1)}{n_c r_{ca}}\left(\frac{1}{n} + \frac{CCT}{nr_{cp}}\right) + \frac{n_c - 1}{n_c^2 r_{ca}}\left(\frac{n_c}{n} - \frac{CCT(n-n_c)}{nr_{cp}}\right)\right) + \left(P_G - \frac{n-n_s}{n}\left(\frac{1}{r_{la}} - \frac{1}{r_{lp}}\right) + \frac{LT(n-n_s)^2}{n.n_s r_{la} r_{lp}}\right)\left(\frac{ACD}{n.r_{pc}} + \frac{CCT}{n_c r_{ac}}\left(\frac{ACD(n-n_c)}{n.r_{cp}} - 1\right) - \frac{n_c ACD}{n \cdot n_c r_{ac}} - \frac{n_c - 1}{n_c^2 r_{ca}}\left(CCT\left(\frac{ACD(n-n_c)}{n.r_{cp}} - 1\right) - \frac{n_c ACD}{n}\right) - \frac{n_c - 1}{n_c r_{ca}}\left(\frac{ACD}{n} + \frac{ACD \cdot CCT}{n \cdot r_{cp}}\right)\right)\left(P_G - \left(\frac{1}{r_{la}} - \frac{1}{r_{lp}}\right)\frac{n - n_s}{n} + \frac{LT(n - n_s)^2}{n.n_s r_{la} r_{lp}}\right)$$

Cornea thickness (CCT)

$$\frac{\partial SE}{\partial CCT} = \frac{-n\left(-1 + \left(\frac{\frac{\partial A}{\partial CCT}C - (A-1)\frac{\partial C}{\partial CCT}}{C^2}\right)\right)}{\left(L - CCT - ACD - LT + \frac{A-1}{C}\right)^2} - n\left(\frac{\partial C}{\partial CCT}\right)$$

with

$$\frac{\partial A}{\partial CCT} = \frac{(n_c - 1)\left(\frac{ACD(n - n_c)}{nr_{cp}} - 1\right)\left(\frac{LT(n - n_s)}{n_s r_{la}} + 1\right)}{n_c r_{ca}} + \frac{LT(n - n_c)(n_c - 1)}{n_c\, n_s r_{ca} r_{cp}}$$

$$\frac{\partial C}{\partial CCT} = \frac{(n_c - 1)\left(\frac{ACD(n - n_c)}{nr_{cp}} - 1\right)\left(P_G - \frac{\left(\frac{1}{r_{la}} - \frac{1}{r_{lp}}\right)(n - n_s)}{n} + \frac{LT(n - n_s)^2}{n\, n_s r_{la} r_{lp}}\right)}{n_c r_{ca}} + \frac{\left(\frac{LT(n - n_s)}{n_s r_{lp}} - 1\right)(n - n_c)(n_c - 1)}{n.n_c r_{ca} r_{cp}}$$

APPENDIX E: Ocular biometry

Table F1: Mean ± SD values for ocular components. The number of subjects is given in parentheses. [31]

Age	6 y	7 y	8 y	9 y	10 y	11 y	12 y	13 y	14 y
Number of subjects (n)	1626	824	567	436	370	496	285	193	111
Axial length (AL) (mm)	22.5 ±0.66	22.78 ±0.73	23.0 ±0.81	23.2 ±0.81	23.3 ±0.83	23.45 ±0.89	23.5 ±0.89	23.62 ±0.93	23.65 ±1.15
Lens power (P_l) (D)	24.80± 2.08	23.63 ±2.27	22.93 ±2.13	22.26± 2.05	21.93± 2.28	22.23± 2.11	21.54± 2.19	21.44± 2.09	21.93± 2.1
Total corneal power (P_c) (D)	42.34 ±1.01	42.24 ± 1.12	42.13 ±1.11	41.98± 1.1	41.99± 1.22	42.15± 1.11	42.18± 1.5	42.14± 1.15	41.99± 1.07
Anterior chamber depth (ACD) (mm)	3.53 ±0.24	3.56 ±0.23	3.6 ±0.24	3.59 ± 0.23	3.62 ±0.26	3.7 ±0.25	3.69±0. 24	3.69±0. 26	3.65±0. 31
Refractive index of the ocular humour (n) (unitless)	1.336±0 .002	1.336 ±0.00 2	1.336 ±0.00 2	1.336±0 .002	1.336±0 .002	1.336±0 .002	1.336±0 .002	1.336±0 .002	1.336±0 .002
Position 2nd corneal pp from the cornal vertex (pp_{c2}) (unitless)	-0.006	-0.006	-0.006	-0.006	-0.006	-0.006	-0.006	-0.006	-0.006
Position 1st lens pp from the corneal vertex (pp_{l1}) (unitless)	5.61	5.65	5.68	5.7	5.72	5.74	5.85	5.76	5.77
Position 2nd ocular pp from corneal vertex (pp_{eye2}) (unitless)	2.21	2.19	2.17	2.15	2.13	2.12	2.11	2.1	2.1

F2: Mean ± SD values for ocular components[32]

Age	0.25 y (3 mo)	0.75 y (9 mo)	1.5 y (18 mo)	3 y	4.5 y	6.5 y
Axial length (AL)	19.19 ± 0.69 (292)	20.29 ± 0.64 (257)	20.71±0.7 (257)	21.42±0.68 (240)	21.96±0.7 (160)	22.39±0.71 (196)
Lens power (P_l) (D)	40.3 ± 2.58 (286)	37.2 ± 2.09 (251)	35.1 ± 2.24 (250)	31.7 ± 1.94 (237)	28.9 ±1.76 (154)	27.4 ± 1.86 (195)
Total corneal power(P_c) (D)	42.57± 1.54 (289)	41.60 ± 1.48 (272)	41.41± 1.53 (259)	41.21± 1.41 (241)	41.12±1.36 (156)	41.12± 1.33 (196)
Anterior chamber depth (ACD) (mm)	2.83 ± 0.32 (292)	3.06 ± 0.36 (257)	3.01 ± 0.35 (257)	3.15 ± 0.30 (240)	3.29 ±0.31 (160)	3.42 ± 0.30 (196)
Refractive index of the ocular humour (n) (unitless)	1.336±0.002	1.336±0.002	1.336±0.002	1.336±0.002	1.336±0.00 2	1.336±0.00 2
Position 2nd corneal pp from the corneal vertex (pp_{c2}) (unitless)	-0.057	-0.057	-0.057	-0.057	-0.057	-0.057
Position 1st lens pp from the corneal vertex (pp_{l1}) (unitless)	5.15	5.2	5.30	5.44	5.54	5.63
Position 2nd ocular pp from corneal vertex (pp_{eye2}) (unitless)	2.47	2.43	2.39	2.31	2.26	2.2
Lens thickness (LT) (mm)	3.91 ± 0.16 (292)	3.87 ± 0.18 (259)	3.83 ± 0.17 (257)	3.81 ± 0.16 (240)	3.70 ±0.17 (160)	3.60 ± 0.16 (196)

Table F3: Mean ± SD values for ocular components of new-born infants aged 0-3 days[33]

Parameters	Values	Number of subjects
Axial length (L) (mm)	16.53±0.48	59
Lens power (P_l) D)	49.34±3.27	52
Total corneal power (P_c) (D)	47.91±1.97	56
Anterior chamber depth (ACD) (mm)	1.73 ±0.16	59

Table F4: Mean ± SD values for ocular components of premature infants with or without ROP[34]

Parameters	Stage	T1 (32 wk)	T2 (36 wk)	T3(40 wk)	T4(44 wk)	T5(52 wk)
Number of subjects	**n**	**107**	**113**	**120**	**115**	**90**
Axial length (L)(mm)	0	15.4 (0.42)	16.1 (0.45)	16.8 (0.46)	17.4 (0.48)	18.6 (0.54)
	1	15.2 (0.33)	16.1 (0.37)	16.6 (0.61)	17.2 (0.55)	18.6 (0.39)
	2	15.1 (0.50)	15.8 (0.44)	16.7 (0.51)	17.2 (0.57)	18.6 (0.75)
	3	15.3 (0.51)	16.2 (0.63)	16.8 (0.44)	17.4 (0.56)	18.8 (0.82)
	3+	14.9 (0.38)	15.9 (0.50)	16.4 (0.40)	16.9 (0.65)	18.2 (1.1)
Lens thickness (LT) (mm)	0	3.8 (0.22)	3.9 (0.18)	4.0 (0.19)	4.0 (0.22)	4.0 (0.21)
	1	3.8 (0.23)	4.0 (0.15)	4.0 (0.27)	4.0 (0.15)	3.9 (0.19)
	2	3.9 (0.33)	4.0 (0.21)	4.0 (0.14)	4.1 (0.26)	4.0 (0.14)
	3	4.0 (0.14)	4.1 (0.14)	4.0 (0.29)	4.0 (0.19)	3.9 (0.17)
	3+	3.9 (0.00)	4.0 (0.11)	4.1 (0.11)	4.1 (0.21)	4.1 (0.31)
Anterior corneal radius of curvature (r_{ca}) (mm)	0	6.1(0.41)	6.4 (0.24)	6.9 (0.24)	7.2(0.28)	7.6(0.31)
	1	5.9 (0.34)	6.2 (0.26)	6.8 (0.23)	7.1 (0.29)	7.5(0.36)
	2	5.9 (0.30)	6.3 (0.28)	6.6 (0.39)	7.0 (0.48)	7.5(0.17)
	3	5.7 (0.23)	6.5 (0.48)	6.9 (0.44)	7.2 (0.24)	7.5(0.26)
	3+	4.9 (0.00)	6.2 (0.18)	6.7 (0.44)	7.1 (0.34)	7.3(0.31)
Anterior chamber depth (ACD) (mm)	0	2.0 (0.19)	2.1 (0.32)	2.3 (0.19)	2.4 (0.23)	2.8 (0.25)
	1	2.1 (0.38)	2.1 (0.24)	2.2 (0.23)	2.3 (0.22)	2.8 (0.25)
	2	2.0 (0.19)	2.0 (0.21)	2.2 (0.20)	2.3 (0.34)	2.7 (0.35)
	3	1.9 (0.29)	2.0 (0.38)	2.2 (0.28)	2.4 (0.18)	2.8(0.21)
	3+	2.0 (0.05)	2.0 (0.17)	2.1 (0.11)	2.3 (0.25)	2.5(0.29)

Table F5: Mean ± SD values for ocular components of diabetes and control group.[35] Errors are 95% confidence intervals.

Parameters and numbers in groups (diabetes/control)	Diabetes group	Control group
Axial length (L) (mm)(74/64)	23.74±0.92	23.95±0.88
Lens power (P_l) D)(67/62)	25.06±0.8	24.28±0.59
Total corneal power (P_c) (D)(74/64)	43.49±1.17	43.16 ± 1.5
Anterior chamber depth (ACD) (mm)(74/64)	2.75 ±0.09	2.89 ±0.09

APPENDIX F: Physiological constraints of visual pathway lead to more efficient coding of information in retina

Previously published as:

Arezoo Farzanfar, Farzaneh Shayegh, Behzad Nazari, Saeid Sadri
Physiological constraints of visual pathway lead to more efficient coding of information in retina

Journal of Theoretical Biology, 2020;506:110418.

This paper studied how physiological constraints in the visual pathway affect the efficiency of information encoding in the retina, an important neural tissue that enables our perception of the surrounding environment. Retina translates light intensity into electrical signals for the brain, optimizing information transfer while addressing biological limitations. This paper emphasizes the retina's role in transmitting visual data through photoreceptors that respond to input images and retinal ganglion cells (RGCs) that forward encoded signals to the visual cortex. Synaptic connections between sets of photoreceptors, represented by a weight matrix *W*, play a crucial role in the formation of receptive fields for each ganglion cell. Consequently, optimizing the coding of this weight matrix is important to ensure effective representation and transmission of visual information to the brain. Natural images exhibit inherent spatial and temporal correlations, so this paper investigates the importance of redundancy reduction in sensory coding. Traditional methods, such as Principal Component Analysis (PCA) and Independent Component Analysis (ICA), have been used to address this challenge but did not consider essential physiological constraints. The proposed model in this paper builds upon these frameworks by incorporating additional biological constraints, specifically the spatial organization of photoreceptor projective fields and correlations among RGCs. These factors yield an encoding matrix that aligns with the center-surround receptive field structures observed in experimental studies, offering a realistic depiction of retinal signal processing.
This study evaluates the proposed model using metrics like Mean Squared Error (MSE), channel redundancy, and information transfer efficiency. Results demonstrate that while the model introduces a slightly higher MSE compared to simpler frameworks, it significantly reduces redundancy and optimally utilizes neural capacity.

In summary, this thesis advances the understanding of efficient visual information encoding by emphasizing the necessity of integrating physiological constraints into computational models.

APPENDIX G: Publications

Farzanfar A, Shayegh F, Nazari B, Sadri S. Physiological constraints of visual pathway lead to more efficient coding of information in retina. J. Theor. Biol. 2020; 506 (2020): 110418.

Farzanfar A, Lockett-Ruiz V, Navarro R, Koppen C, Rozema JJ. The influence of variations in ocular biometric and optical parameters on differences in refractive error. Ophthalmic Physiol. Opt. 2024;44(5):1000-9.

Farzanfar A, Rozema JJ. Bi-exponential description for different forms of refractive development. J. Vis. 2024;24(7):3-.

Rozema JJ, Farzanfar A, Refractive development II: Modelling normal and myopic eye growth. Ophthalmic Physiol. Opt. 2024

Farzanfar A, Manuel González-Méijome J, Macedo de Araújo R.J, Queirós Pereira A, Rozema J.J, The influence of color and defocus on contrast sensitivity function.

APPENDIX H: Author contributions

Chapter	Author	Concept	Data curation	Formal analysis	Investi-gation	Methodo-logy	Software	Valida-tion	Writing (original)	Writing (review)	Funding	Super-vision
3	Farzanfar	Lead	Equal	Equal	Equal	Equal	Lead	Equal	Equal	Equal		
	Lockett-Ruiz	Equal	Equal	Equal	Equal	Equal	Equal	Equal	Equal	Equal		
	Navarro	Equal	Equal	Equal	Equal	Equal	Equal	Equal	Equal	Equal		
	Koppen										Equal	Equal
	Rozema	Equal			Equal	Equal					Equal	Equal
4	Farzanfar	Equal	Equal	Equal	Equal	Lead	Lead	Lead	Equal	Equal		
	Rozema	Equal	Equal	Equal	Equal	Equal	Equal	Equal	Equal	Equal	Equal	Equal
5	Rozema	Lead	Lead	Lead	Lead	Lead	Lead	Lead	Lead	Lead	Lead	
	Farzanfar	Sup-port	Sup-port	Sup-port	Sup-port	Sup-port	Sup-port	Sup-port	Support	Sup-port	Sup-port	Sup-port
6	Farzanfar	Lead	Equal	Equal	Equal	Equal	Lead	Equal	Equal	Equal		
	González-Méijome	Equal			Equal	Equal				Equal		
	Macedo de Araújo	Equal			Equal	Equal				Equal		
	Queirós Pereira			Equal		Equal	Equal			Equal		
	Rozema	Equal		Equal	Equal	Equal				Equal		

English abstract

This thesis investigates the dynamics of refractive development by analyzing axial and total refractive power using bi-exponential functions to model different refractive development courses reported in the literature, including instant emmetropization, persistent hypermetropia, and myopia. The model was further adjusted to simulate refractive development in school-age myopia and pseudophakia up to 20 years, showing strong alignment with literature. Myopia, which arises from an imbalance between the axial length and optical power of the eye, is driven by genetic and environmental factors, including near-vision activities and reduced time outdoors, and its global prevalence is expected to increase significantly. Insights from animal studies confirmed the role of retinal signals and visual stimuli, such as chromatic cues and image degradation, in regulating eye growth and the onset of myopia. However, the limitations of animal models to fully represent human ocular responses underscore the need for more precise models. For example, while animal studies suggest that choroidal thickening may counteract myopia, its effectiveness in humans remains uncertain.

In response to this gap, this thesis proposes an active emmetropization model by integrating bi-exponential functions for axial length and total refractive power with retinal feedback mechanisms, aiming to simulate ocular growth processes more accurately. This approach uses two ordinary differential equations incorporating both closed-loop and open-loop components to represent retinal blur and excessive axial growth, respectively. Controlled by 18 parameters, the model successfully replicates refractive development in both normal and myopic eyes, demonstrating that early onset of myopia, excessive axial growth, and maximal crystalline lens power are associated with higher degrees of myopia. Validation was achieved through cross-sectional and longitudinal studies from literature.

Additionally, this thesis explores how environmental factors, specifically defocus and chromatic cues, influence contrast sensitivity function (CSF) in both emmetropic and myopic individuals. The findings reveal that defocus and color significantly impact CSF, with green filters enhancing and blue filters reducing sensitivity. Myopic eyes showed a greater decline in CSF with increasing defocus compared to emmetropic eyes, providing key insights into how environmental conditions shape ocular development. Future research will focus on refining the proposed eye growth model by incorporating additional variables such as color and defocus to further enhance its predictive accuracy.

Furthermore, the thesis examines how variations in ocular biometry contribute to refractive errors at a population level. Using an error propagation method across two ocular modeling techniques—the simple and matrix methods, the study identifies axial length as the primary driver of refractive error variation, particularly during myopia progression, with secondary influences from corneal and lens power.

In conclusion, this research offers a novel theoretical framework for understanding refractive development through retinal feedback-based modeling. The findings provide a foundation for future investigations aimed at refining eye growth models and developing interventions to mitigate the impact of myopia.

Nederlands abstract

Deze thesis onderzoekt de dynamiek van refractieve ontwikkeling aan de hand van de axiale en totale refractieve sterkte in de vorm van bi-exponentiële functies. Hiermee kunnen verschillende in de literatuur gerapporteerde trajecten van refractieve ontwikkeling worden gemodelleerd, waaronder directe emmetropisatie, aanhoudende hypermetropie en bijziendheid. Het model werd verder aangepast om de refractieve ontwikkeling bij schoolgaande kinderen met bijziendheid en pseudofakie tot 20 jaar te simuleren, hetgeen een sterke overeenstemming met de literatuur laat zien. Bijziendheid, die ontstaat door een onevenwicht tussen de aslengte en de optische kracht van het oog, wordt gedreven door genetische en omgevingsfactoren, waaronder activiteiten waarbij men vaak dichtbij kijkt en minder tijd buitenshuis doorbrengt. De wereldwijde prevalentie van bijziendheid zal naar verwachting aanzienlijk toenemen. Inzichten uit dierstudies gaven aan dat retinale signalen en visuele stimuli, zoals chromatische signalen en beeldverslechtering, een belangrijke rol spelen in het reguleren van ooggroei en het ontstaan van bijziendheid. Maar diermodellen zijn te beperkt om menselijke oogreacties volledig te vertegenwoordigen, hetgeen de noodzaak van preciezere modellen benadrukt. Bijvoorbeeld, terwijl dierstudies suggereren dat verdikking van het choroidea mogelijk bijziendheid tegengaat, blijft de effectiviteit hiervan bij mensen onzeker.

Om dit probleem aan te pakken, stelt deze thesis een actief emmetropisatiemodel voor gebaseerd op bi-exponentiële functies die axiale en totale refractieve kracht integreren met retinale feedbackmechanismen en zo meer nauwkeurige simulaties te verkrijgen van de ooggroei. Deze benadering gebruikt twee gewone differentiaalvergelijkingen die zowel closed-loop en open-loop feedback gebruiken die respectievelijk de retinale onscherpte en overmatige axiale groei vertegenwoordigen. Het model, aangestuurd door 18 parameters, slaagt erin om refractieve ontwikkeling in zowel normale als bijziende ogen te repliceren, hetgeen aantoont dat vroege bijziendheid, overmatige axiale groei en maximale kracht van de ooglens geassocieerd zijn met hogere graden van bijziendheid. Dit werd gevalideerd door middel van dwarsdoorsnede- en longitudinale studies uit de literatuur.

Daarnaast verkent deze thesis hoe omgevingsfactoren zoals defocus en chromatische signalen de contrastgevoeligheids-functie (CSF) beïnvloeden in emmetrope en bijziende individuen. De resultaten tonen aan dat defocus en kleur significante invloed hebben op CSF, waarbij groene filters de gevoeligheid vergroten en blauwe filters deze verminderen. Bijziende ogen vertonen een sterkere afname van CSF met toenemende defocus in vergelijking met emmetrope ogen, wat aangeeft hoe omgevingsomstandigheden de ontwikkeling van het oog beïnvloeden. Toekomstig onderzoek zal zich richten op het verfijnen van het voorgestelde ooggroeimodel door extra variabelen zoals kleur en defocus te integreren om de voorspellende nauwkeurigheid verder te verbeteren.

Verder onderzoekt de thesis hoe variaties in oogbiometrie bijdragen aan refractieve fouten op populatieniveau. Met behulp van een foutpropagatiemethode over twee technieken voor oogmodellering, de eenvoudige en matrixmethode, identificeert de studie axiale lengte als de belangrijkste oorzaak van variatie in refractieve fouten, met name tijdens de progressie van bijziendheid, met secundaire invloeden van corneale en lenskracht.

Kortom, dit onderzoek biedt een nieuw theoretisch kader om de refractieve ontwikkeling beter te begrijpen door middel van een model gebaseerd op retinale feedback. Deze bevindingen vormen een basis voor toekomstig onderzoek gericht op het verfijnen van ooggroeimodellen en het ontwikkelen van interventies om de impact van bijziendheid te verminderen.

Acknowledgements

We all have dreams and aspirations guiding us in our professional and academic journey. My career path began to take shape when I chose to focus my master's thesis on efficient coding of visual information in the retina.

After completing my master's degree, I decided to pursue my passion for eye modeling during my PhD degree. This decision led me to search for PhD opportunities abroad. Fortunately, I came across the profile of Professor Jos Rozema and immediately reached out to him via email. One of the most remarkable and encouraging moments at the start of this journey was Professor Rozema's prompt and detailed response, guiding me to apply for a position under the Marie Curie Fellowship program.
What stood out to me from the very beginning was his unwavering support and responsiveness, despite his busy schedule. Professor Rozema consistently answered emails with speed, precision, and care—qualities that are invaluable and reassuring for any PhD student. I feel truly fortunate and proud to have such an exceptional and compassionate supervisor.

A few months after submitting my application, I received incredible news: I was selected as ESR-9 for the OBERON PhD project under the Marie Curie Fellowship! This was a monumental moment for me. On one hand, I was thrilled to be part of a large-scale international project, and on the other, I was grateful to have one of the most brilliant, supportive, and inspiring supervisors—a professor many of my peers dream of working with.

The OBERON project was an intense and ambitious endeavor that needed to be completed within three years, a timeframe that was both challenging and stressful. However, Professor Rozema made this journey much smoother for me. His excellence as a scientist was only matched by his exceptional personal qualities. One of his most admirable traits was his ability to maintain calm and provide clarity during high-pressure moments when multiple tasks needed to be completed simultaneously.
Our weekly meetings played a crucial role in my success. These sessions provided a safe space to discuss challenges and receive thoughtful and constructive feedback. Not only did these meetings advance my research, but they also brought me peace of mind and encouragement throughout the process.
I am incredibly proud to have been part of the VOLANTIS team — a group of creative, curious, and hardworking individuals. This experience has been one of the most enriching periods of my life, and I am deeply grateful for the opportunity.

I would also like to express my gratitude to Prof. Dr. Carina Koppen, head of the ophthalmology department at the UZA Hospital. Her humility, warmth, and kindness were evident from our very first interaction, and I consider it an honor to have had the chance to work with her. Having a supervisor of her caliber has been a truly inspiring and valuable experience.
My PhD journey also allowed me to broaden my horizons through enriching research visits and collaborations. I had the privilege of spending time at the University of Zaragoza in Spain under the guidance of Professor Rafael Navarro to explore the contribution of biometric factors to variations of

refractive error. I also conducted research at the University of Minho in Portugal with Professor José Manuel Gonzalez Meijome, focusing on measuring contrast sensitivity in emmetropic and myopic groups under various defocus and color conditions. Additionally, I will gain invaluable experience during my time at Essilor in Paris, which will remain a lasting and treasured memory.

The annual OBERON meetings were another highlight of this journey. These gatherings provided an excellent opportunity to exchange ideas with colleagues, participate in professional training sessions, and engage in workshops on topics like grant writing and public speaking—skills that significantly contributed to our professional development.

I am deeply grateful to the coordinators and supervisors of the OBREON project for their unwavering support and dedication to creating such impactful opportunities for both scientific and personal growth. A special thanks goes to my wonderful friends in the VOLANTIS group, Hosna and Sharon, for the joyful and memorable moments we shared. I sincerely wish you all the best in your future endeavors and happiness in all that you do. I also extend my warmest wishes to my friends in the ARGOS group for their continued success.

To my dear husband, whose unwavering support, patience, and endless love carried me through the most challenging times. I owe my deepest gratitude. Words cannot adequately express the extent of your love, sacrifices, and encouragement.

To my parents and mother-in-law, who have always been my pillars of strength, showering me with unconditional love, faith, and encouragement at every step of my life, I thank you from my heart.
Thank you all for being an integral part of this journey and making it an unforgettable and fulfilling experience.